

Improving Secrecy Performance in Optical HAPS Communications Through Site Selection Under Harsh Weather Conditions

Eylem Erdogan¹ , Evla Safahan Ahrazoglu² , Emre Berker Bakirci² , and Ibrahim Altunbas² 

¹ Department of Electrical and Electronics Engineering, Izmir Institute of Technology, Izmir, 35430, Turkey

² Department of Electronics and Communication Engineering, Istanbul Technical University, Istanbul, 34469, Turkey

Abstract: The physical layer security of non-terrestrial networks (NTNs) has recently garnered increasing attention from both academia and industry as the information can be intercepted in aerial transmissions, especially when an illegitimate user positions itself near the transmitter or receiver. To address this vulnerability, we investigate the secrecy performance of a high altitude platform station (HAPS) system using optical communications in the presence of an aircraft eavesdropper. Specifically, we assess the secrecy-reliability trade-off by considering both outage and interception probability, and explore the secrecy outage probability. In the proposed setup, we evaluate a practical scenario in which the HAPS communicates with multiple ground stations located at different altitudes, examining the system's physical layer security performance for different types of attenuators including fog, clouds and air pollution. The findings indicate that weather conditions significantly affect the secrecy performance of optical HAPS communications. However, placing ground stations at higher altitudes or selection among multiple ground stations can improve the overall security performance of the system.

Keywords: HAPS systems, optical communication, physical layer security.

Zorlu Hava Koşulları Altında Yer İstasyonu Seçimi Yoluyla Optik HAPS İletişiminde Gizlilik Başarımının Arttırılması

Özet: Son zamanlarda, havasal iletimlerde bilginin ele geçirilebilmesi nedeniyle, karasal olmayan ağların (non-terrestrial networks, NTNs) fiziksel katman güvenliği hem akademide hem de endüstride artan bir ilgiyle karşılanmaktadır; özellikle de yetkisiz bir kullanıcının vericiye veya alıcıya yakın bir konumda bulunması durumunda güvenlik riskleri artmaktadır. Olası güvenlik açıklarını ele almak amacıyla, bu çalışmada optik haberleşme kullanan bir yüksek irtifa platform istasyonu (high altitude platform station, HAPS) sisteminin gizlilik performansı, bir gizli dinleyicinin varlığı altında incelenmiştir. Özellikle, kesinti ve ele geçirilme olasılıklarını dikkate alarak önerilen sistemin gizlilik-güvenilirlik dengesi değerlendirilmiş ve gizlilik kesinti olasılığı hesaplanmıştır. Önerilen senaryoda, HAPS'in farklı yüksekliklerde konumlanmış birden fazla yer istasyonu ile iletişim kurduğu pratik bir durumu ele alarak, sistemde sis, bulutlar ve hava kirliliği gibi farklı zayıflatıcı etmenlerin etkisi incelenmiştir. Sonuçlar, hava koşullarının optik HAPS iletişimlerinin gizlilik performansını önemli ölçüde etkilediğini göstermektedir. Ancak, yer istasyonlarının daha yüksek irtifalarda konumlandırılması veya birden fazla yer istasyonu arasından seçim yapılması sistemin genel güvenlik performansını arttırabilmektedir.

Anahtar Kelimeler: HAPS sistemleri, optik haberleşme, fiziksel katman güvenlik.

RESEARCH PAPER

Corresponding Author: Eylem Erdogan, eylemerdogan@iyte.edu.tr

Reference: E. Erdogan, E. S. Ahrazoglu, E. B. Bakirci, and I. Altunbas, (2025), "Improving Secrecy Performance in Optical HAPS Communications Through Site Selection Under Harsh Weather Conditions," *ITU-Journ. Wireless Comm. Cyber.*, 2, (1) 1–10.

Submission Date: Nov, 26, 2024

Acceptance Date: Mar, 2, 2025

Online Publishing: Mar, 28, 2025

1 INTRODUCTION

Due to the foreseen increase in requested data rates from the users, different techniques aiming to convey more information to the users are among the key topics of interest for researchers today. Free space optics (FSO) offers a promising solution to the growing demand for higher data rates, leveraging the broader bandwidth available at optical frequencies to transmit large volumes of data. One distinctive feature of optical signals is their highly directional beams, which restricts their use to line-of-sight (LOS) scenarios, unlike traditional radio frequency (RF) communication where a LOS link is not always required. However, this signal characteristic also addresses another critical issue: data privacy [1]. Unlike RF signals, where electromagnetic wave propagation raises security concerns, an eavesdropper in FSO systems must be positioned close to the LOS link to be able to listen the legitimate user, thereby enhancing the security of transmitted data [2].

An alternative approach to address user privacy concerns can be established by using physical layer security (PLS) techniques, which provide information-theoretic security by exploiting the inherent randomness in wireless channels, such as noise and fading characteristics. PLS techniques ensure secure communication as long as the legitimate user's channel quality surpasses those of potential eavesdroppers [3]. Compared to the traditional cryptographic methods, PLS techniques offer greater computational efficiency and ease of implementation, making them a topic of increasing interest among both researchers and industry professionals in the recent years [4].

Aiming to satisfy both high data rate and security requirements, various scenarios that utilize FSO technique have been analyzed in the literature. [1] and [5] derive the secrecy performance of a single hop FSO link under different turbulence channels. Reference [6] extends the single hop analysis to multiple scenarios for different eavesdropper locations, and [2] focuses on secrecy performance under different eavesdropper locations. Moreover, [7] and [8] add an RF link to the single hop scenarios, with and without an additional RF eavesdropper, respectively. Finally, [9] and [10] analyze multi hop hybrid FSO/RF scenarios with maximum ratio combining (MRC) and selection combining (SC) diversity reception techniques respectively.

Another promising approach for providing stable and high-rate data transmission to targeted users is the implementation of vertical networks, which can be realized through unmanned aerial vehicles (UAVs), high-altitude platform stations (HAPS), or low Earth orbit (LEO) satellites. In HAPS enabled communications, stronger and less disrupted LOS communication can be provided to a large number of user, with enhanced data rates, and reliable communication performance [11]. However, as these networks serve a large number of users, higher privacy demands arise. Consequently, the need for comprehensive

research and detailed analysis of vertical network scenarios becomes essential to address these growing privacy concerns effectively.

In the recent years, secrecy performance of vertical networks with PLS techniques have been investigated in the literature. Among them, [12] analyzes a downlink satellite communication scenario where the receiver and the eavesdropper are equipped with multiple antennas. Reference [13] explores the impact of satellite orbits on secrecy performance, while [3] examines a satellite communication scenario that incorporates channel estimation errors and considers the presence of multiple receivers along with multiple eavesdroppers. Moreover, [14] analyzes the secrecy performance of a scenario in which multiple relays are fed from a satellite and paired with multiple users, and [15] includes power optimization and trajectories of UAV's to improve secrecy performance. Finally, [16] focuses on the secrecy performance of a multiple UAV relay assisted system setup. In addition to the aforementioned studies, numerous papers in the literature have explored the integration of the high data rates provided by FSO techniques with the extensive coverage capabilities of vertical networks to enhance secrecy. For instance, [17] examines the secrecy performance of a single-hop FSO link between a LEO satellite and a HAPS system. Similarly, [18] explores various scenarios in non-terrestrial networks, including LEO satellite-to-HAPS, HAPS-to-HAPS, and HAPS-to-ground links. Furthermore, [19] introduces a hybrid FSO/RF link in addition to the FSO link between a LEO satellite and a HAPS, enhancing communication robustness.

In addition to the above-mentioned studies, several secrecy analyses have been conducted in the literature, combining both the high data rate output of FSO techniques and the robustness of vertical networks. For instance, [17] examines the secrecy performance of a single-hop FSO link between a LEO satellite and a HAPS. Similarly, [18] explores various scenarios in non-terrestrial networks, including LEO satellite-to-HAPS, HAPS-to-HAPS, and HAPS-to-ground links. Furthermore, [19] introduces a hybrid FSO/RF link in addition to the FSO link between a LEO satellite and a HAPS, enhancing communication robustness.

Building upon the principles of FSO communication and PLS, this study presents a comprehensive analysis of physical layer security in HAPS systems utilizing optical communication. Given the growing demand for secure and high-rate communication in non-terrestrial networks, particularly with the unique characteristics of FSO such as narrow beamwidth and high directivity, our research focuses on evaluating the secrecy performance of HAPS-based optical communication links. The contributions of this paper can be summarized as follows:

- By integrating the strengths of optical transmission with the security benefits offered by PLS techniques, we

provide a thorough investigation into how these systems can ensure secure communication against potential eavesdropping threats. To do so, we consider different site deployment scenarios in the presence of various attenuators, including fog, clouds, and air pollution.

- The analysis is crucial as HAPS systems, positioned in the stratosphere, present distinct challenges and opportunities in terms of maintaining high-quality, secure communication links over vast areas. To establish a practical scenario, we consider an aerial eavesdropper positioned close to the HAPS node, trying to intercept optical communication.
- In this study, we analyze the impact of various weather conditions and deployment scenarios on system performance, with a primary focus on the secrecy outage probability. Furthermore, we examine the security-reliability trade-off by jointly considering outage probability and intercept probability. By evaluating these factors in the proposed scenario, we aim to provide a deeper understanding of how environmental conditions and site configurations influence both the security and reliability of the system.

The paper is organized as follows. In Section 2.1, a general system model is described, followed by explanations about atmospheric attenuation and turbulence-induced fading channel in Section 2.2. Section 2.3 focuses on clarifying different scenarios that will be used throughout the paper. Section 3 focuses on statistical properties of SNR and analytical expressions about secrecy performance of the proposed system. Simulation results are talked upon in Section 4, and the results are summarized in Section 5.

2 SYSTEM AND CHANNEL MODEL

2.1 System Model

In this study, we introduce a scenario for an eavesdropping attack on the communication link between a HAPS system and a ground station. Specifically, we analyze the case where HAPS A is communicating with the best site B_k^* , among possible sites B_k , $k \in \{1, 2, \dots, N\}$ in the footprint of A . This capability allows A to enhance the secrecy performance of the communication by strategically choosing the optimal site from a range of possible candidates [20]. Meanwhile, the aircraft eavesdropper E , positioned in close proximity to A , is actively attempting to intercept and gather information transmitted through the optical beam as illustrated in Fig. 1. Positioning itself above the troposphere enhances E 's eavesdropping performance by mitigating the impacts of weather-dependent effects. However, despite this advantage, intercepting information in optical communication remains challenging, as any eavesdropper in close proximity to A must block the LOS communication between

A and B_k to successfully gather the data. Alternatively, E could function as a passive optical beam splitter, capturing a small fraction r_E of the laser beam's irradiance, while allowing the remainder r_{B_k} to be transmitted to B_k satisfying $r_{B_k} + r_E = 1$ [1]. For the proposed structure, the received signals at B_k and E can be written as

$$y_{B_k} = \sqrt{r_{B_k} P_A} I_{B_k} g_{B_k} x + n_{B_k}, \quad (1)$$

and

$$y_E = \sqrt{r_E P_A} I_E g_E x + n_E, \quad (2)$$

where P_A is the transmit power of A , n_{B_k} stands for the additive white Gaussian noise (AWGN) with one-sided noise power N_0 , I_{B_k} is turbulence induced fading channel coefficient, and g_{B_k} denotes the atmospheric attenuation between A and B_k respectively. Moreover, I_E and g_E are the turbulence induced fading coefficient and attenuation between A and E , and n_E is the AWGN noise at passive eavesdropper with one-sided noise power N_0 . Accordingly, the instantaneous SNRs at B_k and E can be written as

$$\gamma_j = \frac{r_j P_A}{N_0} I_j^2 g_j^2 = \bar{\gamma}_j I_j^2, \quad (3)$$

where $j \in \{B_k, E\}$, and $\bar{\gamma}_j = \frac{r_j P_A}{N_0} g_j^2$ is the average SNR with $E[I_j^2] = 1$.

2.2 Channel Model

The optical signal's quality is influenced by various atmospheric factors, such as weather conditions, turbulence, and random fluctuations as it travels through the atmosphere. Key factors include atmospheric conditions like cloud formations, fog, dust, rain, and snow, which cause scattering, absorption, and attenuation of the signal due to changes in the refractive index along the transmission path. In this section, we briefly summarize these limiting effects.

2.2.1 Atmospheric attenuation

In optical communication systems, atmospheric attenuation is caused by scattering and absorption, both of which are affected by atmospheric particles and weather phenomena, especially fog and clouds.¹ Mathematically, atmospheric attenuation is expressed as $g_{B_k} = g_{B_k}^{\text{mie}} g_{B_k}^{\text{geo}}$, where $g_{B_k}^{\text{mie}}$ and $g_{B_k}^{\text{geo}}$ represent the attenuation due to Mie scattering and geometrical scattering, respectively. Mie scattering occurs when the wavelength of operation is similar to the size of the particles in the transmission medium, and its behavior can be described as [21]

¹ As a HAPS eavesdropper, E remains impervious to weather-dependent effects. Consequently, the analysis presented herein remains applicable to the communication between A and B_k .

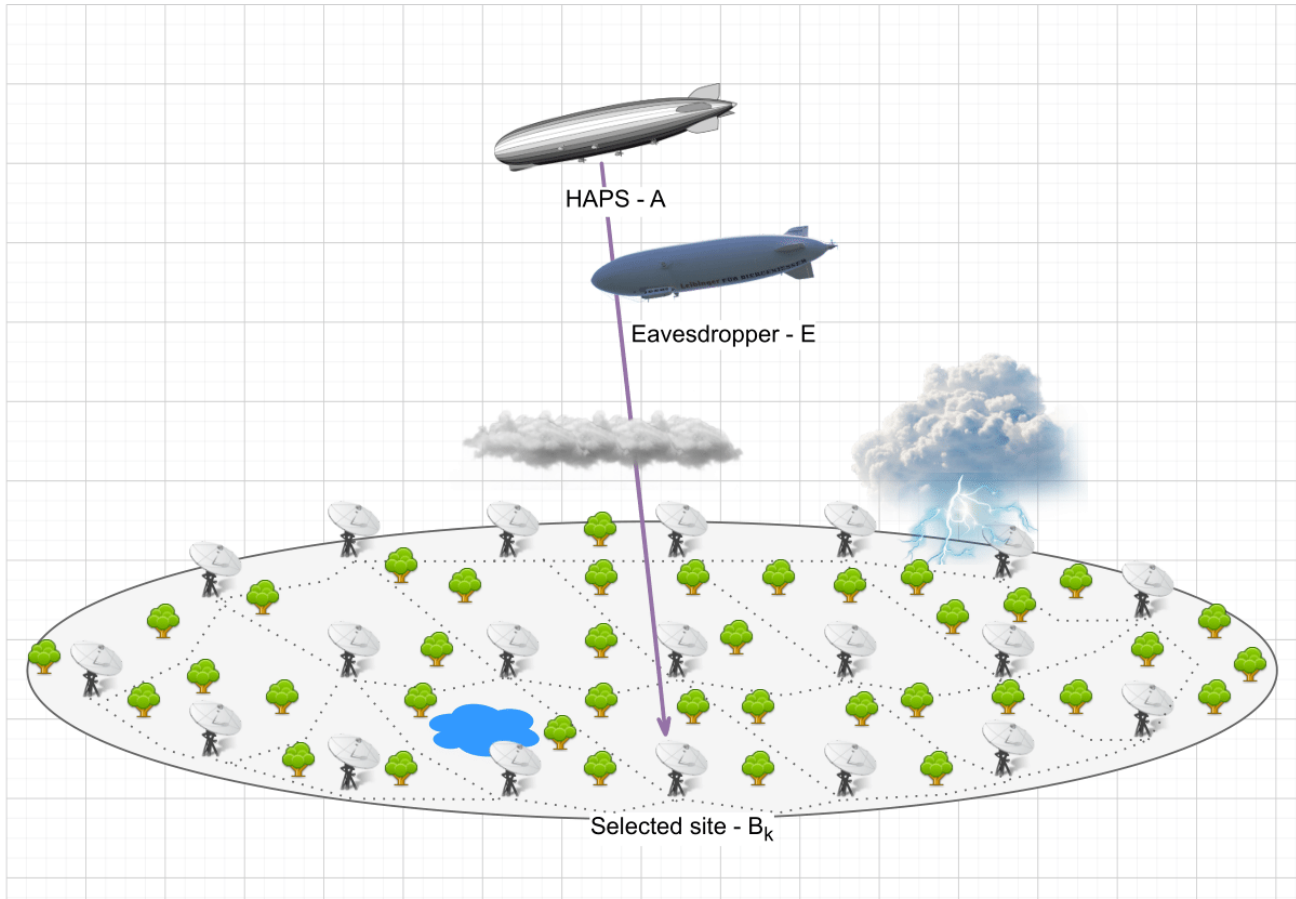


Fig. 1 Illustration of HAPS to ground station communication with a HAPS eavesdropper.

$$g_{B_k}^{\text{mic}} = \exp\left(-\frac{\rho'}{\sin(\theta_{B_k})}\right), \quad (4)$$

where θ_{B_k} is the elevation angle between A and B_k -th site. Here, ρ' denotes the extinction ratio and it is defined as [21]

$$\rho' = a'h_{B_k}^3 + b'h_{B_k}^2 + c'h_{B_k} + d', \quad (5)$$

where h_{B_k} is the height of the selected site above mean sea level. a' , b' , c' , and d' depend on the signal wavelength λ through the following equations

$$\begin{aligned} a' &= -0.000545\lambda^2 + 0.002\lambda - 0.0038, \\ b' &= 0.00628\lambda^2 - 0.0232\lambda + 0.0439, \\ c' &= -0.028\lambda^2 + 0.101\lambda - 0.18, \\ d' &= -0.228\lambda^3 + 0.922\lambda^2 - 1.26\lambda + 0.719. \end{aligned} \quad (6)$$

Geometrical scattering, on the other hand, is associated with the optical visibility range, which is influenced by cloud/fog formations and atmospheric pollution. Based on the Kim's model, the attenuation caused by geometrical scattering can be expressed as [22]

$$g_{B_k}^{\text{geo}} = \exp(-\varphi_{B_k} D_{B_k}^{\text{geo}}), \quad (7)$$

where $D_{B_k}^{\text{geo}}$ is the distance of the fraction of the link between A to B_k that experiences geometrical scattering, and φ_{B_k} denotes the attenuation coefficient, defined as [22]

$$\varphi_{B_k} = \frac{3.91}{V_{B_k}} \left(\frac{\lambda}{550}\right)^{-\psi_{B_k}}, \quad (8)$$

where ψ_{B_k} and V_{B_k} are the particle size coefficient and optical visibility, and ψ_{B_k} is determined by the Kim's model as [23]

$$\psi_{B_k} = \begin{cases} 1.6 & V_{B_k} > 50 \\ 1.3 & 6 < V_{B_k} < 50 \\ 0.16V_{B_k} + 0.34 & 1 < V_{B_k} < 6 \\ V_{B_k} - 0.5 & 0.5 < V_{B_k} < 1 \\ 0 & V_{B_k} < 0.5. \end{cases} \quad (9)$$

Herein, V_{B_k} is defined as [23]

$$V_{B_k} = \frac{1.002}{(\mathcal{W}_{B_k} \mathcal{C}_{B_k})^{0.6473}} \text{ [km]}, \quad (10)$$

where \mathcal{W}_{B_k} and \mathcal{C}_{B_k} denote liquid water content and cloud number concentration. The values of \mathcal{W}_{B_k} , \mathcal{C}_{B_k} , and V_{B_k} , under $\lambda = 1550\text{nm}$, for various cloud formations are presented in Table 1. Moreover, V_{B_k} and φ_{B_k} values for fog formations and different atmospheric pollution levels are provided in Table 2 and 3, respectively.

Table 1 Geometrical scattering parameters for different cloud formations at $\lambda = 1550\text{ nm}$ [23]

Cloud formation	\mathcal{W}_{B_k} [cm^{-3}]	\mathcal{C}_{B_k} [g/m^{-3}]	V_{B_k} [km]
Cumulus	250	1.0	0.028
Stratus	250	0.29	0.0626
Stratocumulus	250	0.15	0.0959
Altostratus	400	0.41	0.0369
Nimbostratus	200	0.65	0.0429
Cirrus	0.025	0.06405	64.66
Thin cirrus	0.5	3.128×10^{-4}	290.69

Table 2 Geometrical scattering parameters for different fog formations [24]

Fog formation	V_{B_k} [km]	φ_{B_k} [dB/km]
Dense	0.05	339.62
Thick	0.2	84.9
Moderate	0.5	33.96
Light	0.77	16.67
Thin	1.9	4.59

Table 3 Geometrical scattering parameters for different atmospheric pollution levels [25]

Atmospheric pollution	V_{B_k} [km]	φ_{B_k} [dB/km]
Extremely polluted atm.	1 (low)	16.98
Normal atm.	10 (mod)	0.442
Non-polluted atm. (clear)	145 (high)	0.022

2.2.2 Turbulence-induced fading

Atmospheric temperature fluctuations give rise to turbulent eddies with randomly varying refractive indices. As these

eddies function like dynamic optical lenses, they introduce random variations in the amplitude of the transmitted signal, a phenomenon termed turbulence-induced fading. This fading can be effectively modeled using the exponentiated Weibull distribution (EW) [26], where the probability density function (PDF) and cumulative distribution function (CDF) characterize the statistical behavior of signal fluctuations as

$$f_I(I) = \frac{\alpha\beta}{\eta} \left(\frac{I}{\eta}\right)^{\beta-1} \exp\left[-\left(\frac{I}{\eta}\right)^\beta\right] \left(1 - \exp\left[-\left(\frac{I}{\eta}\right)^\beta\right]\right)^{\alpha-1}, \quad (11)$$

and

$$F_I(I) = \left(1 - \exp\left[-\left(\frac{I}{\eta}\right)^\beta\right]\right)^\alpha, \quad (12)$$

respectively. Here, α and β are the distribution parameters, and η is the scale parameter. The parameters can be expressed as [27]

$$\alpha = \frac{7.22\sigma_I^{2/3}}{\Gamma(2.487\sigma_I^{2/6} - 0.104)},$$

$$\beta = 1.012(\alpha\sigma_I^2)^{-13/25} + 0.142, \quad (13)$$

$$\eta = \frac{1}{\alpha\Gamma(1 + 1/\beta)g_1(\alpha, \beta)},$$

where $g_1(\alpha, \beta)$ is defined as

$$g_1(\alpha, \beta) \triangleq \sum_{k=0}^{\infty} \frac{(-1)^k \Gamma(\alpha)}{k!(k+1)^{1+1/\beta} \Gamma(\alpha-k)}. \quad (14)$$

In this formulation, the fluctuation level can be obtained by using the scintillation index σ_I^2 , which is determined by the Rytov variance σ_R^2 as [28]

$$\sigma_I^2 = \exp\left[\frac{0.49\sigma_R^2}{(1 + 1.11\sigma_R^{12/5})^{7/6}} + \frac{0.51\sigma_R^2}{(1 + 0.69\sigma_R^{12/5})^{5/6}}\right] - 1, \quad (15)$$

and the Rytov variance σ_R^2 is related with the physical parameters, including transmitter and receiver altitudes, wind speed, wave number and the zenith angle. Further details about the calculation of σ_R^2 can be found in [28].

2.3 Site Deployment Model

In the forthcoming generation of optical wireless communication systems, multiple ground stations may be strategically positioned at varying altitudes above mean sea level to optimize coverage and enhance performance. Specifically,

deploying multiple stations within NTN offers a viable solution for mitigating signal attenuation caused by adverse weather conditions. With practical deployment in mind, we propose three distinct deployment strategies in this work.

In the scenario of ground level deployment, we consider that all sites available for communication are situated at ground level, precisely $h_0 = 0$ km above the surface and $h_E = 0.01$ km above mean sea level, where the wind speed is 2.8 m/s, and $\lambda = 1550$ nm. In the configuration of mid-level deployment, we assume the ground stations are positioned at mid-altitudes, such as on hills, low mountainous regions, or foothills, to minimize signal attenuation. The altitudes are set to $h_0 = 0.5$ km and $h_E = 0.7$ km. As a result, the wind speed experiences a slight increase to 5.1 m/s, with an operational wavelength of $\lambda = 1550$ nm. In the setup of high-level deployment, the ground stations are located at very high altitudes, like high plateau, or mountains. As a result, h_0 and h_E are taken as $h_0 = 2$ km and $h_E = 2.2$ km, and the wind speed increases up to 10.0 m/s, with the same operational wavelength as given above.

3 SECURITY PERFORMANCE ANALYSIS

In this section, we first present the statistical properties of SNR. Thereafter, we analyze the proposed system in terms of secrecy outage probability (SOP) and provide a security-reliability trade-off.

3.1 Statistical Properties of SNR

The proposed site selection method relies on the maximization of SNR. Mathematically, the best site is selected as

$$k^* = \arg \max_{1 \leq k \leq N} [\gamma_{B_k}], \quad (16)$$

and similarly, the end-to-end SNR at the legitimate link can be written as

$$\gamma_B = \max_{1 \leq k \leq N} [\gamma_{B_k}]. \quad (17)$$

Assuming independent identically distributed Exponentiated Weibull random variables in each link, with the aid of (12) and (17) CDF of the overall SNR can be expressed as

$$F_{\gamma_B}(\gamma_B) = \prod_{k=1}^N \left(1 - \exp \left[- \left(\frac{\gamma_B}{(\eta_{B_k} g_{B_k})^2 \tilde{\gamma}_{B_k}} \right)^{\beta_k/2} \right] \right)^{\alpha_k}. \quad (18)$$

3.2 Secrecy Outage Probability

In the physical layer security, SOP stands as one of the most extensively employed metrics for evaluating secrecy performance in academic literature. Within the context of wireless communications, HAPS *A* must ensure that the information is transmitted at a fixed secrecy rate, denoted by

R_s . For secure communication to be maintained, this secrecy rate is required to be less than the secrecy capacity C_s , meaning that the condition $C_s > R_s$ must hold true to prevent a breach in secrecy [29]. Mathematically, SOP can be defined as

$$P_{SO} = \Pr[C_s < R_s], \quad (19)$$

where $R_s = \log_2 \gamma_{th}$, and C_s can be written as

$$C_s = \begin{cases} \log_2(1 + \gamma_B) - \log_2(1 + \gamma_E), & \gamma_B > \gamma_E \\ 0, & \text{otherwise.} \end{cases} \quad (20)$$

As we assume a turbulence-free communication model between *B* and *E*, due their close proximity, the SNR at *E*, denoted as γ_E , can be represented by its average value $\bar{\gamma}_E$, given by $\gamma_E = \bar{\gamma}_E = \frac{r_E P_A}{N_0}$ [1]. Therefore, by invoking (20) into (19), P_{SO} can be written as

$$P_{SO} = \Pr[\gamma_B < \gamma_{th}(1 + \bar{\gamma}_E) - 1], \quad (21)$$

and with the aid of (21), and (18), P_{SO} can be expressed as

$$P_{SO} = \prod_{k=1}^N \left(1 - \exp \left[- \left(\frac{\gamma_{th}(1 + \bar{\gamma}_E) - 1}{(\eta_{B_k} g_{B_k})^2 \tilde{\gamma}_{B_k}} \right)^{\beta_k/2} \right] \right)^{\alpha_k}. \quad (22)$$

3.3 Security-Reliability Trade-off

The security-reliability trade-off (SRT) is characterized by the balance between the intercept probability (IP) and the outage probability (OP) in communication systems [30]. IP refers to the probability that *E* successfully intercepts and decodes the transmitted signal. This happens when the *E*'s SNR exceeds a certain threshold, allowing it to capture the data. On the contrary, OP measures the probability that the signal quality, typically quantified by SNR of the legitimate link, falls below a certain threshold γ_{th} . By taking IP and OP into consideration, the SRT can be expressed as [30]

$$P_{SRT} = \Pr[\gamma_B \leq \gamma_E, \gamma_E > \gamma_{th}]. \quad (23)$$

Please note that IP and OP are statistically independent. Therefore the above expression can be written as $P_{SRT} = \Pr[\gamma_B \leq \gamma_E] \Pr[\gamma_E > \gamma_{th}]$. Therefore, P_{SRT} can be expressed

$$\begin{aligned} P_{SRT} &= \Pr[\gamma_B \leq \gamma_E] \Pr[\gamma_E > \gamma_{th}] \\ &= \Pr[\gamma_E > \gamma_{th}] \prod_{k=1}^N \left(1 - \exp \left[- \left(\frac{\tilde{\gamma}_E}{(\eta_{B_k} g_{B_k})^2 \tilde{\gamma}_{B_k}} \right)^{\beta_k/2} \right] \right)^{\alpha_k}. \end{aligned} \quad (24)$$

Moreover, SRT can be asymptotically evaluated by using the high SNR Taylor expansion of $\exp(x) \cong 1 - x$ as

$$P_{SRT}^{\infty} = \Pr[\gamma_E > \gamma_{th}] \prod_{k=1}^N \left(\frac{\tilde{\gamma}_E}{(\eta_{B_k} g_{B_k})^2 \tilde{\gamma}_{B_k}} \right)^{\alpha_k \beta_k/2}. \quad (25)$$

4 NUMERICAL RESULTS

In this section, the SOP and SRT performances of the proposed system are illustrated, and theoretical findings are validated by Monte-Carlo simulations. It is assumed that HAPS A is employed at an altitude of 30 km as recommended in [31] and that the eavesdropper E is located at very close proximity of HAPS A . Due to close distance between A and E , we assume that $\Pr[\gamma_E > \gamma_{th}] = 0.9$. The zenith angles between the A and all possible sites are assumed to be $\zeta = 10^\circ$. Three different site deployment scenarios are considered as described in Section 2.3, and the fading parameters are found as $\alpha = 3.209$, $\beta = 2.505$, $\eta = 0.81$ for the ground level deployment, $\alpha = 3.113$, $\beta = 2.657$, $\eta = 0.827$ for the mid-level deployment, and $\alpha = 3.135$, $\beta = 2.621$, $\eta = 0.823$ for the high-level deployment. The distances $D_{B_k}^{\text{geo}}$ are calculated through measurement results in [32]. Additionally, the fixed secrecy rate is taken as $R_s = 1$ bit/s, and the fraction of the power received by the eavesdropper is set to $r_E = 0.2$. Also, the received SNR at the eavesdropper is assumed as $\bar{\gamma}_E = 5$ dB.

In Fig. 2, the SOP performance of the system is shown for the ground level deployment scenario in the presence of thin cirrus cloud formation with $D_{B_k}^{\text{geo}} = 0.1$ km for different number of sites. It can be seen here that the theoretical results are perfectly matched with the simulations. Moreover, it is inferred from the figure that the slopes of the curves increase with the increasing number of sites. This stems from larger diversity order offered by higher number of sites. Hence, it can be deduced that enhanced security can be achieved by deploying higher number of sites.

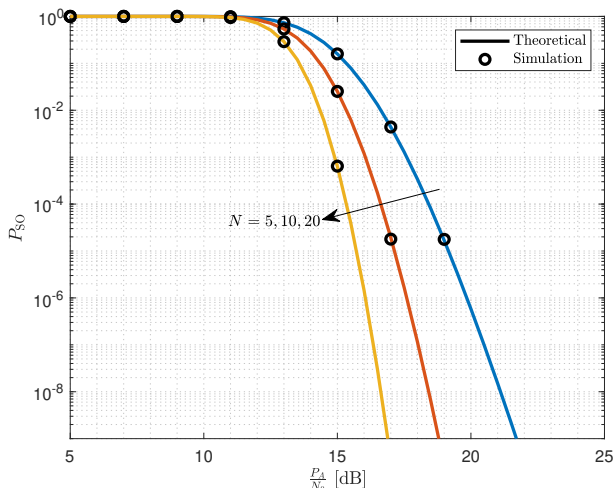


Fig. 2 SOP performance of the system under thin cirrus cloud formation for the ground level deployment and $N = 5, 10, 20$.

The SOP curves for $N = 10$ sites are illustrated in Fig. 3 for different deployment scenarios in the presence of thin cirrus cloud formation with $D_{B_k}^{\text{geo}} = 0.1$ km. It can be observed from the figure that the system performance is en-

hanced from ground level to mid-level deployment and from mid-level to high-level deployment. Therefore, it can be said that utilizing higher altitudes for sites improves the system performance. Notice here that the slopes of the curves are almost the same, and the system performance is improved in terms of power gain. This can be attributed to lower loss levels owing to high-level deployment and shorter link distance.

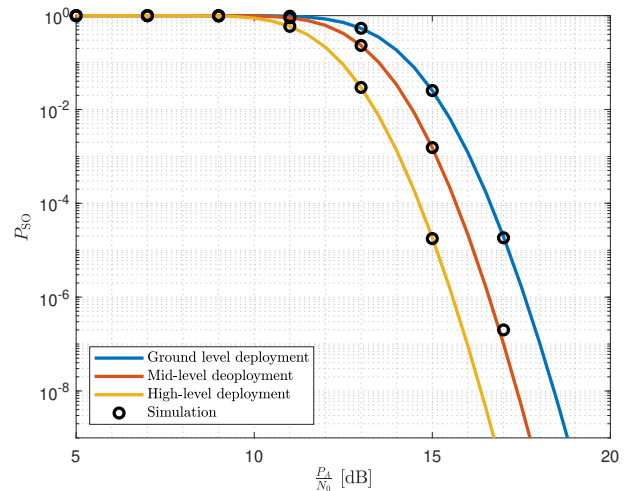


Fig. 3 SOP performance of the system under thin cirrus cloud formation for different deployment scenarios and $N = 10$.

In Fig. 4, the SOP performance is presented with respect to r_E for different deployment scenarios, fixed $P_A/N_0 = 15$ dB, and $N = 10$ number of sites. Here, thin cirrus cloud formation is considered with $D_{B_k}^{\text{geo}} = 0.1$ km. It can be inferred from the figure that deploying sites at higher altitudes significantly improves the system performance for lower values of r_E . However, for higher values of r_E , SOP dramatically increase. This can be explained by the fact that the eavesdropper receives very large fraction of the transmitter power and the legitimate sites receive very small fraction of the power. Thus, secure communication becomes infeasible for high values of r_E .

In Fig. 5, the SOP curves are illustrated for $N = 10$ number of sites with mid-level deployment under different atmospheric conditions. Here, thin cirrus cloud formation with $D_{B_k}^{\text{geo}} = 0.1$ km, thin fog with $D_{B_k}^{\text{geo}} = 1.01$ km, and normal polluted atmosphere with $D_{B_k}^{\text{geo}} = 3.04$ km are considered to examine the effects of various visibility levels. It can be deduced from the figure that for a SOP of 10^{-9} , atmospheric pollution results in ~ 2.5 dB SNR loss in system performance, whereas thin fog formation introduces ~ 9 dB SNR loss. Hence, it can be concluded that the system performance significantly affected by the atmospheric conditions.

SRT performance of the proposed system is presented in Fig. 6 for $N = 5$ and mid-level deployment scenario under non-polluted, normal polluted, and extremely polluted

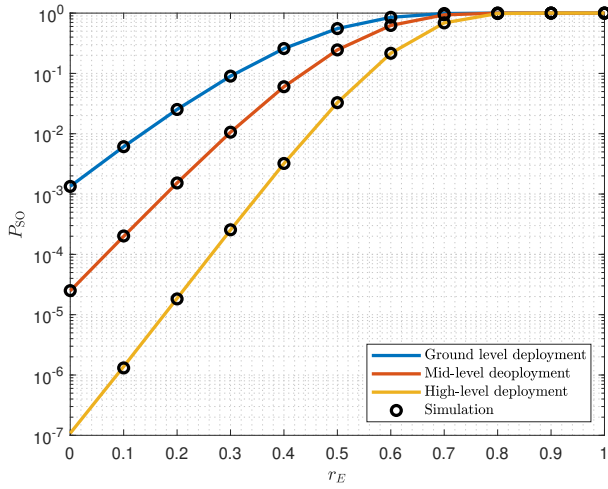


Fig. 4 SOP performance of the system with respect to r_E under thin cirrus cloud formation for $N = 10$ and $\frac{P_A}{N_0} = 15$ dB.

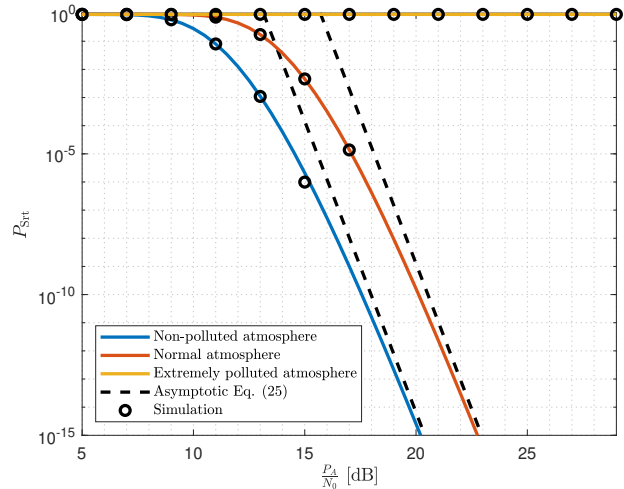


Fig. 6 Impact of pollution on SRT performance of the system for $N = 5$ and mid-level deployment scenario.

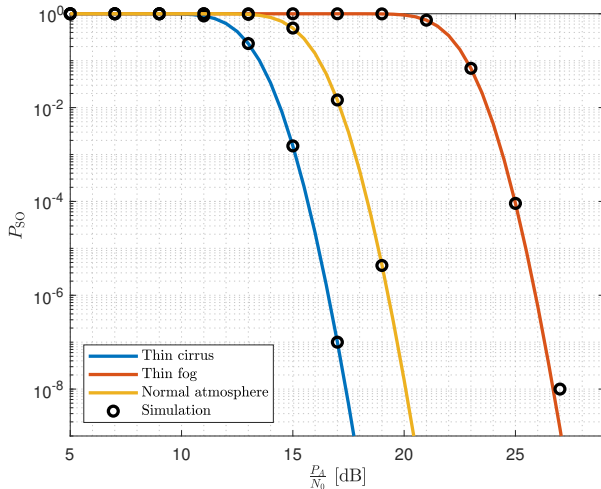


Fig. 5 SOP performance of the system under thin cirrus cloud formation, thin fog formation, normal polluted atmosphere for $N = 10$ and mid-level deployment.

atmospheric conditions all with $D_{B_k}^{\text{geo}} = 3.04$ km. It can be seen here that asymptotic curves perfectly depicts the system performance in high SNR region. Moreover, the figure reveals that different pollution regimes results in significant SNR loss in the system performance. Under extremely polluted atmosphere, reliable communication is not achievable with reasonable SNR values. Therefore it can be deduced that atmospheric pollution is critically important in SRT performance of the system.

In Fig. 7, SRT performance of the system is illustrated with respect to r_E for different deployment scenarios. Here, thin cirrus cloud formation with $D_{B_k}^{\text{geo}} = 0.1$ km, $N = 10$ sites, and $\frac{P_A}{N_0} = 15$ dB are considered. It can be deduced from the figure that deploying legitimate sites at higher altitudes

enhances the SRT performance of the system, similar to Fig. 4. Additionally, high values of r_E results in poor SRT performance, increasing up to probability of 1. This stems from the eavesdropper gathering most of the transmitted power, thus, secure communication between HAPS A and legitimate sites becomes infeasible.

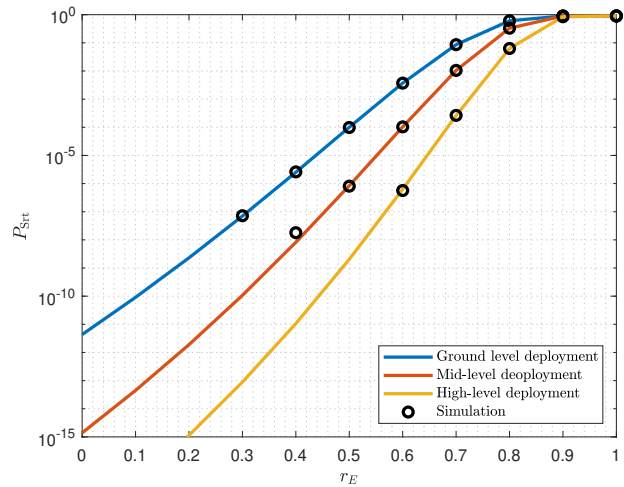


Fig. 7 SRT performance of the system with respect to r_E under thin cirrus cloud formation for $N = 10$ and $\frac{P_A}{N_0} = 15$ dB.

5 CONCLUSION

This study highlights the critical role that weather conditions play in the physical layer security of optical HAPS communications, particularly in the presence of an airborne eavesdropper. By evaluating the secrecy-reliability trade-off through interception and outage probabilities, we have demonstrated that adverse weather conditions, such as fog,

clouds, and air pollution, can severely degrade system performance. However, our results also show that strategically positioning ground stations at higher altitudes offers a viable solution to enhance overall secrecy. These insights provide valuable guidance for the design and deployment of secure non-terrestrial networks, emphasizing the need for careful consideration of environmental factors and system configuration in maintaining secure communications.

REFERENCES

- [1] F. J. Lopez-Martinez, G. Gomez, and J. M. Garrido-Balsells, "Physical-layer security in free-space optical communications," *IEEE Photonics Journal*, vol. 7, no. 2, pp. 1–14, 2015.
- [2] P. V. Trinh, A. Carrasco-Casado, A. T. Pham, and M. Toyoshima, "Secrecy analysis of FSO systems considering misalignments and eavesdropper's location," *IEEE Transactions on Communications*, vol. 68, no. 12, pp. 7810–7823, 2020.
- [3] K. Guo, K. An, Y. Huang, and B. Zhang, "Physical layer security of multiuser satellite communication systems with channel estimation error and multiple eavesdroppers," *IEEE Access*, vol. 7, pp. 96 253–96 262, 2019.
- [4] R. Chen, C. Li, S. Yan, R. Malaney, and J. Yuan, "Physical layer security for ultra-reliable and low-latency communications," *IEEE Wireless Communications*, vol. 26, no. 5, pp. 6–11, 2019.
- [5] M. J. Saber and S. M. S. Sadough, "On secure free-space optical communications over Málaga turbulence channels," *IEEE Wireless Communications Letters*, vol. 6, no. 2, pp. 274–277, 2017.
- [6] Y. Ai, A. Mathur, G. D. Verma, L. Kong, and M. Cheffena, "Comprehensive physical layer security analysis of FSO communications over Málaga channels," *IEEE Photonics Journal*, vol. 12, no. 6, pp. 1–17, 2020.
- [7] D. R. Pattanayak, V. K. Dwivedi, V. Karwal, I. S. Ansari, H. Lei, and M.-S. Alouini, "On the physical layer security of a decode and forward based mixed FSO/RF co-operative system," *IEEE Wireless Communications Letters*, vol. 9, no. 7, pp. 1031–1035, 2020.
- [8] X. Pan, H. Ran, G. Pan, Y. Xie, and J. Zhang, "On secrecy analysis of DF based dual hop mixed RF-FSO systems," *IEEE Access*, vol. 7, pp. 66 725–66 730, 2019.
- [9] S. Althunibat, S. C. Tokgoz, S. Yarkan, S. L. Miller, and K. A. Qaraqe, "Physical layer security of dual-hop hybrid FSO-mmWave systems," *IEEE Access*, vol. 11, pp. 58 209–58 227, 2023.
- [10] D. R. Pattanayak, V. K. Dwivedi, V. Karwal, P. K. Yadav, and G. Singh, "Physical layer security analysis of multi-hop hybrid RF/FSO system in presence of multiple eavesdroppers," *IEEE Photonics Journal*, vol. 14, no. 6, pp. 1–12, 2022.
- [11] M. Alzenad, M. Z. Shakir, H. Yanikomeroglu, and M.-S. Alouini, "FSO-based vertical backhaul/fronthaul framework for 5G+ wireless networks," *IEEE Communications Magazine*, vol. 56, no. 1, pp. 218–224, 2018.
- [12] Y. Zhang, J. Ye, G. Pan, and M.-S. Alouini, "Secrecy outage analysis for satellite-terrestrial downlink transmissions," *IEEE Wireless Communications Letters*, vol. 9, no. 10, pp. 1643–1647, 2020.
- [13] Y. Xiao, J. Liu, Y. Shen, X. Jiang, and N. Shiratori, "Secure communication in non-geostationary orbit satellite systems: A physical layer security perspective," *IEEE Access*, vol. 7, pp. 3371–3382, 2019.
- [14] W. Cao, Y. Zou, Z. Yang, *et al.*, "Secrecy outage analysis of relay-user pairing for secure hybrid satellite-terrestrial networks," *IEEE Transactions on Vehicular Technology*, vol. 71, no. 8, pp. 8906–8918, 2022.
- [15] X. Zhou, Q. Wu, S. Yan, F. Shu, and J. Li, "UAV-enabled secure communications: Joint trajectory and transmit power optimization," *IEEE Transactions on Vehicular Technology*, vol. 68, no. 4, pp. 4069–4073, 2019.
- [16] B. Ji, Y. Li, D. Cao, C. Li, S. Mumtaz, and D. Wang, "Secrecy performance analysis of UAV assisted relay transmission for cognitive network with energy harvesting," *IEEE Transactions on Vehicular Technology*, vol. 69, no. 7, pp. 7404–7415, 2020.
- [17] O. B. Yahia, E. Erdogan, G. K. Kurt, I. Altunbas, and H. Yanikomeroglu, "Optical satellite eavesdropping," *IEEE Transactions on Vehicular Technology*, vol. 71, no. 9, pp. 10 126–10 131, 2022.
- [18] E. Erdogan, O. B. Yahia, G. K. Kurt, and H. Yanikomeroglu, "Optical HAPS eavesdropping in vertical heterogeneous networks," *IEEE Open Journal of Vehicular Technology*, vol. 4, pp. 208–216, 2023.
- [19] V. Bankey, S. Sharma, S. R., and A. S. Madhukumar, "Physical layer security of HAPS-based space-air-ground-integrated network with hybrid FSO/RF communication," *IEEE Transactions on Aerospace and Electronic Systems*, vol. 59, no. 4, pp. 4680–4688, 2023.
- [20] E. Erdogan, I. Altunbas, G. K. Kurt, M. Bellemare, G. Lamontagne, and H. Yanikomeroglu, "Site diversity in downlink optical satellite networks through ground station selection," *IEEE Access*, vol. 9, pp. 31 179–31 190, 2021.

- [21] *Prediction Methods Required for the Design of Earth-Space Telecommunication Systems*, Rec. ITU-R P.1622, International Telecommunication Union, Geneva, Switzerland, 2003.
- [22] I. I. Kim, B. McArthur, and E. J. Korevaar, "Comparison of laser beam propagation at 785 nm and 1550 nm in fog and haze for optical wireless communications," vol. 4214, E. J. Korevaar, Ed., pp. 26–37, 2001.
- [23] M. S. Awan, E. Leitgeb, B. Hillbrand, F. Nadeem, M. Khan, *et al.*, "Cloud attenuations for free-space optical links," in *2009 International Workshop on Satellite and Space Communications*, IEEE, 2009, pp. 274–278.
- [24] O. B. Yahia, E. Erdogan, G. K. Kurt, I. Altunbas, and H. Yanikomeroglu, "Haps selection for hybrid RF/FSO satellite networks," *IEEE Transactions on Aerospace and Electronic Systems*, vol. 58, no. 4, pp. 2855–2867, 2022.
- [25] S. Sabetghadam and F. Ahmadi-Givi, "Relationship of extinction coefficient, air pollution, and meteorological parameters in an urban area during 2007 to 2009," *Environmental Science and Pollution Research*, vol. 21, pp. 538–547, 2014.
- [26] R. Barrios and F. Dios, "Exponentiated weibull distribution family under aperture averaging for Gaussian beam waves," *Opt. Express*, vol. 20, no. 12, pp. 13 055–13 064, Jun. 2012.
- [27] R. Barrios Porras, "Exponentiated Weibull fading channel model in free-space optical communications under atmospheric turbulence," Ph.D. dissertation, Dept. of Signal Theory and Commun., Univ. Politècnica de Catalunya, Barcelona, 2013.
- [28] L. C. Andrews and R. L. Phillips, *Laser Beam Propagation Through Random Media: Second Edition*, 2005.
- [29] E. Erdogan, I. Altunbas, G. K. Kurt, and H. Yanikomeroglu, "The secrecy comparison of RF and FSO eavesdropping attacks in mixed RF-FSO relay networks," *IEEE Photonics Journal*, vol. 14, no. 1, pp. 1–8, 2022.
- [30] W. M. R. Shakir, J. Charafeddine, H. Hamdan, I. A. Alshabeeb, N. G. Ali, and I. E. Abed, "Security-reliability tradeoff analysis for multiuser FSO communications over a generalized channel," *IEEE Access*, vol. 11, pp. 53 019–53 033, 2023.
- [31] *Impact of uplink transmission from fixed service using high altitude platform stations in the 27.5-28.35 GHz and 31-31.3 GHz bands on the Earth exploration-satellite service (passive) in the 31.3-31.8 GHz band*, Rec. ITU-R F.1570-2, International Telecommunication Union, Geneva, Switzerland, 2010.
- [32] M. Hess, P. Koepke, and I. Schult, "Optical properties of aerosols and clouds: The software package OPAC," *Bulletin of the American Meteorological Society*, vol. 79, no. 5, pp. 831–844, 1998.

Sustainable Communication in 5G/6G Wireless Sensor Networks: A Survey on Energy-Efficient Collaborative Routing

Muhammed Yasir Yılmaz¹ , Berk Üstüner¹ , Ömer Melih Gül² , Hakan Ali Çırpan¹ 

¹ Department of Electronics and Communication Engineering, Istanbul Technical University, Istanbul, 34469, Turkey

² Informatics Institute, Istanbul Technical University, Istanbul, 34469, Turkey

Abstract: Wireless sensor networks (WSNs) play an important role in modern communication systems with the advances in 5G/6G technologies. These networks have a wide range of applications, from smart cities to industrial automation, from environmental monitoring systems to healthcare applications. However, since sensor nodes have limited energy resources, energy efficiency remains a critical issue for the sustainability of these networks. Low-power routing protocols are needed to ensure the long lifespan and efficient operation of sensor nodes. This study comprehensively studies cooperative energy-efficient routing protocols designed to achieve sustainability in WSNs. First of all, the basic principles of cooperative routing methods are discussed and approaches to optimize data transmission between nodes are reviewed. Then, different energy-efficient routing protocols are compared and the pros and cons of hierarchical, planar and location-based protocols are analyzed. It is shown that by integrating artificial intelligence (AI) and machine learning (ML) techniques into routing protocols, it is possible to dynamically optimize node selection processes and extend the network lifetime. This survey summarizes the current status of energy-efficient routing protocols, discusses the challenges encountered and suggests potential directions for future research.

Keywords: Wireless sensor networks, energy efficiency, routing protocols, 5G/6G, artificial intelligence.

5G/6G Kablosuz Sensör Ağlarında Sürdürülebilir Haberleşme: Enerji Verimli İşbirliğine Dayalı Rotalama Üzerine Literatür Taraması

Özet: Kablosuz sensör ağları (KSA'lar), 5G/6G teknolojilerindeki gelişmelerle birlikte yeni iletişim sistemlerinde önemli bir rol oynamaktadır. Bu ağlar, akıllı şehirlerden endüstriyel otomasyona, çevre izleme sistemlerinden sağlık uygulamalarına kadar geniş bir uygulama yelpazesine sahiptir. Ancak, sensör düğümlerinin sınırlı enerji kaynaklarına sahip olması nedeniyle, enerji verimliliği bu ağların sürdürülebilirliği için kritik bir konu olmaya devam etmektedir. Sensör düğümlerinin uzun ömürlü ve verimli çalışmasını sağlamak için düşük güçlü yönlendirme protokollerine ihtiyaç vardır. Bu çalışma, KSA'larda sürdürülebilirliği sağlamak için tasarlanmış işbirlikçi enerji verimli yönlendirme protokollerini incelemektedir. Her şeyden önce, işbirlikçi yönlendirme yöntemlerinin temel prensipleri tartışılmakta ve düğümler arasında veri iletimini optimize etme yaklaşımları incelenmektedir. Ardından, farklı enerji verimli yönlendirme protokolleri karşılaştırılmakta ve hiyerarşik, düzlemsel ve konum tabanlı protokollerin artıları ve eksileri analiz edilmektedir. Yapay zeka ve makine öğrenimi tekniklerinin yönlendirme protokollerine entegre edilmesiyle, düğüm seçim süreçlerinin dinamik olarak optimize edilmesinin ve ağ ömrünün uzatılmasının mümkün olduğu gösterilmektedir. Bu literatür taraması, enerji açısından verimli yönlendirme protokollerinin mevcut durumu özetlenmiş, karşılaşılan zorluklar tartışılmış ve gelecekteki araştırmalar için olası yönler önermiştir.

Anahtar Kelimeler: Kablosuz sensör ağları, enerji verimliliği, yönlendirme protokolleri, 5G/6G, yapay zeka.

REVIEW PAPER

Corresponding Author: Ömer Melih Gül, omgul@itu.edu.tr

Reference: M. Y. Yılmaz, B. Üstüner, Ö.M. Gül, and H. A. Çırpan, (2025), "Sustainable Communication in 5G/6G Wireless Sensor Networks: A Survey on Energy-Efficient Collaborative Routing," *ITU-Journ. Wireless Comm. Cyber.*, 2, (1) 11–26.

Submission Date: Feb, 13, 2025

Acceptance Date: Mar, 17, 2025

Online Publishing: Mar, 28, 2025

1 INTRODUCTION

WSNs have become an essential element in modern communication systems, especially in applications such as environmental monitoring, healthcare, smart cities, and industrial automation. With the advances in 5G and 6G networks, WSNs can do more by offering very reliable communication, low latency, and fast data transfer rates. However, energy efficiency remains one of the key challenges in ensuring the sustainability of WSNs, especially considering the limited resources and energy resources of sensor nodes and their typical deployment in inaccessible locations. Efficient utilization of energy is important to extend the network lifetime, but is also essential to maintain the reliability of the communication infrastructure. Thus, the study of energy efficiency and sustainability has been a major challenge for WSNs. Routing protocols have received considerable attention in recent research [1], [2]. The introduction of collaborative tracking of targets and connections in modern networks exacerbates the energy efficiency problem in WSNs.

Walid Demiga and others [3] have highlighted the importance of collaborative target tracking to reduce redundant probes and optimize communication between nodes to minimize energy consumption. In this context, cooperation between sensor nodes ensure that only the necessary information is available to all nodes participating in the probe and communication process, significantly increasing the network lifetime. Similarly, energy-efficient communication methods, e.g., as discussed by Igor Stanoev et al. [4], the impact of teamwork on improving reliability and reducing energy consumption while communicating, such as the optimized Hybrid Automatic Repeat Request (HARQ) protocol. Efforts towards building collaborative intelligent environments provide a significant positive impact on the sustainable design of WSNs. By leveraging the outcomes of the Internet of Things (IoT) and artificial intelligence (AI), these environments are developing systems that save energy, reduce costs and improve user comfort and safety. According to the work in [5], the interconnected intelligent devices of a Collaborative Smart Environment (CSE) manage their energy consumption more efficiently. This approach, combining different technologies, leads to integrated energy management solutions to improve everyday life.

To improve the energy efficiency of WSNs, many energy-efficient routing protocols have been proposed. T.M. Behera et al. [6] provide a review of various hierarchical clustering protocols, such as the Low Energy Adaptive Clustering Hierarchy (LEACH), and their variations for optimizing energy usage in WSNs. The LEACH protocol, which organizes the sensor nodes into clusters with cluster heads, reduces direct communication to the base station (BS). Different modifications of LEACH, such as LEACHC (LEACH Central) and LEACH-DCS (Deterministic Cluster Selec-

tion), have been developed to further optimize the selection of cluster heads based on residual energy and leads to more balanced clusters and networks with increased lifetimes [7]. Other approaches discussed in [8], focus on reducing energy waste through traffic distribution techniques to ensure optimized energy consumption across the network. C. Nakas et al. [9] provides a review of energy-efficient routing protocols for wireless sensor networks and classify them into hierarchical and location-based categories. Each type has its own advantages and disadvantages in terms of energy-efficient savings. Hierarchical routing is notable for reducing duplicate data transmissions and increasing network lifetime by collecting data at the cluster head before transmitting it to the BS. H. L. Gururaj et al. [10] proposed an energy-efficient routing protocol for 5G/6G WSNs that uses RL to improve cluster head selection and the data routing. RL-based methods select nodes with more remaining energy and adjust the routing path based on the current state. This brings sustainable communication in WSNs.

The literature offers a fascinating perspective on the use of autonomous robots for data collection in terrestrial WSNs. By lowering the energy consumption of cluster heads and UAV robots, several research suggested mobile sinks for gathering data from clustered networks [11]–[15]. The work in [16] considers a similar data collection problem by considering underwater communication challenges via an autonomous underwater vehicle (AUV). The underwater system is more costly than terrestrial wireless sensors, although autonomous robots help decrease the energy cost of sensor equipment. The papers [17]–[19] tackle scheduling problem for data collection in single-hop energy harvesting WSN by considering throughput and fairness.

The work [20] suggested a cluster head selection approach for energy-sensitive routing issues in UASNs and examined the impact of predicted available energy on cluster head selection while considering stochastic energy harvesting methods of individual sensors. The paper addresses the same problem and suggests a new reinforcement learning-based approach to identify cluster heads (CHs) that takes into account estimated collected energy as well as the locations and remaining energy of the sensor nodes [1]. Energy harvesting awareness makes underwater sensors last longer. This is shown by numerical results that show our proposed method greatly increases the amount of energy collected, which in turn extends the network's useful life.

Mobility and heterogeneous networks (HetNets) brings extra problems to energy-efficient routing. When you mix macro and small cells in HetNets, you get more handoffs, more signaling overhead, and different types of nodes need more energy. Gures et al. [21] describes mobility handling problems in 5G HetNets, including frequent handover failures, the ping-pong effect, and increased energy usage due

to redundant signaling. Addressing these issues requires advanced mobility management techniques such as beam-level mobility, dual connectivity, and mobility resilience optimization (MRO). These approaches help WSNs to maintain reliable communication without wasting energy. The study of Wang in [22] shows that how mobility affects coverage and energy consumption in WSNs.

AI techniques can improve energy efficiency of WSNs. AI-driven approaches introduced by Parag Biswas et al. [23] include reinforcement learning, genetic algorithms, and neural networks to decrease power consumption for sustainable communication and enable dynamic decision-making that adapts routing and energy management strategies according to real-time network conditions. Pasqualetto in [24] have demonstrated the value of multi-agent systems (MAS) in building smart energy management systems that can process big amount of data from various sensors and devices, optimizing energy usage in the network and the role of MAS and big data is also discussed.

While energy efficiency is considered for WSNs, security should also be considered for sensors. Sensor nodes, often deployed in open environments and susceptible to attacks, make security a critical factor in WSNs. However, traditional security methods such as encryption spend a lot of energy, which poses a problem considering the limited resources of WSNs. M. Mahamat et al. [25] review recent energy-aware security approaches that balance strong protection with low energy consumption. For example, context-aware security avoids unnecessary energy consumption by adjusting protection levels according to the current environment and threat level. M. Biradar and B. Mathapathi [20] describe a trust-based routing protocol that increases security while keeping energy consumption low. These protocols create link between nodes and save energy. New research looks into how metaheuristic and biologically inspired algorithms can be used to make routing in wireless sensor networks more energy-efficient. R. Priyadarshi [26] reviews techniques such as particle swarm optimization (PSO), artificial bee colony (ABC) and artificial bee colony optimization (ACO). Natural behaviors, like the flight of bees or foraging ants, inspire these algorithms to determine energy-efficient routes. An approach combining PSO and ACO shows the potential to increase the strengths of algorithms to improve data collection and extend network lifetime.

In conclusion, making 5G and 6G WSNs more energy efficient requires a mix of collaborative routing, mobility management, AI-assisted optimization, and security issues that are aware of energy use. This paper looks at previous research that has been done on energy-efficient routing protocols, collaborative techniques to lower energy use, the effects of mobility and heterogeneous networks, optimizing AI/ML techniques for energy use, and systems that are limited by energy. Covering these areas summarizes current achievements.

1.1 Main Contributions of the Paper

The main contributions of this paper is summarized below:

- This paper provides an overview of collaborative energy-efficient routing protocols designed for 5G/6G WSNs. It categorizes different routing approaches, including hierarchical, planar, and location-based protocols, and compares their advantages and disadvantages.
- We discuss the impact of mobility management and heterogeneous network structures on energy efficiency, focusing on beam-level mobility and handover optimization.
- The study includes how AI algorithms like reinforcement learning, genetic algorithms, and neural networks, can be integrated into routing protocols to optimize node selection and extend the overall lifetime of the network.
- The paper highlights the security concerns in low-power WSNs, evaluating lightweight encryption, trust-based routing and AI-based approaches to ensure secure and efficient communication.
- This survey brings potential future research directions, emphasizing AI-based routing, mobility management, and sustainable communication solutions for 5G/6G WSNs.
- Instead of diving too deep into details, this survey gives a general idea about the problem and fundamental concepts to deal with it, thus providing a basis for further advancements and new solutions.

1.2 Organization of the Paper

We organize the rest of the paper as follows. Section 2 presents energy-efficient protocols in 5G/6G WSNs. Section 3 presents collaborative approaches for energy-efficient routing. Section 4 exhibits impact of mobility and heterogeneous networks. Section 5 introduces AI/ML-based techniques in energy-efficient routing. Section 6 provides security challenges in energy-efficient routing. Section 7 concludes the paper.

2 PROTOCOLS FOR ENERGY EFFICIENCY IN 5G/6G WSNs

Energy-saving routing protocols are important for wireless sensor networks, especially for advanced systems such as 5G and 6G. WSN nodes have limited battery power, so using energy wisely ensures that the network operates efficiently for a long time. Figure 1 presents an example model of a clustered WSN. This section focuses on the various protocols developed to conserve energy, how they work,

and how they can be adapted to the needs of 5G/6G networks. Misra et al. shows that multimedia streaming in WSNs introduces unique challenges in terms of energy-efficient data transmission and real-time communication [27].

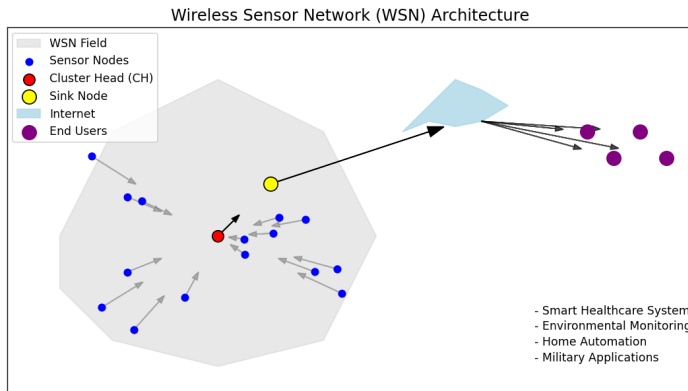


Fig. 1 WSN architecture showing sensor nodes, cluster head, sink node, and data flow to end users for various applications.

Behera et al. [6] also discussed the LEACH protocol in WSNs. LEACH divides sensor nodes into clusters, and cluster heads (CHs) manage the communication within these clusters. This arrangement reduces the number of nodes that transmit data directly to the master station, thus saving energy. However, LEACH's method of randomly selecting CHs are not that efficient. Selecting a low-energy node as a CH quickly exhausts it, leading to a short network lifetime. To solve this problem, LEACH-C (Central LEACH) is used. LEACH-C selects CHs by a centralized system depending on the remaining energy of the nodes. This creates a more balanced cluster and increases the network lifetime, but requires additional infrastructure such as GPS, which increases energy consumption [8], [28]. The another paper deeply reviews clustering protocols in WSNs, analyzing existing classifications, problems encountered and future research directions [29]. Hosseinzadeh et al. propose cluster based trusted routing method in WSNs using Fire Hawk Optimizer (FHO) for better security and efficiency [30]. They show this method improves network performance by optimizing energy in sensor nodes. Also, the study by Hegde et al. shows that the Improved Grey Wolf Optimization (IGWO)-based LEACH protocol significantly enhances network lifetime in Wireless Sensor Networks (WSNs) compared to traditional LEACH and GWO-based methods. Their findings indicate that IGWO optimizes cluster head selection by considering factors such as energy balance and intra-cluster distance and helps to substantially improve the number of operational rounds and energy efficiency in both small- and large-scale WSN deployments [31].

Behera and his team also mention another variation called LEACH-DCS (Deterministic Cluster Selection). This method optimizes the CH selection process by considering whether the node was a CH before and its current energy level. Therefore, high energy sensors are selected as CHs, resulting in a more balanced energy distribution. The authors also consider a distributed LEACH method with solar power. This method uses solar-powered nodes as CHs, thereby reducing the energy consumption of battery-powered nodes.

This approach has been successful in extending the network lifetime, especially in outdoor areas with sufficient sunlight. However, it depends on the environmental conditions [6]. They also highlight the use of multi-hop LEACH. In this method, CHs do not send data directly to the BS, but through intermediate nodes. This method is especially important for large-scale WSNs, as it extends the network lifetime by reducing the energy load in long-distance transmissions [6].

Schurgers and Srivastava [8] focus on local methods and traffic distribution techniques to save energy usage in WSNs. The paper propose to combine data from closer sensor nodes before sending it to the master station. This reduces the amount of data transmitted and saving energy amount. Instead of using fixed cluster heads, they use Data Convergence Units (DCEs) for processing the data locally. If there is a failure, these DCEs quickly adapt, making the system more reliable and energy efficient. They also propose to prevent a single node from running out of power by distributing traffic across the network. Methods such as Gradient-Based Routing (GBR) send data through the path with the largest gradient difference for balancing energy usage and extend the lifetime of the network [8].

Another method focuses on choosing nodes with more energy for routing, which avoids putting too much work on weaker nodes and helps save energy [8], [32]. Nakas, Kandris, and Visvardis [9] provide a detailed review of energy-efficient routing protocols in WSNs, dividing them into four categories: Flat, Hierarchical, Location-Based, and QoS-Based protocols. They emphasize the importance of hierarchical protocols like LEACH and its improved versions for saving energy. These protocols group nodes into clusters, with one node acting as the cluster head (CH) to collect and send data. Upgraded versions like LEACH-C and LEACH-M improve CH selection by considering how much energy each node has left, helping to spread energy use more evenly across the network. The survey also looks at location-based protocols, such as Geographic Adaptive Fidelity (GAF) and Greedy Perimeter Stateless Routing (GPSR), which use location data for better routing. For example, GAF divides the network into grids and activates only one node in each grid to save energy while keeping good coverage. QoS-based protocols, like Sequential Assignment Routing (SAR), are designed to balance

energy saving with network performance. SAR chooses paths based on QoS needs, such as delay limits and packet loss rates, making it useful for critical tasks where reliability is important [9]. Table 1 presents a brief comparison of location-based topology protocols in terms of their advantages, disadvantages, scalability, mobility, routing, robustness.

Gururaj et al. [10] have a new idea for how to send data in 5G and 6G sensor networks. They call it CEERP (Collaborative Energy-Efficient Routing Protocol). It uses a type of machine learning, reinforcement learning, to make groups of sensors, or clusters, change as needed. A key part is how it picks the leaders of these groups, the cluster heads. It looks at how much power each sensor has left. This helps spread out the work and keeps any one sensor from running out of power too soon. This makes the whole network last longer. They also use something called MOISA (Multi-Objective Improved Seagull Algorithm). This helps make the network even better by saving energy, sending data faster, and just making the whole process more efficient. By considering multiple objectives simultaneously, MOISA ensures efficient energy management in complex 5G/6G scenarios where high data rates and reduced latency are essential. The authors demonstrate that CEERP significantly outperforms traditional protocols in terms of energy consumption, throughput, and network longevity, with a 50% reduction in energy consumption compared to conventional methods. This collaborative and adaptive approach makes CEERP particularly suitable for 5G/6G WSNs, which require scalable and energy-efficient solutions for sustainable communication [10].

Eriş et al. [47], [48] introduce a new medium access policy for underwater sensor networks that uses reinforcement learning (RL) within the Time Division Multiple Access (TDMA) system to improve energy efficiency. They focus on solving the energy challenges in underwater environments, where high energy use is caused by acoustic communication and environmental noise. Their proposed method uses a cooperative multi-agent RL algorithm that allows nodes to assign TDMA time slots on their own based on energy harvesting opportunities. The work in [49], [50] also considers a similar problem and proposed a novel reinforcement learning based routing algorithm for energy management in networks.

This reduces wasted energy and helps the network last longer. The method also uses multi-armed bandit modeling to help nodes learn the best times to transmit data, making better use of the energy they collect. Simulations show big improvements in metrics like half node dead (HND) and last node dead (LND), meaning the nodes stay active much longer than with older scheduling methods. Additionally, piezoelectric energy harvesting is used to capture mechanical energy from water flow, providing a sustainable energy source and making the network more resilient to underwa-

ter challenges. The study concludes that combining energy harvesting with RL-based TDMA scheduling is a promising way to boost energy efficiency and communication reliability in underwater sensor networks [48]. Yari et al. studies the energy-efficient routing algorithm using sensors to increase longevity by adjusting sensor positions dynamically and optimizing data paths to reduce energy consumption in WSNs [51].

5G networks are expected to achieve significant efficiency improvements, with a goal of improving spectrum efficiency by 90/100 compared to 4G, while future 6G systems are designed to operate at lower power consumption while supporting land, air, and sea connections. A key aspect of this transition is the integration of AI/ML algorithms for intelligent resource management, enabling dynamic adjustments to transmission power, network topology, and service configuration. AI-based technologies such as adaptive beamforming and deep reinforcement learning will enable BS and radio access networks (RAN) for optimized power allocation based on real-time traffic demand, then reducing unnecessary energy consumption [52].

Energy harvesting is another key for achieving energy efficiency in 6G networks. Unlike 5G, which focuses on optimizing power management, 6G aims to integrate renewable energy sources, such as solar and ambient RF energy harvesting into powering the network. This will reduce reliance on traditional carbon-based power grids and align with global sustainable development goals. In addition, ultra-low power communication strategies such as device-to-device (D2D) networks and non-orthogonal multiple access (NOMA) are expected to minimize energy consumption at the user end by enabling localized data exchange and spectrum reuse rather than relying on centralized, power-hungry infrastructure [52].

In addition, 3GPP has defined a set of key performance indicators (KPIs) for mobile network energy efficiency, focusing on reducing the power consumption of core network components while maintaining better high data rates and low latency. These include database sleep mode optimization, adaptive bandwidth allocation, and intelligent scheduling mechanisms that allow mobile devices and network nodes to enter low-power states during inactivity. 6G is expected to be 10 times more energy efficient than 5G while providing higher spectral efficiency, lower power consumption per bit, and sustainable network operation [52].

Mobile Ad Hoc Networks (MANETs) are dynamic, infrastructure-less wireless networks in which nodes function as both hosts and routers, necessitating efficient routing protocols to manage communication and variations in network topology. Roy et al. conducted a performance comparison of leading MANET routing protocols, specifically AODV (Ad Hoc On-Demand Distance Vector), DSR (Dynamic Source Routing), and DSDV (Destination-Sequenced Distance Vector), based on three key perfor-

Table 1 A Synopsis of Location-Based Topology Protocols

Protocol	Advantages	Disadvantages	Scalability	Mobility	Routing	Robustness
GEAR [33]	It balances energy ingestion and extends network lifetime. It efficiently routes messages	The periodic table exchanges increase overhead.	Good	Limited	The best route is selected.	Good
GEM [34]	and offers void and obstacle tolerance. It has fault tolerance and reduced end-to-end latency.	It overloads low-level nodes.	Good	Limited	The shortest route is selected.	Low
IGF [35]	It has uniform energy dissipation.	It depends on the up-to-date local neighbor table.	Good	Limited	The best route is used.	Good
SELAR [36]	It is easy to apply and offers lower path and hop stretch.	It does not work well with nodes with holes.	Good	Limited	The highest residual power route.	Good
GDSTR [37]	It has uniformity of energy consumption.	It suffers from the local dead-end problem.	Good	Limited	The shortest route is used.	Low
MERR [38]	It offers superior energy saving and handles void.	It wastes energy when nodes are close.	Limited	Limited	The minimum energy ingestion route is used.	Low
OCF [39]	It manages low overhead of routing.	It depends on the up-to-date local neighbor tables.	Good	Limited	The best route is used.	Good
PAGER-M [40]	It has reduced end-to-end delay.	It is stateless location-based.	Good	Limited	The shortest route using the greedy algorithm is used.	Low
HGR [41]	Fault tolerance is established.	The reduced delay is not guaranteed.	Good	Limited	The minimum energy ingestion route is used.	Good
MECN [42]	Both link maintenance cost and number of hops are reduced.	The link maintenance consumes energy.	Good	Limited	The optimal route in a sparse graph is used.	Good
SMECN [43]	Network lifetime is extended.	High amount of edges increases overhead.	Low	Limited	The optimal route in a sparse graph is used.	Good
GAF [44]	Redundant data are reduced.	Nodes neither aggregate nor merge data.	Low	Limited	The least cost route within the virtual grid is used.	Low
PASC ACO [45]	It avoids the energy hole problem and extends network lifetime.	Energy holes are more evident.	Good	Limited	The highest residual energy route.	Good
PASC-AR [46]		GPS increases energy consumption.	None	Limited	The optimal path by using ACO is used.	Low

mance metrics: average end-to-end delay (EED), packet delivery fraction (PDR), and throughput. Their findings revealed that AODV is better than DSR and DSDV regarding end-to-end delay, as AODV employs a hop-by-hop mechanism that reduces buffering delays. Consequently, DSDV demonstrated the highest packet delivery fraction (PDR) due to its proactive routing characteristics, making it more reliable in stable environments. Although DSR is effective under controlled network conditions, it exhibited fluctuations in throughput due to route caching mechanisms that occasionally led to stale routes, impacting performance. The study underscored that reactive protocols (AODV, DSR) are more suitable for dynamic network environments, whereas proactive protocols (DSDV) provide improved packet delivery in static scenarios. The authors concluded that no single routing protocol is optimal for all network conditions, and future research should explore hybrid and AI-enhanced routing strategies to enhance efficiency across various network scenarios [53].

In conclusion, the protocols discussed in this section investigate the importance of energy-efficient routing in WSNs, particularly for advanced 5G/6G environments. LEACH and its variants, reinforcement learning-based approaches like CEERP, and localized strategies such as GBR and TDMA with RL all contribute to enhancing energy efficiency and extending the operational lifetime of sensor networks. These protocols emphasize the need for adaptive, scalable, and sustainable solutions to meet the growing demands of next-generation communication systems, where energy efficiency remains a critical concern.

3 COLLABORATIVE APPROACHES FOR ENERGY EFFICIENCY ROUTING

Energy-efficient routing allows nodes in WSNs to cooperate and reduce energy consumption. This cooperation is especially important in 5G/6G systems to ensure that the network operates longer and more efficiently. Research has shown how nodes can perform better sensing and communication with less energy consumption. Thanks to these methods, the network's lifetime is increased and its efficiency is improved.

Demigha et al. [3] studied cooperative target-tracking techniques used to improve the energy efficiency of WSNs. Researchers classify these techniques into two main groups: perception-related methods and communication-related methods. These methods reduce unnecessary operations and allow the network to operate for a longer period of time. A representative cooperative method is the predictive model. In this method, nodes predict the future position of the target and activate only the necessary nodes. Thus, unnecessary data collection and data transfer are prevented, resulting in energy savings. Also, the sensor selection problem (SSP), which is part of this method, focuses on determining which nodes will work to obtain

the best tracking results with the least energy consumption. This technique is an effective way to save energy in WSNs by maintaining tracking accuracy while reducing energy usage. Sabakrou et al. proposes that intelligent distributed sensor activation algorithms optimize the energy usage while maintaining high tracking accuracy in WSNs [54]. Zhang et al. investigated sensor collaboration for parameter tracking using energy harvesting sensors [55]. They show optimal collaboration improve tracking accuracy and energy efficiency in wireless sensor networks.

Demigha et al. [3] state that self-organizing systems are also important for energy saving. There are two common methods: cluster-based and tree-based. In cluster-based methods, the sensors are divided into groups, and each group has a cluster head. The cluster head organizes the groups in real-time based on the target location and activates only the nodes that is required [56]. The other nodes go into sleep mode for saving energy. In tree-based methods, nodes form a hierarchical structure and only the nodes that are best suited to track the target are activated while the others remain in sleep mode. Figure 2 exhibits target tracking process in a WSN, showing active nodes, detecting nodes, estimated target positions, and the predicted path [3].

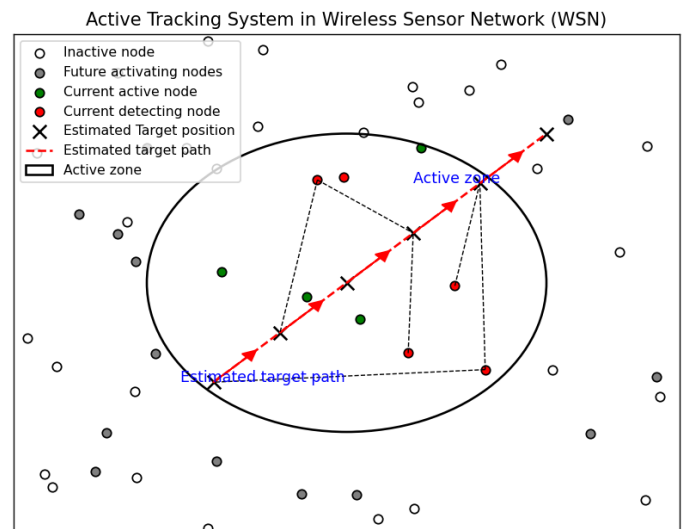


Fig. 2 Target tracking process in a sensor network, showing active nodes, detecting nodes, estimated target positions, and the predicted path [3].

In addition, interoperability of sensing and communication systems is very important for energy saving. Instead of sending raw data from all nodes, the system combines data from the nodes and sends only the processed and important information. This method reduces communication, prevents unnecessary energy consumption, and makes the network work more efficiently. These teamwork methods

allow the system to save a lot of energy while still tracking targets effectively. In Javapdour et al., it is stated that integrating MAC layer techniques with active nodes can increase the target tracking accuracy and energy efficiency in WSNs [3], [57].

The work by Stanojev et al. [4] extends the discussion on collaborative energy-saving techniques by exploring the use of Hybrid Automatic Repeat reQuest (HARQ) protocols. The study compares the energy efficiency of non-collaborative and collaborative HARQ versions. The authors evaluate three types of HARQ protocols—HARQ Type I (HARQ-TI), Chase Combining (HARQ-CC), and Incremental Redundancy (HARQ-IR)—and analyze the impact of using a relay for retransmissions. In collaborative HARQ settings, energy consumption is reduced by involving a relay, which improves communication reliability while balancing the energy load across the network. The relay helps retransmit data, thereby decreasing the number of retransmissions needed by the source and destination nodes, which directly impacts the energy used in communication. However, the authors note that while collaborative HARQ can save energy over long distances, it is not always advantageous in scenarios where circuitry energy dominates the total energy budget. This is particularly evident in cases where transmission distances are short, and the energy cost of activating additional circuitry (such as relays) outweighs the benefits of reduced transmission power. This highlights the need for a balanced approach when choosing collaborative techniques for energy efficiency, ensuring that the energy costs of both transmission and circuitry are considered. It is stated that energy-harvesting sensors enable optimal sensor collaboration for tracking parameters and extending network lifetime while ensuring data reliability [4], [55], [58].

Felicetti et al. [5] propose a collaborative model that extends the idea of energy efficiency to residential environments through Collaborative Smart Environments (CSEs). The authors introduce a Home Energy Management System (HEMS) as a central control unit to manage energy consumption by smart devices within a household. The proposed model leverages recent advances in the Internet of Things (IoT) and Information and Communication Technologies (ICT) to enable effective communication between different smart devices within a home. The centralized control unit (CCU) collects data from sensors, smart plugs, and other devices, ensuring that energy use is optimized through real-time monitoring and control. By managing energy supply, demand, and appliance use collaboratively, the system can reduce energy consumption while maintaining user comfort and cost efficiency. The smart plugs and smart boxes in the CSE architecture allow existing appliances to become part of the energy management system, providing additional intelligence and connectivity that enable these appliances to adapt to real-time energy

demand and supply conditions [48], [59].

The paper talks about how important it is for smart devices to work well together in smart environments. One big problem in making a Collaborative Smart Environment (CSE) is making sure all devices can connect and work without issues. The system suggested in the paper uses smart plugs and a "smart box" to help regular home appliances talk to a central control unit (CCU). This setup helps the system control energy better, like using stored energy or shared energy systems. It also changes energy use in real time to match what users need and how much energy is available, making the system more efficient.

Felicetti et al. [5] talk about how predicting energy use can help save power. They explain a method that looks at past energy usage to find patterns and predict future needs. This helps the system decide the best time to run appliances or charge local energy storage. With tools like machine learning and simple math models, the central control unit (CCU) can guess how much energy is needed and control devices to use power better. This way, energy is saved while still keeping everything running smoothly and making sure users are comfortable [5].

To sum up, prediction-based schemes, self-organization, collaborative HARQ protocols, and home energy management are some collaborative energy-efficient techniques that show a lot of promise for lowering energy use in WSNs and smart environments. These methods focus on intelligent coordination between network nodes and devices to conserve energy while meeting performance requirements. Prediction based schemes and adaptive clustering help in optimizing the activation of nodes, thereby conserving energy in target tracking.

Collaborative HARQ protocols enhance communication reliability while managing energy costs effectively. Home energy management systems in smart environments use advances in ICT and IoT to dynamically manage energy consumption and optimize household energy use. Together, these techniques represent a promising approach to tackling the challenge of energy efficiency in next-generation communication networks and smart systems.

4 IMPACT OF MOBILITY AND HETEROGENEOUS NETWORKS

Understanding the effects of mobility and heterogeneous networks is key to developing future communication systems that are both energy-efficient and reliable, especially for advanced WSNs and 5G/6G networks.

As more heterogeneous network designs are introduced, combining macro and small cells, new challenges arise in managing mobility while maintaining good performance. This section reviews how mobility and heterogeneity affect network performance, focusing on the difficulties of mobility management, energy use, and maintaining reliable handovers. The study by Gures et al. [21] provides an

extensive analysis of mobility management in 5G heterogeneous networks (HetNets), emphasizing the complexity brought on by the deployment of a large number of small cells alongside macro cells. These HetNets offer higher capacity and enhanced coverage, but at the cost of frequent handovers (HOs), leading to issues like HO failures (HOFs), ping-pong HOs, and increased energy consumption. These challenges have a significant impact on user experience, with frequent HOs leading to increased power consumption and reduced battery life for user equipment (UE). To address these challenges, 5G mobility management includes mechanisms such as beam-level mobility and beam management, which allow for more stable connections between UE and BS. Beam-level mobility enables dynamic routing of transmission to maintain connectivity with moving devices, especially in 5G/6G WSNs. Beam-level management helps reduce unnecessary HOs by maintaining directional links to the UE, even as it moves between cells [21].

Gures et al. talk about network slicing as an important part of handling mobility in networks. Network slicing enables a physical network to be divided into virtual network slices with different services, each of which is provided with customized resources and services. It lets many virtual networks run on the same physical system, giving different services based on what is needed. For example, IoT devices and machine-to-machine (M2M) systems can have their own slices with mobility settings that match their needs. IoT devices, which can handle short breaks in connection, are treated differently than services like IP telephony, which need a stable connection all the time. The paper also explains handover methods like XN-based and N2-based handovers, which help reduce connection breaks and keep communication smooth. These methods are very important in crowded HetNet setups where handovers happen often. By avoiding interruptions, they make sure users have a good experience [21].

Managing mobility in HetNets comes with challenges in paging and registration processes, which need to balance saving power and keeping delays low. The 5G Radio Resource Control (RRC) Inactive state is a helpful solution to this problem. This state works as a middle ground between the RRC Idle and Connected states, lowering both delay and energy use by keeping the user equipment (UE) context. This means the device can reactivate quickly without needing a full reconfiguration. This improvement makes handling frequent handovers more efficient, reducing signaling and saving energy, which helps optimize mobility management in HetNets [21].

In their study, Wang et al. [22] explore the impact of mobility and heterogeneity on coverage and energy consumption in WSNs, providing insights into how these factors influence network performance. The authors analyze different sensor deployment schemes, such as uniform deployment and Poisson deployment, to understand their effects on

coverage and energy use. In uniform deployment, sensors are placed randomly and uniformly across the operational area, while Poisson deployment uses a 2-dimensional Poisson point process to model sensor placement. The authors focus on blanket coverage (full coverage of an area) and k -coverage (where each point is covered by at least k sensors), both of which are essential for ensuring network reliability in applications such as environmental monitoring and surveillance [22].

A significant concept introduced by Wang et al. is the equivalent sensing radius (ESR), which is used to assess coverage performance in heterogeneous WSNs, where nodes have different sensing capabilities. The study finds that ESR is a critical factor in determining whether full coverage can be achieved, especially under different mobility models, including i.i.d. mobility (independent and identically distributed) and 1-dimensional random walk mobility. The authors show that mobility can significantly enhance coverage by repositioning sensors to improve overall area coverage, which highlights the positive impact of controlled node movement on network performance [22], [60].

The study also addresses the effects of sensor heterogeneity on coverage and energy consumption. Heterogeneous WSNs consist of sensors with varying capabilities, such as different sensing radii or power levels. The authors demonstrate that while heterogeneity can lead to slightly increased energy consumption under certain mobility models, it can also result in better coverage without proportional increases in energy use. For example, under the 1-dimensional random walk mobility model, sensor heterogeneity slightly increases sensing energy, but it also reduces overall network costs by making efficient use of sensors with different capabilities. This trade-off suggests that, under appropriate mobility settings, heterogeneity can enhance coverage without significantly impacting energy consumption, making it a valuable approach for large-scale deployments [22].

The survey by Tashan et al. [61] focuses on Mobility Robustness Optimization (MRO) in future HetNets, emphasizing the importance of optimizing mobility to maintain stable communication in high-mobility environments. The paper highlights the challenges of managing handover (HO) in HetNets, especially due to the deployment of numerous small base stations (SBSs) alongside macro cells. While these SBSs enhance network capacity and coverage, they also increase the frequency of HOs, which can lead to handover pingpong and radio link failures (RLFs). These issues degrade user QoE and require effective handover control parameters (HCPs), such as Time-To-Trigger (TTT) and Handover Margin (HOM), to be optimized for better performance. The authors discuss several MRO algorithms that dynamically adjust HCPs based on network conditions to minimize unnecessary HOs and maintain optimal connectivity, especially in ultra-dense networks [61].

Tashan et al. also explore the use of machine learning (ML) in MRO to enhance adaptability. Techniques like fuzzy logic controllers (FLC) and Q-learning are used to dynamically adjust handover parameters based on real-time data such as received signal strength (RSS), user speed, and cell load. These ML-based approaches help address the challenges posed by heterogeneous cell sizes and different radio access technologies (RATs) in HetNets, making handover decisions more efficient and reducing unnecessary HOs. For instance, fuzzy Q-learning combines reinforcement learning with fuzzy logic to provide adaptive solutions that optimize HCPs with minimal computational overhead. This use of ML highlights the importance of intelligent handover management in maintaining stable connectivity and improving user QoE in HetNets [61], [62].

Figure 3 shows the concept of resource management in HetNets under four main categories. These are power allocation, user assignment, mode selection, and spectrum allocation. While power allocation is evaluated in terms of efficiency, energy saving, and spectrum usage, user assignment is considered based on SINR (signal-to-noise ratio) and data rate. Mode selection is divided into static and dynamic, while spectrum allocation is performed over conventional bands, millimeter wave (mmWave) and terahertz (THz). This structure provides a core for efficient resource utilization and performance optimization in 5G/6G WSN networks. [63]

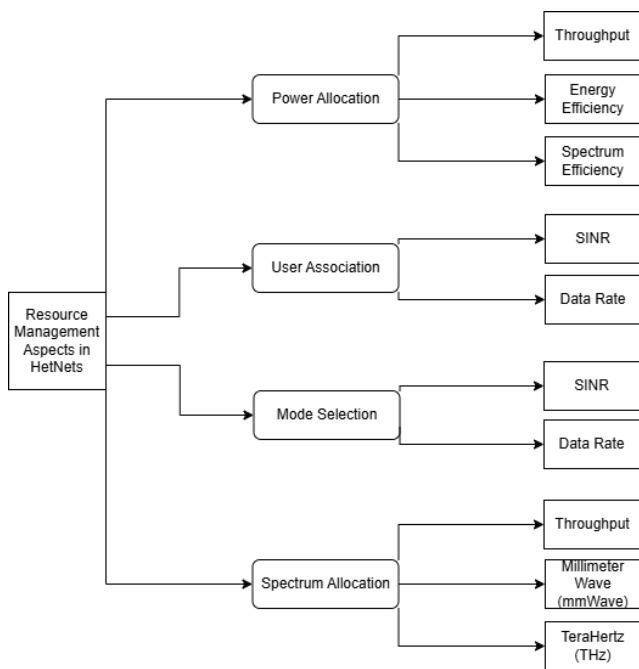


Fig. 3 Key resource management aspects in HetNets [63].

In conclusion, the impact of mobility and heterogeneity on WSNs and HetNets is multifaceted, involving challenges related to frequent handovers, coverage, and energy efficiency.

Mobility management in HetNets, as highlighted in [21], requires advanced solutions like beam-level mobility and network slicing to handle frequent HOs and provide tailored services for different types of devices. The work [22] emphasize the positive effects of mobility on coverage and the role of sensor heterogeneity in optimizing energy use in WSNs. Lastly, Tashan et al. [61] underline the importance of robust mobility optimization through self-optimizing algorithms and machine learning techniques to manage HOs in future HetNets effectively. These studies show that two main things are important for better wireless networks, especially with 5G and 6G. First, how devices move around. Second, how different devices are used together. In Yang et al. it is also emphasized that tracking mobile targets in WSNs requires specialized protocols that efficiently manage node coordination and communication overhead [64]. Doing them well can help networks cover more area, use less power, and keep working even when things go wrong.

5 AI/ML TECHNIQUES IN ENERGY-EFFICIENT ROUTING

Lots of people are now looking at using AI and machine learning to help WSNs save power. These networks often work in tough places where it's really important to not waste energy. AI and machine learning can assist by intelligently managing the network's resource usage and making more informed decisions about data transmission. This helps the networks work for way longer. Here, we'll dive into how researchers are using AI and machine learning to make data travel through the network using less power. We'll look at the latest studies on this. Biswas et al. [23] provide a detailed review of how AI is used to optimize power consumption, showing its impact on saving energy in various areas, including WSNs. The authors highlight that AI not only helps achieve sustainability goals but also lowers operational costs. The authors delve into various AI techniques, such as Reinforcement Learning (RL), Genetic Algorithms (GA), and Neural Networks (NN), that enable real-time energy management. For instance, they apply Reinforcement Learning (RL) to manage changing energy demands in HVAC systems, enabling real-time adjustments that save energy while maintaining user comfort. Fuzzy Logic Control (FLC) is another technique they mention, known for managing nonlinear power systems, such as air conditioners, where it achieved up to 25% energy savings. These AI-driven methods show great potential for improving energy efficiency and ensuring a stable energy supply [23]. The another paper presents an approach to optimize the power consumption of wireless sensor nodes by developing a novel power control technique, to improve energy efficiency and extending the network lifetime [65].

Pasqualetto et al. [24] look into how AI can make energy management in smart buildings more efficient and help with global sustainability efforts. They focus on Multi-Agent Sys-

tems (MAS), which use decentralized decision-making to create smart environments. MAS is based on the "Belief-Desire Intention" (BDI) model, where different agents work together to optimize energy use. Each agent manages specific tasks like temperature control or HVAC systems, making the building more energy-efficient overall. The paper also highlights the role of Big Data in improving AI models. Data collected from sensors and devices in smart buildings is essential for understanding energy usage, predicting future needs, and managing resources in real-time. The authors discuss Artificial Neural Networks (ANNs) and Genetic Algorithms (GA) as useful tools. ANNs help predict how much energy will be needed, while GAs optimize energy usage based on changing prices. These AI methods offer practical ways to manage energy better, meet user needs, and support sustainability[24].

The survey by Samara et al. [66] focuses on energy efficient routing algorithms in WSNs, emphasizing the need for effective routing to minimize energy consumption in sensor nodes. The authors discuss several well-known algorithms, such as LEACH (Low Energy Adaptive Clustering Hierarchy), TEEN (Threshold Sensitive Energy Efficient Sensor Network Protocol), and APTEEN (Adaptive Periodic Threshold Sensitive Energy Efficient Sensor Network Protocol). These algorithms use clustering strategies to minimize data transmissions, thereby reducing energy consumption. LEACH, for example, organizes nodes into clusters, with Cluster Heads (CHs) responsible for aggregating and forwarding data to the BS. However, the random selection of CHs can sometimes result in inefficient energy usage, especially when selecting nodes with low residual energy. TEEN and APTEEN improve upon LEACH by introducing threshold-based mechanisms to minimize unnecessary data transmissions, especially in event driven scenarios, thus extending the network lifetime. The authors also explore AI-based approaches, such as genetic algorithms and neural networks, to optimize CH selection and routing paths, highlighting their ability to dynamically adapt to changing network conditions and energy levels, which significantly enhances energy efficiency in WSNs [66], [67]. Figure 4 provides a general architecture of data aggregation approach from [66].

Priyadarshi [26] provides an in-depth review of meta-heuristic and AI-based algorithms for energy-efficient routing in WSNs. Some of the optimization algorithms talked about in the paper are Particle Swarm Optimization (PSO), ABC, Ant Colony Optimization (ACO), Genetic Algorithm (GA), Firefly Algorithm (FA), and Bacterial Foraging Optimization (BFO). These bio-inspired algorithms are based on how animals act naturally, like how bees use swarm intelligence or how ants use pheromones to find the best routes. WSNs use these algorithms to solve challenging routing problems. PSO, for instance, helps nodes find the best transmission paths by mimicking the social be-

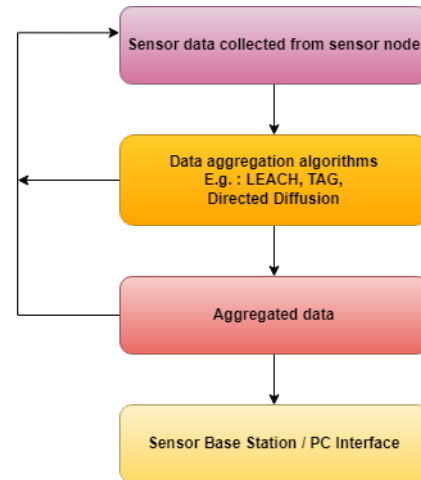


Fig. 4 The general architecture of data aggregation approaches.

havior of birds, while ACO uses pheromone trails to determine the most energy efficient routes. The author also explores hybrid optimization techniques, such as combining PSO with ACO, to enhance data collection and prolong network longevity [68]. Combining different algorithms can make things even better, especially when it comes to saving energy and keeping the network running for a long time. Priyadarshi's work also suggests that AI and certain smart search methods are really useful for tackling power issues in these sensor networks. This makes them more reliable and able to adapt to different uses, like keeping an eye on the environment, running factory equipment, and building smart cities [26], [69], [70].

The study from Rovira-Sugranes et al. concludes that AI-based routing protocols bring significant advantages over traditional routing mechanisms, especially in dynamic and resource-constrained networks. Traditional protocols such as AODV, DSR, and OLSR rely on predefined routing tables and periodic updates, also this can lead to high operational costs and slow convergence in rapidly changing environments. In contrast, AI-driven approaches, such as Q-learning and reinforcement learning (RL)-based protocols, reduce latency and improve packet delivery rates by adapting to changes in network topology in real time. AI-based methods also integrate predictive analytics, enabling proactive route adjustments and better handling of connection failures. However, these intelligent routing solutions often require more computational resources and extensive training data to perform optimally. While traditional routing protocols provide stability and low computational cost, they lack scalability and adaptability in highly mobile networks. In contrast, AI-powered protocols offer superior performance in terms of throughput, reduced latency, and energy efficiency, making them ideal for unmanned aerial vehicles and next-generation wireless networks [71].

AI-driven routing has come with smart ways to manage

network traffic, predict congestion, and fix problems automatically. For example, RL models such as Deep Q Networks (DQN) and Proximal Policy Optimization (PPO) help networks choose the best path in real time applications. On the other hand, supervised learning is mainly used to detect unusual network activity and classify traffic. Deep learning methods, such as Recurrent Neural Networks (RNNs) and Transformer-based models, improve predictions but need a lot of computing power. Since studies do not compare these AI techniques properly, it is difficult to know which one works best for different network conditions. Without a clear evaluation system, it is unclear whether AI-based routing is better for quick decision-making, security, or managing traffic over time. This lack of clarity makes it harder to use AI-driven routing effectively in SDN (Software-Defined Networking), cloud systems, and 5G/6G WSN networks [72].

Despite WSNs' advantages, they face significant real-world challenges, including hardware limitations, environmental constraints, and deployment issues. One of the primary constraints is energy consumption, as sensor nodes rely on battery power, making efficient energy utilization a key concern. Furthermore, harsh environmental conditions such as extreme temperatures, humidity, and electromagnetic interference can severely impact the reliability of WSNs. The scalability issues arises when large-scale deployments increase network congestion and brings all problems in data routing and synchronization. To address these concerns, researchers emphasize the need for energy-efficient protocols, adaptive deployment strategies, and AI-driven optimizations to make the robustness better and the longevity of WSN applications [73].

In summary, AI and ML are useful tools for better energy-efficient routing in WSNs. Methods like reinforcement learning, genetic algorithms, fuzzy logic control, and using groups of intelligent agents has also been a good way to make these networks better and last longer. These "multi-agent systems" offer adaptable and smart ways to handle energy problems, so the networks can run for longer and more reliably. Combining different optimization methods, especially ones inspired by nature, also looks promising. These can simplify data gathering, spread out the work evenly, and save power. Basically, using AI and machine learning for energy-efficient routing makes these sensor networks more sustainable and prepares them for all sorts of future uses in smart homes, cities, and other places.

6 SECURITY CHALLENGES IN ENERGY-EFFICIENT ROUTING

Keeping data safe is a big deal when designing ways for devices in the IoT and WSNs to send information while saving power. These networks often don't have much energy to spare, so adding security is tricky. We need to protect the data and make sure it's reliable and private, all while trying to use as little power as possible. This section looks

at recent research on the tough problem of designing both secure and energy-efficient routing algorithms, particularly for networks with limited resources [74].

For example, Mahamat et al. [25] talk about how difficult it is to have both good security and low energy use in IoT networks. Due to the frequent placement of these devices in vulnerable areas and their limited power, maintaining a balance becomes crucial. They say that many current security methods use up too much energy, which means the network won't last as long.

We need fresh ideas for security that don't drain the battery. This paper suggests using AI and software-defined networking (SDN) to build flexible security. AI and SDN can tweak security settings instantly based on what's happening around the devices, which saves power and keeps things secure. Think of it like this: simple security rules made for the limited brains of IoT devices are key to protecting data without killing the battery [25].

Mahamat et al. also stress the need for "smart" security, where the level of protection changes based on the actual threat. By constantly checking what's going on, IoT devices can adjust their security. When things are dangerous, they can ramp up the protection. When things are calm, they can dial it back and save power. This not only helps the devices last longer but also finds a good middle ground between strong security and efficient energy use. AI can make this kind of adaptable security possible, which could be a big step forward for making IoT networks both secure and sustainable in ever-changing situations [25]. Figure 5 provides elements needed to provide a security solution balancing the provided security level and energy consumption [25].

Biradar and Mathapathi [20] looked at the tricky job of designing ways for WSNs to send data securely, reliably, and without wasting power. They sorted these data-sending methods into three groups: proactive, reactive, and hybrid. Then, they checked how each group handles energy use and security. Their main point is that it's really tough to build systems that both save power and keep data safe, particularly for important jobs like watching the environment or military operations. Reactive methods are more energy-efficient than proactive ones, as they establish data routes only when necessary. Proactive methods, on the other hand, use up extra energy constantly updating their route maps, even when they're not sending data [20]. They also explore different ways to make these routing methods both secure and energy-efficient. They mention that grouping sensors into clusters, like with LEACH method, can help save power because the cluster leaders can gather and process data more efficiently. They also states that it's vital to have trust-based routing and secure location tracking to keep data safe and stop unauthorized access. Simple encryption methods are also key for adding security to these power-limited networks. Finally, they suggest that machine learning could be promising to boost security with much

less energy, so that's the future work [20].

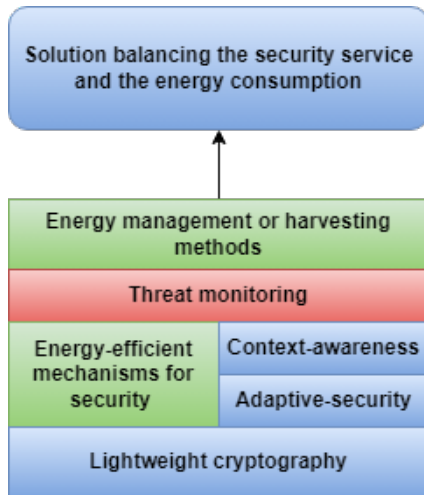


Fig. 5 Elements needed to provide a security solution balancing the provided security level and energy consumption [25].

Both Mahamat et al. and Biradar and Mathapathi highlight the constant struggle to balance saving energy and keeping things secure in IoT and WSNs. Strong security is a must to protect data and keep these networks running reliably. But, because IoT devices and sensor nodes have limited battery power, security measures have to be really energy-efficient. AI-powered, context-aware solutions and lightweight encryption seem like good ways to tackle this problem. These methods make sure that security adjusts to what's happening in network right now, so you can save power while still keeping your data reasonably safe [75].

To wrap things up, building routing methods for IoT and WSNs that both save energy and solve security problems is a tough but essential job. Smart security systems that use AI, software-defined networking, and simple encryption can help keep data safe without draining the battery. By creating systems that adapt to their surroundings and using clever optimization techniques, researchers can make these networks more robust, reliable, and sustainable. This will be crucial for important applications where both security and energy efficiency are paramount [20], [25].

7 CONCLUSION

This study investigates energy-efficient routing protocols for 5G/6G WSNs. Cooperative routing techniques, hierarchical clustering methods, AI, and machine learning (ML) applications reduces unnecessary energy consumption and extend the network lifetime. Protocols such as LEACH and its derivatives (LEACH-C, LEACH-DCS) save energy by selecting more balanced nodes, and AI techniques such as reinforcement learning and genetic algorithms make routing dynamic to have sustainable communication. In mobility and heterogeneous networks, frequent handovers and

excessive signaling traffic increases the energy consumption. Solutions such as beam-level mobility and mobility role optimization (MRO) have been proposed to minimize these issues. This review provides an organized comparison of the energy-efficient routing protocols and highlights developing trends that contribute to the sustainable development of 5G/6G WSNs.

Energy-efficient security solutions use lightweight encryption, trust-based routing, and context-aware security mechanisms to secure the network while reducing energy consumption [76]. However, large and rapidly changing networks require scalable and low-power solutions. Future research should focus on AI-assisted routing, advanced mobility management, and the integration of renewable energy sources. These developments will contribute to the widespread adoption of reliable and energy-efficient communication systems in many areas, including smart cities, environmental monitoring, and industrial automation.

Additionally, studies in the future should explore the scalability of AI-driven routing algorithms for very large-scale WSN deployments. They need to optimize the energy consumption without compromising performance. The integration of energy-harvesting techniques, such as solar-powered sensor nodes, brings an exciting research direction for sustainable WSNs. Furthermore, interdisciplinary collaborations between network engineers, AI researchers, and experts can lead to innovative solutions. Practical validation methods, including real-world testbeds and large-scale simulations, will be important for evaluating the feasibility and effectiveness of these proposed solutions.

REFERENCES

- [1] D. Kandris and E. Anastasiadis, "Advanced wireless sensor networks: Applications, challenges and future directions," *Electronics*, vol. 13, no. 12, p. 2268, 2023. DOI: 10.3390/electronics13122268.
- [2] D. Kannaujaiya and A. K. Dwivedi, "Challenges, issues, and applications of wireless sensor networks: A review," in *Proc. IEEE Int. Conf. Innovative Computing and Communication Technologies (ICICAT)*, 2023. DOI: 10.1109/ICICAT57735.2023.10263699.
- [3] O. Demigha, W.-K. Hidouci, and T. Ahmed, "On energy efficiency in collaborative target tracking in wireless sensor network: A review," *IEEE Communications Surveys & Tutorials*, vol. 15, no. 3, pp. 1210–1221, 2013.
- [4] I. Stanojev, O. Simeone, Y. Bar-Ness, and D. H. Kim, "Energy efficiency of non-collaborative and collaborative hybrid-arq protocols," *IEEE Transactions on Wireless Communications*, vol. 8, no. 1, pp. 326–337, 2009.
- [5] C. Felicetti, R. D. Rose, C. Raso, A. M. Felicetti, and S. Ammirato, "Collaborative smart environments for energy-efficiency and quality of life," *International Journal of Engineering and Technology*, vol. 7, no. 2, pp. 543–552, 2015.

- [6] T. M. Behera, U. C. Samal, S. K. Mohapatra, *et al.*, “Energy-efficient routing protocols for wireless sensor networks: Architectures, strategies, and performance,” *Electronics*, vol. 11, no. 15, p. 2282, 2022.
- [7] A. Al-Shaikh, H. Khattab, and S. Al-Sharaeh, “Performance comparison of leach and leach-c protocols in wireless sensor networks,” *Journal of Computing & Communication*, vol. 9, no. 5, pp. 219–236, 2018. DOI: 10.5614/itbj.ict.res.appl.2018.12.3.2.
- [8] C. Schurgers and M. B. Srivastava, “Energy efficient routing in wireless sensor networks,” in *Proceedings of IEEE International Conference on Communications*, vol. 1, 2001, pp. 357–361.
- [9] C. Nakas, D. Kandris, and G. Visvardis, “Energy efficient routing in wireless sensor networks: A comprehensive survey,” *Algorithms*, vol. 13, no. 3, p. 72, 2020.
- [10] H. L. Gururaj, R. Natarajan, N. A. Almujaally, F. Flammini, S. Krishna, and S. K. Gupta, “Collaborative energy-efficient routing protocol for sustainable communication in 5g/6g wireless sensor networks,” *IEEE Open Journal of the Communications Society*, vol. 4, pp. 2050–2061, 2023.
- [11] O. M. Gul and A. M. Erkmen, “Energy-efficient cluster-based data collection by a uav with a limited-capacity battery in robotic wireless sensor networks,” *Sensors*, vol. 20, p. 5865, 2020.
- [12] O. M. Gul, A. M. Erkmen, and B. Kantarci, “Uav-driven sustainable and quality-aware data collection in robotic wireless sensor networks,” *IEEE Internet of Things Journal*, vol. 9, pp. 25 150–25 164, 2022.
- [13] O. M. Gul and A. M. Erkmen, “Energy-aware uav-driven data collection with priority in robotic wireless sensor network,” *IEEE Sensors Journal*, vol. 23, pp. 17 667–17 675, 2023.
- [14] O. M. Gul, A. M. Erkmen, and B. Kantarci, “Ntn-aided quality and energy-aware data collection in time-critical robotic wireless sensor networks,” *IEEE Internet of Things Magazine*, vol. 7, pp. 114–120, 2024.
- [15] O. M. Gul, “Uav-driven robust and energy-aware data collection in robotic wireless sensor networks,” in *2024 15th IFIP Wireless and Mobile Networking Conference (WMNC)*, vol. 1, 2024, pp. 17–24.
- [16] O. M. Gul, “A novel energy-aware path planning by autonomous underwater vehicle in underwater wireless sensor networks,” *Turkish Journal of Maritime and Marine Sciences*, vol. 10, pp. 81–94, 2024.
- [17] O. M. Gul and M. Demirekler, “Average throughput performance of myopic policy in energy harvesting wireless sensor networks,” *Sensors*, vol. 17, p. 2206, 2017.
- [18] O. M. Gul and M. Demirekler, “Asymptotically throughput optimal scheduling for energy harvesting wireless sensor networks,” *IEEE Access*, vol. 6, pp. 45 004–45 020, 2018.
- [19] O. M. Gul, “Achieving near-optimal fairness in energy harvesting wireless sensor networks,” in *2019 IEEE Symposium on Computers and Communications (ISCC)*, vol. 1, 2019, pp. 1–6.
- [20] M. Biradar and B. Mathapathi, “Secure, reliable and energy efficient routing in wsn: A systematic literature survey,” in *2021 International Conference on Advances in Electrical, Computing, Communication and Sustainable Technologies (ICAECT)*, IEEE, 2021, pp. 1–7. DOI: 10.1109/ICAECT49130.2021.9392561.
- [21] E. Gures, I. Shaye, A. Alhammedi, M. Ergen, and H. Mohamad, “A comprehensive survey on mobility management in 5g heterogeneous networks: Architectures, challenges and solutions,” *IEEE Access*, vol. 8, pp. 195 883–195 901, 2020.
- [22] X. Wang, X. Wang, and J. Zhao, “Impact of mobility and heterogeneity on coverage and energy consumption in wireless sensor networks,” in *31st International Conference on Distributed Computing Systems*, 2011, pp. 477–484.
- [23] P. B. et al., “Ai-driven approaches for optimizing power consumption: A comprehensive survey,” *Journal of Energy Informatics*, vol. 12, no. 3, pp. 234–256, 2024.
- [24] A. Pasqualetto, L. Serafini, and M. Sproccati, *Artificial Intelligence Approaches for Energy Efficiency: A Review*. Department of Information Engineering, University of Padua, 2024.
- [25] M. Mahamat, G. Jaber, and A. Bouabdallah, “Achieving efficient energy-aware security in iot networks: A survey of recent solutions and research challenges,” *Wireless Networks*, vol. 29, pp. 787–808, 2023. DOI: 10.1007/s11276-022-03170-y.
- [26] R. Priyadarshi, “Energy-efficient routing in wireless sensor networks: A meta-heuristic and artificial intelligence-based approach: A comprehensive review,” *Journal of Intelligent Systems*, vol. 15, no. 4, pp. 231–256, 2024.
- [27] S. Misra, M. Reisslein, and G. Xue, “A survey of multimedia streaming in wireless sensor networks,” *IEEE Communications Surveys & Tutorials*, vol. 10, no. 4, pp. 18–39, 2008. DOI: 10.1109/SURV.2008.080404.
- [28] K. Tebessi and F. Semchedine, “An improvement on leach-c protocol (leach-ccmsn),” *Russian Journal of Electrical Engineering*, vol. 56, no. 1, pp. 10–16, 2022. DOI: 10.3103/S0146411622010102.
- [29] P. Rawat and S. Chauhan, “Clustering protocols in wireless sensor network: A survey, classification, issues, and future directions,” *Computer Science Review*, vol. 41, p. 100 396, 2021. DOI: 10.1016/j.cosrev.2021.100396.
- [30] M. Hosseinzadeh, J. Yoo, and S. A. et al., “A cluster-based trusted routing method using fire hawk optimizer (fho) in wireless sensor networks (wsns),” *Scientific Reports*, vol. 13, p. 13 046, 2023. DOI: 10.1038/s41598-023-40273-8.
- [31] K. H. M and R. Dilli, “Wireless sensor networks: Network life time enhancement using an improved grey wolf optimization algorithm,” *Engineered Science*, vol. 19, pp. 186–197, 2022, ISSN: 2576-9898. DOI: 10.30919/es8d717.
- [32] S. Sharmin, I. Ahmedy, and R. Md Noor, “An energy-efficient data aggregation clustering algorithm for wireless sensor networks using hybrid pso,” *Energies*, vol. 16, no. 5, 2023, ISSN: 1996-1073. DOI: 10.3390/en16052487.

- [33] Y. Yu, R. Govindan, and D. Estrin, "Geographical and energy aware routing: A recursive data dissemination protocol for wireless sensor networks," UCLA Computer Science Department, Los Angeles, CA, USA, Tech. Rep., 2001, pp. 1–11.
- [34] J. Newsome and D. Song, "Gem: Graph embedding for routing and data-centric storage in sensor networks without geographic information," in *Proceedings of the 1st International Conference on Embedded Networked Sensor Systems*, Los Angeles, CA, USA, 2003, pp. 76–88.
- [35] B. Blum, T. He, S. Son, and J. Stankovic, "Igf: A state-free robust communication protocol for wireless sensor networks," Department of Computer Science, University of Virginia, Charlottesville, VA, USA, Tech. Rep. CS-2003-11, 2003.
- [36] G. Lukachan and M. Labrador, "Selar: Scalable energy-efficient location aided routing protocol for wireless sensor networks," in *Proceedings of the 29th Annual IEEE International Conference on Local Computer Networks*, Tampa, FL, USA, 2004, pp. 694–695.
- [37] B. Leong, B. Liskov, and R. Morris, "Geographic routing without planarization," in *Proceedings of the 3rd Conference on Networked Systems Design and Implementation*, vol. 3, San Jose, CA, USA, 2006, pp. 25–39.
- [38] M. Zimmerling, W. Dargie, and J. Reason, "Energy-efficient routing in linear wireless sensor networks," in *Proceedings of the 4th IEEE International Conference on Mobile Ad-hoc and Sensor Systems (MASS 2007)*, Pisa, Italy, 2007, pp. 1–3.
- [39] D. Chen and P. K. Varshney, "On-demand geographic forwarding for data delivery in wireless sensor networks," *Computer Communications*, vol. 30, no. 14, pp. 2954–2967, 2007, Network Coverage and Routing Schemes for Wireless Sensor Networks, ISSN: 0140-3664. DOI: <https://doi.org/10.1016/j.comcom.2007.05.022>.
- [40] L. Zou, M. Lu, and Z. Xiong, "Pager-m: A novel location-based routing protocol for mobile sensor networks," in *Proceedings of the 2007 ACM SIGMOD International Conference on Management of Data*, Beijing, China, 2007, pp. 1182–1185.
- [41] M. Chen, V. C. M. Leung, S. Mao, Y. Xiao, and I. Chlamtac, "Hybrid geographic routing for flexible energy—delay trade-off," *IEEE Transactions on Vehicular Technology*, vol. 58, no. 9, pp. 4976–4988, 2009. DOI: 10.1109/TVT.2009.2025767.
- [42] V. Rodoplu and T. Meng, "Minimum energy mobile wireless networks," *IEEE Journal on Selected Areas in Communications*, vol. 17, no. 8, pp. 1333–1344, 1999. DOI: 10.1109/49.779917.
- [43] L. Li and J. Halpern, "Minimum energy mobile wireless networks revisited," in *Proceedings of the IEEE International Conference on Communications (ICC)*, Helsinki, Finland, 2001, pp. 278–283.
- [44] Y. Xu, J. Heidemann, and D. Estrin, "Geography-informed energy conservation for ad hoc routing," in *Proceedings of the 7th Annual ACM/IEEE International Conference on Mobile Computing and Networking (MobiCom)*, Rome, Italy, 2001.
- [45] C. Boucetta, H. Idoudi, and L. Saidane, "Ant colony optimization based hierarchical data dissemination in wsn," in *Proceedings of the 2015 International Wireless Communications and Mobile Computing Conference (IWCMC)*, Dubrovnik, Croatia, 2015.
- [46] C. Boucetta, H. Idoudi, and L. Saidane, "Adaptive scheduling with fault tolerance for wireless sensor networks," in *Proceedings of the 2015 IEEE 81st Vehicular Technology Conference (VTC Spring)*, Glasgow, Scotland, 2015.
- [47] C. Eris, O. M. Gul, and P. S. Boluk, "An energy-harvesting aware cluster head selection policy in underwater acoustic sensor networks," in *2023 International Balkan Conference on Communications and Networking (BalkanCom)*, vol. 1, 2023, pp. 1–5.
- [48] Ç. Eriş, Ö. M. Gül, and P. S. Bölük, "A novel medium access policy based on reinforcement learning in energy-harvesting underwater sensor networks," *Sensors*, vol. 24, p. 5791, 2024.
- [49] Ç. Eriş, Ö. M. Gül, and P. S. Bölük, "A novel reinforcement learning based routing algorithm for energy management in networks," *Journal of Industrial Management and Optimization*, vol. 20, p. 12, 2024.
- [50] M. Fathi, V. Maihami, and P. Moradi, "Reinforcement learning for multiple access control in wireless sensor networks: Review, model, and open issues," *Wireless Personal Communications*, vol. 72, 2013. DOI: 10.1007/s11277-013-1028-9.
- [51] M. Yari, P. Hadikhani, M. Yaghoubi, R. Nowrozy, and Z. Asgharzadeh, "An energy efficient routing algorithm for wireless sensor networks using mobile sensors," *arXiv preprint*, vol. 2103.04119, 2021. DOI: 10.48550/arXiv.2103.04119.
- [52] D. A. Milovanovic and Z. S. Bojkovic, "Exploring 5g/6g energy-efficiency in mobile communications for sustainable future," in *Intelligent and Sustainable Engineering Systems for Industry 4.0 and Beyond*, CRC Press, 2023, ch. 13, pp. 259–284. DOI: 10.1201/9781003511298-13.
- [53] A. Roy and T. Deb, "Performance comparison of routing protocols in mobile ad hoc networks," in *Proceedings of the International Conference on Computing and Communication Systems*, ser. Lecture Notes in Networks and Systems, vol. 24, Springer, 2018, pp. 33–48. DOI: 10.1007/978-981-10-6890-4_4. [Online]. Available: https://doi.org/10.1007/978-981-10-6890-4_4.
- [54] M. Sabokrou, M. Fathy, and M. Hoseini, "Idsa: Intelligent distributed sensor activation algorithm for target tracking with wireless sensor network," *arXiv preprint*, vol. 1506.00122, 2015.

- [55] S. Zhang, S. Liu, V. Sharma, and P. K. Varshney, "Optimal sensor collaboration for parameter tracking using energy harvesting sensors," *IEEE Transactions on Signal Processing*, vol. 66, no. 10, pp. 2647–2659, 2018. DOI: 10.1109/TSP.2018.2827319.
- [56] H. Y. Shwe, A. Kumar, and P. H. J. Chong, "Building efficient multi-level wireless sensor networks with cluster-based routing protocol," *KSII Transactions on Internet and Information Systems*, vol. 10, pp. 4272–4286, 2016. DOI: 10.3837/tiis.2016.09.014.
- [57] A. Javadpour, "An optimize-aware target tracking method with combine mac layer and active nodes in wireless sensor networks," *arXiv preprint*, vol. 2005.06598, 2020.
- [58] H. Wang, N. Agoulmine, M. Ma, and Y. Jin, "Network lifetime optimization in wireless sensor networks," *IEEE Journal on Selected Areas in Communications*, vol. 28, no. 7, pp. 1127–1137, 2010. DOI: 10.1109/JSAC.2010.100917.
- [59] A. K. Salama and M. M. Abdellatif, "Aiot-based smart home energy management system," in *Proc. 2022 Global Conference on Artificial Intelligence of Things (GCAIoT)*, 2022, pp. 177–181. DOI: 10.1109/GCAIoT57150.2022.10019091.
- [60] H. Wang, J. Zhang, and Z. Chen, "Coverage and energy consumption control in mobile heterogeneous wireless sensor networks," *International Journal of Sensor Networks*, vol. 12, no. 4, pp. 273–285, 2015.
- [61] W. T. et al., "Mobility robustness optimization in future mobile heterogeneous networks: A survey," *IEEE Access*, vol. 10, pp. 45522–45537, 2022.
- [62] P. E. I. Rivera, M. Elsayed, M. Bavand, R. Gaigalas, S. Furr, and M. Erol-Kantarci, "Hierarchical deep q-learning based handover in wireless networks with dual connectivity," *arXiv preprint*, vol. 2301.05391, 2023. DOI: 10.48550/arXiv.2301.05391.
- [63] H. F. Alhashimi, M. N. Hindia, K. Dimiyati, et al., "A survey on resource management for 6g heterogeneous networks: Current research, future trends, and challenges," *Electronics*, vol. 12, no. 3, p. 647, 2023. DOI: 10.3390/electronics12030647.
- [64] H. Yang and B. Sikdar, "A protocol for tracking mobile targets using sensor networks," in *Proceedings of the First IEEE International Workshop on Sensor Network Protocols and Applications, 2003.*, 2003, pp. 71–81. DOI: 10.1109/SNPA.2003.1203358.
- [65] M. Rajagopal, "Optimal power control technique for a wireless sensor node: A new approach," *International Journal of Computer and Electrical Engineering*, vol. 3, no. 1, p. 1, 2011. DOI: 10.7763/IJCEE.2011.V3.289.
- [66] G. Samara, G. AlBesani, M. Alauthman, and M. A. Khaldy, "Energy-efficiency routing algorithms in wireless sensor networks: A survey," *International Journal of Scientific & Technology Research*, vol. 9, no. 1, pp. 4415–4419, 2020.
- [67] W. Osamy, M. Khedr, A. Salim, A. I. A. Ali, and A. A. El-Sawy, "A review on recent studies utilizing artificial intelligence methods for solving routing challenges in wireless sensor networks," *PeerJ Computer Science*, vol. 8, e1089, 2022. DOI: 10.7717/peerj-cs.1089.
- [68] J. Costa-Requena, *A Hybrid Routing Approach for Ad Hoc Networks*. Tampere University of Technology, Finland, 2005.
- [69] R. Priyadarshi, "Energy-efficient routing in wireless sensor networks: A meta-heuristic and artificial intelligence-based approach: A comprehensive review," *Archives of Computational Methods in Engineering*, vol. 31, no. 4, pp. 2109–2137, May 2024, ISSN: 1886-1784. DOI: 10.1007/s11831-023-10039-6.
- [70] A. Sharma, H. Babbar, S. Rani, D. K. Sah, S. Sehar, and G. Gianini, "Mhseer: A meta-heuristic secure and energy-efficient routing protocol for wireless sensor network-based industrial iot," *Energies*, vol. 16, no. 10, 2023, ISSN: 1996-1073. DOI: 10.3390/en16104198.
- [71] A. Rovira-Sugranes, A. Razi, F. Afghah, and J. Chakareski, "A review of ai-enabled routing protocols for uav networks: Trends, challenges, and future outlook," *Ad Hoc Networks*, vol. 130, p. 102790, 2022, ISSN: 1570-8705. DOI: <https://doi.org/10.1016/j.adhoc.2022.102790>.
- [72] I. Bhattacharjee, "Ai-driven routing: Transforming network efficiency and resilience," *TechRxiv*, vol. Preprint, 2025, Preliminary report, not peer reviewed. DOI: 10.36227/techrxiv.174114640.07395422/v1. [Online]. Available: <https://doi.org/10.36227/techrxiv.174114640.07395422/v1>.
- [73] D. S. Ibrahim, A. F. Mahdi, and Q. M. Yas, "Challenges and issues for wireless sensor networks: A survey," *Journal of Global Scientific Research*, vol. 6, no. 1, pp. 1079–1097, 2021.
- [74] K. Haseeb, A. Almogren, N. Islam, I. Ud Din, and Z. Jan, "An energy-efficient and secure routing protocol for intrusion avoidance in iot-based wsn," *Energies*, vol. 12, no. 21, 2019, ISSN: 1996-1073. DOI: 10.3390/en12214174.
- [75] S. B. Khan, A. Kumar, A. Mashat, D. Pruthviraja, M. K. I. Rahmani, and J. Mathew, "Artificial intelligence in next-generation networking: Energy efficiency optimization in iot networks using hybrid leach protocol," *SN Computer Science*, vol. 5, no. 5, p. 546, May 2024, ISSN: 2661-8907. DOI: 10.1007/s42979-024-02778-5.
- [76] M. Lacoste, G. Privat, and F. Ramparany, "Evaluating confidence in context for context-aware security," in *Ambient Intelligence*, Berlin, Heidelberg: Springer Berlin Heidelberg, 2007, pp. 211–229, ISBN: 978-3-540-76652-0. DOI: https://doi.org/10.1007/978-3-540-76652-0_13.

Details of a Digital Twin for a LoRa Based Forest Fire Management System

Buğra Aydın¹ , and Sema F. Oktuğ¹ 

¹ Department of Computer Engineering, Istanbul Technical University, Istanbul, 34469, Turkey

Abstract: Early detection of forest fires is vital for ecosystems. For this purpose, sensor networks collect data such as temperature and humidity and monitor changes in forests. Long-range and low-energy communication technologies such as LoRa are especially widely used in these networks. However, the management of these networks can be complicated since each forest has different requirements. Digital twin technology allows the simulation of different scenarios and optimization systems by creating virtual copies of physical systems to solve this problem. However, the relational structure of computer networks can be challenging for some artificial intelligence models used in digital twins. Graph neural networks help digital twins to understand and optimize the complicated structure of networks. In addition, it is not feasible for Internet of Things networks to meet digital twins' two-way and continuous communication demand. Therefore, in this study, a forecaster model is designed to facilitate the integration of digital twins into these networks. The forecaster provides the data the digital twin needs by predicting the network's future states from its past states. The first results of the study are promising, especially for small-scale networks. However, as the scale of the network grows, the errors made by the system also increase.

Keywords: Digital twin, IoT, graph neural networks, forest fire detection.

LoRa Tabanlı Bir Orman Yangını Yönetim Sistemi Dijital İkizinin Ayrıntıları

Özet: Orman yangınlarının erken tespiti, ekosistemler için hayati önem taşır. Bu amaçla sensör ağları, sıcaklık ve nem gibi verileri toplayarak ormanlardaki değişiklikleri izler. Özellikle LoRa gibi uzun menzilli ve düşük enerjili iletişim teknolojileri, bu ağlarda yaygın olarak kullanılır. Ancak bu ağların yönetimi, her bir ormanın farklı gereksinimleri olduğundan karmaşık olabilir. Dijital ikiz teknolojisi, bu sorunu çözmek için fiziksel sistemlerin sanal kopyalarını oluşturarak, farklı senaryoları simüle etmeye ve sistemleri optimize etmeye olanak tanır. Lakin bilgisayar ağlarının ilişkisel yapısı dijital ikizde kullanılan bazı yapay zeka modelleri için zorlayıcı olabilir. Grafik sinir ağları ise dijital ikizlerin, ağların karmaşık yapısını anlamasına ve optimize etmesine yardımcı olur. Ayrıca, nesnelerin interneti ağlarının, dijital ikizlerin iki yönlü ve sürekli iletişim talebini karşılaması uygulanabilir değildir. Bu nedenle, bu çalışmada dijital ikizlerin bu ağlara entegrasyonunu kolaylaştıracak bir tahminci modeli tasarlanmıştır. Tahminci ağın geçmiş durumlarından gelecek durumlarını tahmin ederek dijital ikiz için ihtiyacı olan veriyi sağlar. Çalışmanın ilk sonuçları özellikle küçük ölçekli ağlar için umut vericidir. Ancak ağın ölçeği büyüdükçe sistemin yaptığı hatalar da artmaktadır.

Anahtar Kelimeler: Dijital ikiz, nesnelerin interneti, grafik sinir ağları, orman yangını tespiti.

RESEARCH PAPER

Corresponding Author: Sema F. Oktuğ, oktug@itu.edu.tr

Reference: B. Aydın, S. F. Oktuğ, (2025), "Details of a Digital Twin for a LoRa Based Forest Fire Management System," *ITU-Journ. Wireless Comm. Cyber.*, 2, (1) 27–36.

Submission Date: Mar, 2, 2025

Acceptance Date: Mar, 19, 2025

Online Publishing: Mar, 28, 2025

1 INTRODUCTION

The ecology of the world is crucially threatened by forest fires. Rising average temperatures have also increased the frequency of forest fires, including in Turkey. As indicated by the graph in Figure 1, there are more than 2 thousand forest fires every year, which destroy more than 10 thousand hectares of forest area [1].

Early and rapid-fire detection can significantly reduce the devastation of forest fires. Several different techniques are used for these detections such as surveillance of forests with satellites, flying over forests with Unmanned Aerial Vehicles (UAVs), and regularly monitoring forest values with wireless sensor networks. All of these systems have advantages and disadvantages. However, the most cost-effective and fastest fire detection method is Wireless Sensor Network (WSN) solutions. [2].

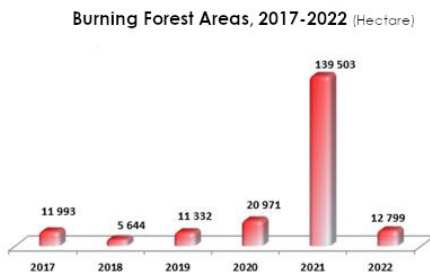


Fig. 1 Area of burned on every year.

Internet of Things (IoT) sensor networks are frequently used in these systems to detect forest fires early. However, forests differ from each other in many aspects, such as size, elevation difference, climatic conditions, tree density, and diversity. Therefore, the demands of forests and the structures of these networks vary widely. This requires specific decisions to be made in the management of each network. Also, due to the size of forests, managing these large networks can be difficult.

Once WSN networks are deployed in forests, their management becomes another problem to be solved. In these sophisticated networks, it may be desirable to minimize packet loss or optimize energy consumption. Digital Twin (DT) technology can help network administrators in this area. DTs are widely used in computer networks for optimization and running test cases. Nonetheless, DTs are challenging to use in IoT networks due to their constant communication requirements. Hence, this paper proposes a forecaster mechanism to facilitate this integration. The proposed model generates the data for DT by predicting the network traffic (packets) in advance.

This paper introduces a digital twin application for forest fire detection systems employing IoT networks. Integrating the digital twin into such networks is key to perceiving their

complexity. It also enables effective and accurate testing of different strategies for network optimization. However, the main challenge in achieving this integration is the need for continuous bidirectional data transfer of digital twins. Since IoT networks have limitations in terms of energy and performance, meeting these requirements is challenging for them. In addition, some use cases can present interesting contradictions. For example, a digital twin modeling network packet delivery rate needs real-time lost packet data from the network. However, the digital twin is not aware of a packet that has not reached the network's server. In networks such as the one studied in this work, where forest fires are specifically investigated, LPWAN communication technologies are widely preferred. The additional limitations of these technologies, such as two-way communication, can make the integration of DTs even more intractable.

Instead of providing real-time network data to the DT, designing a forecaster that predicts the future packets that the network will generate and providing the DT with the predictions it generates from the historical network data can alleviate these problems and enable the integration of DTs into IoT networks. Based on this idea, our study aims to accurately determine the throughput of the simulation which is designed for the forest fire detection network environment with the help of a forecaster. The DT estimates the throughput of the network employing the forecaster's output. Due to the high physical and hardware demands of the network, such as square kilometers of coverage and dozens of sensor devices, this study was conducted by simulation. First, the simulation was run and the generated packets were obtained. Then, the forecaster was trained with the packets generated at a portion of the simulation. Then, these forecasts were forwarded to DT, and the throughput of the network over time was estimated by the DT model. To evaluate the performance of the system, the actual throughput values obtained from the simulation are compared with the predictions. The throughput of the network is affected by the packets generated and the packet losses in the network. The system needs to understand both of these components accurately in order to make successful predictions. Studies in the literature have shown that successful predictions can be made with techniques like Recurrent Neural Network (RNN) based models in sequence data. In addition, Graph Neural Network (GNN) based DT models in the research can successfully comprehend situations such as traffic and packet loss. Hence, it is thought that the results that will emerge with the cooperation of these models could be successful.

The results obtained show that this system works promisingly, especially for small-scale networks. However, as the number of devices in the network increases, the system's performance decreases critically. This result could be caused by the forecasting error of the whole network, which increases cumulatively with the increasing number

of devices.

In the rest of the paper, we first review the literature on the detection and prevention of forest fires from a network perspective and GNN-based DT studies. Then, in Section, the methodology of the study is described. Results and evaluations are given in Section 4. The last section concludes the paper by giving future directions.

2 LITERATURE SURVEY

2.1 Forest Fire Detection Systems

Early detection of forest fires is critical to reducing their damage. However, detecting fires in minutes when they originate in vast forest areas is arduous. To meet this need, forest fire detection systems utilize satellites, UAVs, and sensors. Since it is not feasible to position satellites to continuously monitor the forest, and as UAVs have limited observation areas and need to be recharged for some time, IoT networks have the fastest fire detection capability among these methods.

IoT networks deployed for forest fire detection can be designed in many different ways. First, it is decided how to detect the fire. While fire detection can be done with affordable sensors such as temperature, CO, and humidity, it can also be done with the help of cameras.

In [3], data such as flame, humidity, and temperature were measured and if the designed algorithm detected a fire situation, alarm packets were sent from the nodes to the database server with location information using satellite communication via SAT-202 module.

Next, network topology and communication technologies should be decided. Depending on the frequency of data sent and the network scale, clustered or mesh topologies are often employed. While fault tolerance is higher in mesh networks, clustered topologies provide scalability. In [4], a hierarchical network structure is designed. Two different types of nodes were preferred: central nodes and sensor nodes. Sensor nodes are connected to each other in a tree structure, with the root node being the central node. Zigbee communication is employed in the sensor nodes, the central node also has the cellular network module to send the data to the server. In another study [5], mesh topology is chosen as a network structure. While all nodes are interconnected with LoRa modules, a gateway device sends all generated packets over the internet to the database server. Thanks to Lora's long-distance communication, the authors stated that they could cover an area of 25 square kilometers for less than \$5000 with 100 sensor nodes.

In addition, inexpensive options for sensor nodes can be implemented in networks with fixed Cluster Heads, while in mesh networks, all nodes usually have similar capabilities. As mentioned earlier, communication techniques typically used in wildfire detection are expected to support long-distance transmission. However, for networks in a relatively small forest where the detection range of sensors is limited,

technologies such as Bluetooth could be preferred. However, this technique would be both expensive and difficult to manage to cover large forest areas. For instance, in [6], ZigBee communication is chosen to transfer packets. Despite a fast 6-minute fire detection, a 560-acre park in the city was covered and a mesh topology was proposed for scenarios with more nodes. Once all decisions have been made, the network is deployed in the forest and the collected data is analyzed. Rule-based fire detection can be done, as well as smart systems that can detect false alarms with Artificial Intelligence (AI) techniques. Although fundamental algorithms that make decisions by checking certain threshold values are sufficient for fire detection, data-driven learning techniques are also popular for systems that can operate with high accuracy with minimal false alarms. In [7] to avoid false alarms, an unsupervised dataset was used to cluster alarms into false and true using the k-means technique. Multiple linear regression models were then trained with these data. In [8], the decision was made by RNN models. The model was trained with the data from sensor nodes and then the incoming data was evaluated with this model and the fire decision was made. Also in [9], a similar study was conducted with ANN models. In this study, instead of two classes such as the presence and absence of fire, different classes such as fire is about to start are also included. Predicting the location of fire spread is also important to reduce its impact. In a study [10], wind sensors and artificial intelligence techniques were used to estimate the area of fire spread.

2.2 GNNs in Computer Networks

The main use of GNNs in computer networks is to model networks with high accuracy. Two different studies compare the performance of GNN-based models with queueing theory modeling [11] [12]. In both studies, GNN-based models significantly outperformed the queueing theory based models.

Thanks to GNNs' real-time and accurate network modeling, many network problems can now be optimized. One area of particular interest is packet routing optimization. In [13], the Deep Reinforcement Learning (DRL) agent optimized packet routing to maximize allocated bandwidth using the network's GNN-based DT. The agent not only outperformed the fluid models but also, unlike these models, was able to adapt to dynamic changes in the network such as link failure, and could be generalized for networks with similar characteristics.

In a similar study [14], a GNN called TwinNet was developed for network optimization. Instead of DRL, a classical optimization algorithm was used to optimize the average per-flow delay. The model worked quite successfully compared to RouteNet and Multi Layer Perceptron (MLP) alternatives. It achieved a Mean Absolute Percentage Error (MAPE) of around 3 percent and an R^2 score of more than

97 percent. In optimization, it has been much more successful than fluid-based models, especially in high-density traffic, since those models cannot model queueing delay.

There are also studies on how to model networks using GNNs. In [15], modular GNN models represented in terms of expressiveness and granularity were designed as xNet. For 3 different usage scenarios, the performance of the proposed model was tested. The model was able to predict delay with a MAPE rate of less than 5 percent for data with sampling intervals of ms.

Network slicing is a technology designed for next-generation network applications where the physical network is divided into virtual networks. GNNs are also utilized in the management of these networks. In [16], a scenario with different delay agreements for different network slices was tested by training a Graph Linformer Network (GLN) based DT with Federated Learning (FL) and using a heuristic optimization method for both delay estimation and meeting these agreements. The model both outperformed state-of-the-art GNNs and was able to meet the Service Level Agreement (SLA) requirements of the optimization algorithm. In [17], end-to-end latency was measured for all slices. It was able to predict DT based on GraphSAGE with less than 5 percent error on all slices. Furthermore, link failures and SLA performance were also tested. In addition, the model was trained for jitter in order to show that DT can be trained faster for a different metric.

GNNs are also used to predict network traffic. In [18], the feature extraction technique was used to derive features from the network data and predict the traffic. Similar performance was achieved with the extracted features and the training time was significantly reduced.

3 OUR WORK

Digital Twin Networks (DTNs) continuously obtain data from the network and predict network parameter(s) according to the data. In this work, topology, traffic, and communication type data are collected from the network, and the throughput of the network is forecasted. On the other hand, in IoT networks, obtaining real-time data from the network is not straightforward. Because IoT networks lack reliable and low-latency communication due to power and budget constraints. Also, it is not possible to detect colluded or interfered packets from received packets at the sink server. The latter problem can be solved by using simulations to gather training data for the DT. For the former one, forecasting the current traffic is proposed. The complete model of the proposed system can be seen in Figure 2.

3.1 Simulator Design

In order to collect data, a custom WSN simulator is designed since it is easier to reach and tailor the collected data format as needed. To be sure about the reliability of

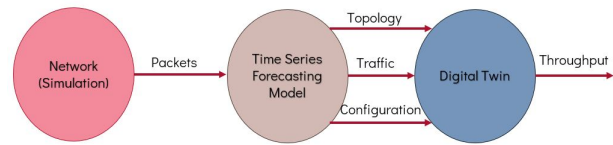


Fig. 2 Model of the System.

the simulator, its results are compared with the results of the OmNet++ simulator for the selected topology and parameters. Since the results of the two simulators are similar, it is concluded that the designed simulator can be used for dataset generation.

Clustered network topology is preferred for the WSNs in our work. Sensor nodes send the packet to the corresponding cluster head via LoRa-like communication technology, and cluster heads aggregate and forward these packets to the server with a GPRS-like radio modulation technique. These communication technologies are chosen because of their long ranges and relatively low power demands. For the path loss model, the Hata model [19] is employed. Sensor nodes and cluster heads are assumed to be installed at 10 meters in height. They are placed on the trees selected randomly. The server’s height is taken as 1000 meters considering variations in the terrain. In the environment, only the thermal noise is calculated, and for simultaneous packets, whether the packet is received successfully is decided based on signal-to-noise and interference ratio (SNIR). Threshold values can be seen in Table 1. The packets of the sensor nodes are considered random events that are generated according to negative exponential distribution. Whereas, cluster heads transmit packets periodically like they are scheduled with TDMA. In case of no received packets, clustered heads may pass their allocated slot without sending a packet. The performance of the model is tested with various number of clustered networks. By changing numbers of clusters, number of sensor nodes, width, and height of the environment, the simulations are repeated. For instance, a 2000x2500 m² area is covered with one cluster network, while a 9-cluster network covers an area of 6000x7500 m². Topologies used in the study can be seen in Figure 3.

The simulator records all transmitted packets with their status, signal strength, transmission start-end times, and source-destination nodes.

3.2 Forecaster Module

The forecaster predicts whether an individual node is transmitting or sleeping at a given time. As sensor nodes sleep most of the time, the problem that the forecaster addresses can be seen as an imbalanced binary classification problem. Therefore, before training the model, undersampling

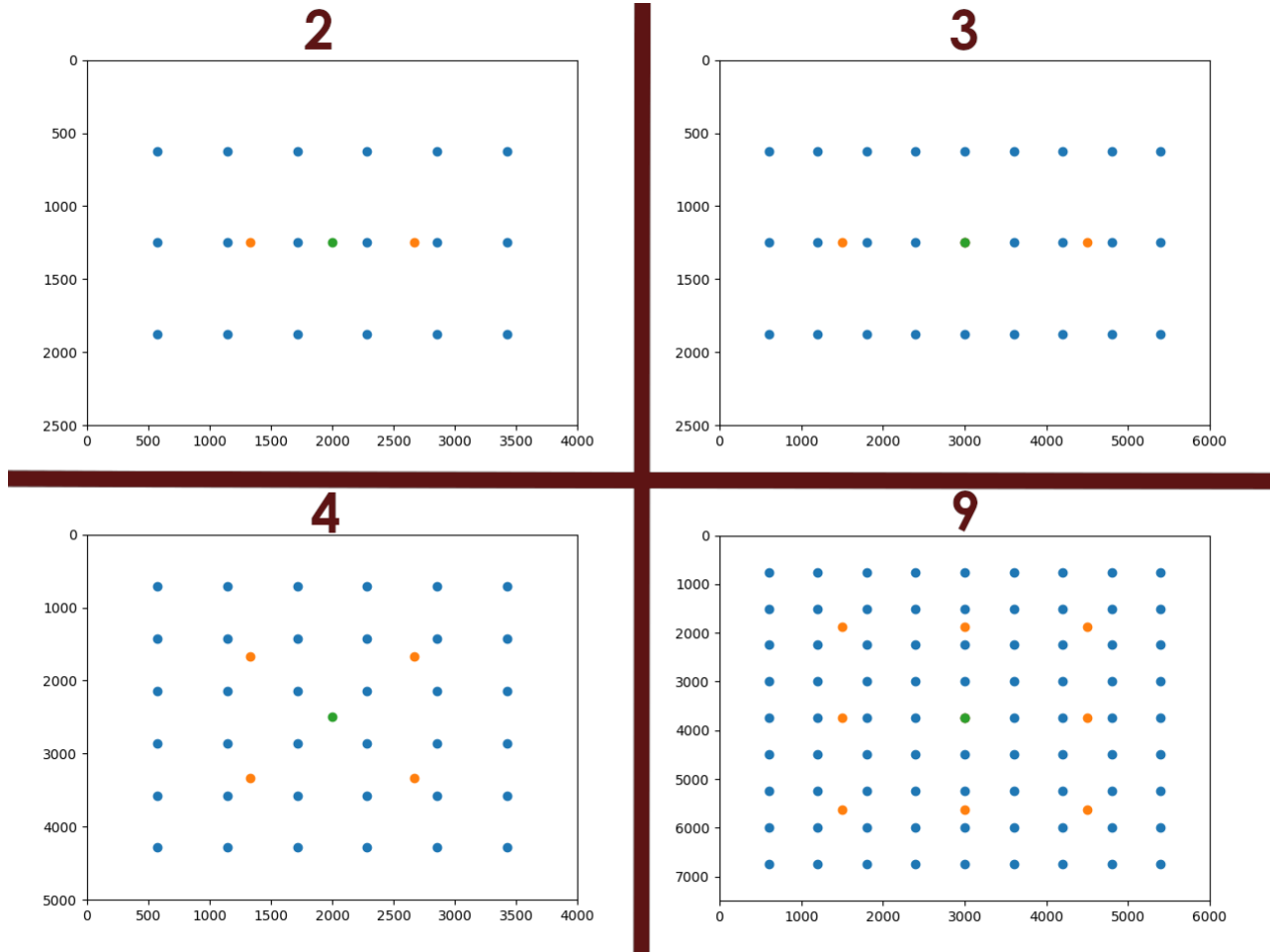


Fig. 3 Various Topologies Tested (having 2, 3, 4, and 9 clusters).

Table 1 Simulation Parameters

Parameter	Value
runtime	24 hrs
packet size	50b
node height	10 meters
GW height	1000 meters
sensor tx power	14 dBm
sensor tx frequency	433 MHz
CH SNIR Threshold	-6 dB
sensor bitrate	5700 Kb/s
mean packet period	1 min
CH min rx power	-130 dBm
GW min rx power	-115 dBm
Temperature	300 K
CH tx power	33 dBm
CH tx frequency	950 MHz
GW SNIR threshold	0 dB
CH bitrate	50000 Kb/s

ted data samples to train the model. A Long-Short Term Memory-based (LSTM) model is chosen for the forecaster. The model has three LSTM layers and one output fully connected layer to predict the state as 0 (sleep) or 1 (transmit). Each LSTM layer has 10 percent dropout rate. From all forecasting results, it is required to retrieve the global state of the network since DT needs it as input. Therefore, after predicting the transmission states of each sensor node and cluster head, the general state of the network including traffic information is constructed. The general state consists of the states of all nodes which are predicted with slight error values. As sleep and transmission states are imbalanced, precision and recall metrics should be considered to decide the performance. F1 score is a metric that combines these two values. The performance of the forecaster is evaluated with the F1 score of the transmit state. Since most of the states are sleep states, the performance of the model for sleep states cannot be trusted.

is applied to the data to prevent bias. Four times as many sleep data samples are randomly selected as the transmit-

3.3 GNN Based Digital Twin

Graph Attention Network (GAT) is used in DTs. After the GAT layer, a four-layered multi-layer perceptron (MLP) is placed to predict the throughput. Therefore, DT has one output. The structure of the model can be seen in Figure 4. This network also has 10 percent dropout ratio. ReLu activation function is applied. A considerably large batch size of 256 is used to train. However, the MLP layers have 128 nodes as the hidden dimension number. The last layer has one node for throughput. Other parameters of the DT can be seen in Table 2. For node attributes, the node type, that is sensor node or cluster head, and the node's status is given to the model. Moreover, the same features are provided for edge attributes.

Table 2 GNN Parameters

Parameter	Value
learning rate	0.001
batch size	256
hidden layer dimension	128
dropout rate	0.1
train ratio	0.8
epoch number	50

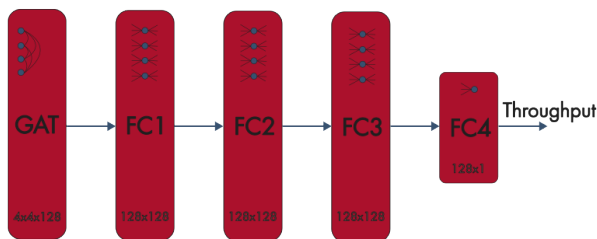


Fig. 4 Structure of the DT.

3.4 How does the System Work?

In the system, traffic was generated in the simulator first. Then, the forecaster was trained by using the a portion of the traffic from the simulator. With, the same packets, DT was also trained. Next, the predictions of the forecaster were fed to the DT to predict the throughput. However, neither the forecaster nor the DT can use the data generated from the previous step directly. Therefore, extra data formation or aggregation steps are added to comply data with the models.

There are five distinct steps of the system. In the first step, packet data is generated with the simulator. The simulator runs the intended simulation and gives reports of generated packets that include: sender and receiver ids, time interval that packet transmits, size of the packet, sig-

nal strength and the receive status of the packet, as it can be seen from Fig 5. The forecaster aims to predict the upcoming packets based on the previous transmissions as in Fig 6. Nevertheless, it is a bit challenging to make this prediction from the simulation report. Thus, the problem is divided into simpler problems that are time series forecasting. To do that, for every node, the node's state, which is either sleep or transmit, is inferred throughout the simulation with predefined sampling intervals. This step is named data augmentation and visualized in Fig 7.

After the augmentation, for every node, time series binary classification is done to predict the future states of the nodes as shown in Fig 8. Yet, as the DT requires the total state of the network to predict the throughput, The entire state of the network must be created from the forecasted states of the nodes for each sampled time that throughput is predicted. The network state generation step creates these states for the DT as shown in Fig 9. Then, finally, the DT predicts the throughput of the network for each generated state. Prediction of DT for an example time sample is demonstrated in Fig 10.

```
12, 36, 0.10568272460712541, 0.18030632452565215, 50, -93.82795462602104, INTERFERED
4, 37, 0.2977671057296664, 0.372511984679166, 50, -93.82795462602104, INTERFERED
28, 39, 0.502746756183371, 0.5763810832426374, 50, -72.26098573014556, SUCCESS
28, 39, 1.1469770499214436, 1.2206113769807099, 50, -72.26098573014556, SUCCESS
8, 36, 3.9479406679361038, 4.021815539193356, 50, -78.71540865496081, SUCCESS
14, 36, 4.2940425854722575, 4.368185096994813, 50, -83.80548606385923, SUCCESS
22, 39, 5.644889517633675, 5.718870448294277, 50, -80.92183722097079, SUCCESS
```

Fig. 5 Generated Packet Reports with Simulator.

```
12, 36, 0.10568272460712541, 0.18030632452565215, 50, -93.82795462602104, INTERFERED
4, 37, 0.2977671057296664, 0.372511984679166, 50, -93.82795462602104, INTERFERED
28, 39, 0.502746756183371, 0.5763810832426374, 50, -72.26098573014556, SUCCESS
28, 39, 1.1469770499214436, 1.2206113769807099, 50, -72.26098573014556, SUCCESS
8, 36, 3.9479406679361038, 4.021815539193356, 50, -78.71540865496081, SUCCESS
14, 36, 4.2940425854722575, 4.368185096994813, 50, -83.80548606385923, SUCCESS
22, 39, 5.644889517633675, 5.718870448294277, 50, -80.92183722097079, SUCCESS

18, 38, 6.829158616441262, 6.903782216359788, 50, -93.82795462602104, INTERFERED
30, 38, 8.475657450405235, 8.550816330854365, 50, -93.82795462602104, INTERFERED
37, 40, 12.0, 12.009778645621509, 50, -50.059535292688224, SUCCESS
22, 39, 14.679678941291861, 14.753659871952465, 50, -80.92183722097079, SUCCESS
```

Fig. 6 Expected Forecasting Operation.

4 RESULTS OBTAINED

In this section, first, the forecaster and DT results are evaluated separately. Then, the performance of the whole system is discussed.

4.1 Performance of the Forecaster

The simulator was run for 24 hours of data transmission for each topology setting. Then, the first 80 percent of the data was used to train the forecaster model. After the training, the forecaster predicted the remaining 20 percent. The results were compared with the ground-truth values collected

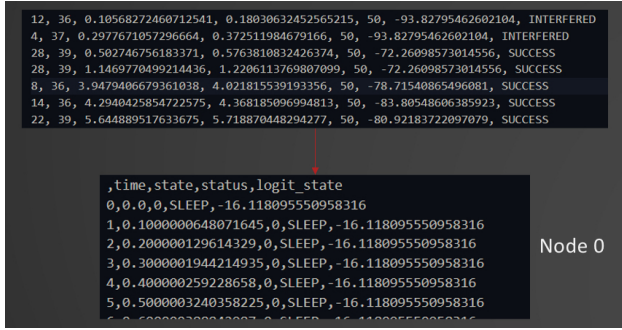


Fig. 7 Data Augmentation for a Node.

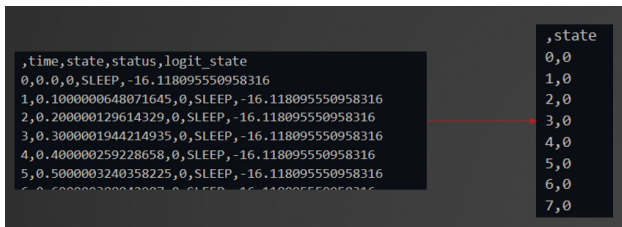


Fig. 8 Forecasting for a Node.

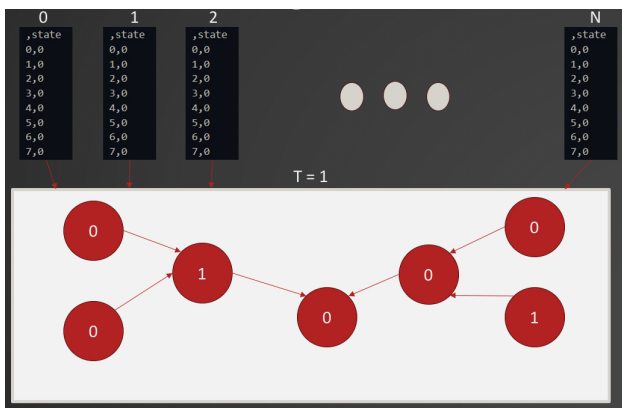


Fig. 9 Network State Generation with Forecasting Results.

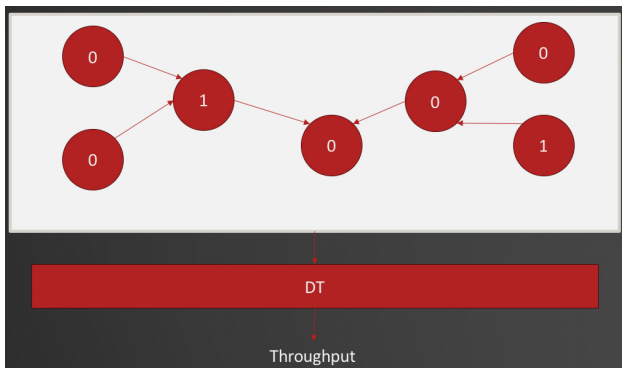


Fig. 10 Throughput Prediction with the DT.

in simulations. The F1 score of the transmission state is calculated to evaluate the model. As forecasting is done for each node separately, the overall result of the forecaster is calculated as the mean and 95 percent confidence interval of all F1 scores of the nodes. The F1 score is calculated as the harmonic mean of the precision and recall values. Since the precision and recall performance of the model is equally important to calculate the throughput accurately, this score is selected as an evaluation metric. It is a prevalent technique for evaluating the performance in imbalanced binary classification problems like the problem that the forecaster solves. Results for the forecaster can be seen in Figure 11. As can be seen, the forecaster can predict the states accurately. Moreover, as the network gets larger, the forecaster's performance is not affected critically. Also, F1 scores of individual nodes in 2-cluster and 3-cluster networks can be observed in Figures 12 and 13, respectively.

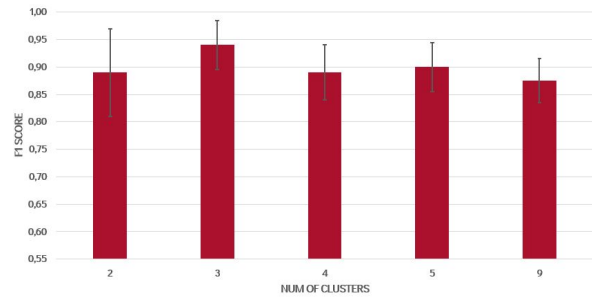


Fig. 11 F1 Scores of Forecaster for Different Topologies.

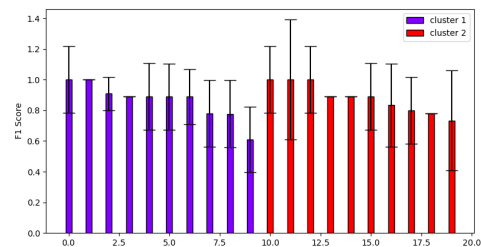


Fig. 12 F1 scores of the nodes in 2 clustered network.

4.2 Performance of the Digital Twin

Ground-truth throughput values were obtained from the simulator. DT also predicted the throughput for test cases following a training. The mean squared error (MSE) and coefficient of determination r -squared (R^2) were used as evaluation criteria for the performance of the DT. The results are given in Figure 14. The GNN-based DT grasps the characteristics of the network as expected. Hence, the R -squared correlation indicator is above 95 percent for all topologies.

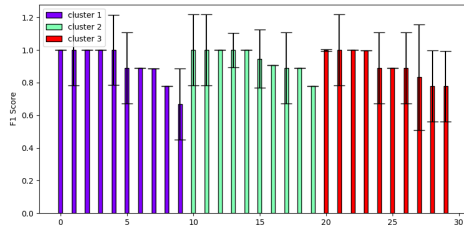


Fig. 13 F1 scores of the nodes in 3 clustered network.

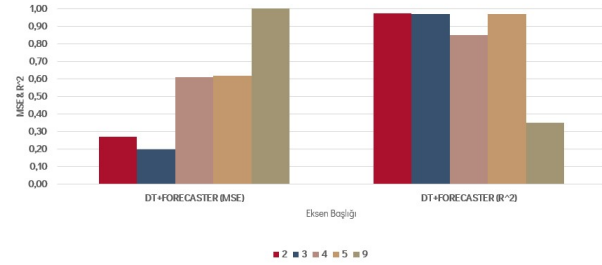


Fig. 15 Performance of the System.

Since the results for all topologies are similar, the scalability of the DT is considered fine.

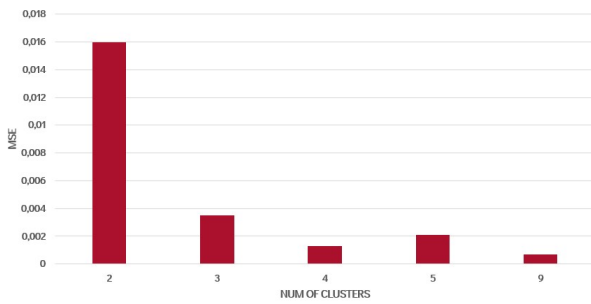


Fig. 14 MSE of the Digital Twin for Different Topologies.

4.3 Performance of the System

To evaluate the integrated performance of the system, the forecaster was run as explained above. In DT, the same training/test split was performed. However, the forecaster’s predictions were used for testing instead of the values obtained from the simulator. The same evaluation metrics were used to test the system’s performance. Figure 15 gives the results of the whole system. Correlation and MSE results do not vary critically for smaller networks. However, the error increases significantly and the r-squared score cannot show the dependency for 9 clustered networks.

Comparing Figures 14 and 15, it can be seen that DT gives significantly varying results when the actual data and the forecast data are employed. Although GNNs are mostly scalable, the whole system’s performance degrades with the increase in the number of nodes here.

The forecaster estimates throughput for each node in the network. Although the prediction performance per node is high, the total error increases as the number of network nodes increases. This causes DT to estimate the throughput with an inaccurate network input. Therefore, the error of the throughput, which is the output of the DT, becomes high. For large networks such as 9 clusters, these estimates are beyond the acceptable limits.

4.4 Effect of Collisions

The results in the previous sections omit the collisions that occurred in the simulations. Although this makes the results unrealistic, the high adaptation and grasping capabilities of GNNs studied by multiple studies in the literature, as well as the system’s performance with the collisions, are expected to be similar. To test the performance difference considering collisions, the system was trained and tested under a collision-enabled simulation environment. In order to integrate collisions with the system, collision information was collected from the simulation and ground truth throughput values were calculated accordingly. As the forecaster module predicts the transmissions of the sensor nodes, collision information is irrelevant to the module. Hence, only the DT was re-trained and used the same forecasting states to better determine the effect of collisions. Results can be seen in Figure 16. As expected, the performance of the system is similar when collisions are considered, because of the GNN’s understanding of spatial information.

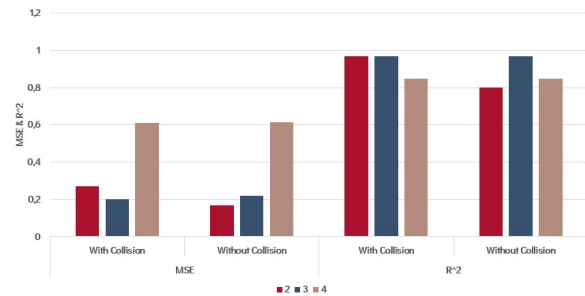


Fig. 16 Collision Effect to the Performance.

5 CONCLUSION

The rise in the average temperature of the world increases the risk of forest fires. Therefore, the importance of forest fire management systems is also increasing. IoT sensor networks are frequently used in these systems to detect forest fires early. However, due to the different requirements of forests, the structures of these networks also vary widely. This requires specific decisions to be made in the manage-

ment of each network. Due to the size of forests, the management of these large networks can be difficult. DT technology can help network administrators in this area. DTs are widely used in computer networks for optimization and test cases. However, DTs are challenging to use in IoT networks due to their continuous communication requirements. This paper proposes a forecaster based mechanism to facilitate such an integration. The proposed model generates the data needed for DT by predicting the network's packets in advance.

In the study, simulations were performed for networks with different number of clusters, and the generated packets were collected. Then, the forecaster, which was trained with these packets, was asked to forecast the upcoming packets. The DT received the packets generated by the forecaster and was expected to determine the throughput at the given instant. The actual throughput values for this duration were also obtained from the simulation and the performance of the system and the modules were evaluated separately.

In the tests, it was observed that the forecaster module correctly recognized the sent packets with an F1 score of approximately 0.9 for each network type. Moreover, the DT module, when trained independently of the forecaster, achieved an MSE score lower than 0.02 and a high R^2 score of 0.8 in each network. In the test of the network's understanding of collisions, the difference between the collision on and off scores is less than 5 percent. However, when the whole system was integrated, the MSE error increased by more than 100 times and the R^2 score dropped below 40 percent for the network with 9 clusters, although similar scores were obtained for the small-scale networks.

The proposed system seems to have a scalability problem. It is assumed that this is due to the accumulation of errors in the individual predictions of all nodes. Currently, we are working to integrate the other state-of-the-art prediction models to the system. Furthermore, a more holistic forecasting approach and a forecasting model based on clusters can be considered as future work. Also, testing the system under different traffic scenarios and environmental conditions could improve the study.

REFERENCES

- [1] OGM. "Official statistics." (accessed: 19/01/2025). (2024), [Online]. Available: <https://www.ogm.gov.tr/tr/e-kutuphane/resmi-istatistikler>.
- [2] V. Chowdary, M. Gupta, and R. Singh, "A review on forest fire detection techniques: A decadal perspective," *International Journal of Engineering & Technology*, vol. 7, p. 1312, Jul. 2018. DOI: 10.14419/ijet.v7i3.12.17876.
- [3] K. Grover, D. Kahali, S. Verma, and B. Subramanian, "Wsn-based system for forest fire detection and mitigation," in *Emerging Technologies for Agriculture and Environment*, B. Subramanian, S.-S. Chen, and K. R. Reddy, Eds., Singapore: Springer Singapore, 2020, pp. 249–260, ISBN: 978-981-13-7968-0.
- [4] A. Molina-Pico, D. Cuesta-Frau, A. Araujo, J. Alejandro, and A. Rozas, "Forest monitoring and wildland early fire detection by a hierarchical wireless sensor network," *Journal of Sensors*, vol. 2016, no. 1, p. 8325845, 2016. DOI: <https://doi.org/10.1155/2016/8325845>. eprint: <https://onlinelibrary.wiley.com/doi/pdf/10.1155/2016/8325845>. [Online]. Available: <https://onlinelibrary.wiley.com/doi/abs/10.1155/2016/8325845>.
- [5] G. Saldamli, S. Deshpande, K. Jawalekar, P. Ghopal, L. Tawalbeh, and L. Ertaul, "Wildfire detection using wireless mesh network," in *2019 Fourth International Conference on Fog and Mobile Edge Computing (FMEC)*, 2019, pp. 229–234. DOI: 10.1109/FMEC.2019.8795316.
- [6] J. Granda Cantuña, D. Bastidas, S. Solórzano, and J.-M. Clairand, "Design and implementation of a wireless sensor network to detect forest fires," in *2017 Fourth International Conference on eDemocracy & eGovernment (ICEDEG)*, 2017, pp. 15–21. DOI: 10.1109/ICEDEG.2017.7962508.
- [7] U. Dampage, L. Bandaranayake, R. Wanasinghe, K. Kottahachchi, and B. Jayasanka, "Forest fire detection system using wireless sensor networks and machine learning," *Scientific Reports*, vol. 12, no. 1, p. 46, Jan. 2022, ISSN: 2045-2322. DOI: 10.1038/s41598-021-03882-9. [Online]. Available: <https://doi.org/10.1038/s41598-021-03882-9>.
- [8] W. Benzekri, A. E. Moussati, O. Moussaoui, and M. Berrajaa, "Early forest fire detection system using wireless sensor network and deep learning," *International Journal of Advanced Computer Science and Applications*, vol. 11, no. 5, 2020. DOI: 10.14569/IJACSA.2020.0110564. [Online]. Available: <http://dx.doi.org/10.14569/IJACSA.2020.0110564>.
- [9] P. Pokhrel and H. Soliman, "Advancing early forest fire detection utilizing smart wireless sensor networks," in *Ambient Intelligence*, A. Kameas and K. Stathis, Eds., Cham: Springer International Publishing, 2018, pp. 63–73, ISBN: 978-3-030-03062-9.
- [10] Imran, N. Iqbal, S. Ahmad, and D. H. Kim, "Towards mountain fire safety using fire spread predictive analytics and mountain fire containment in iot environment," *Sustainability*, vol. 13, no. 5, 2021, ISSN: 2071-1050. DOI: 10.3390/su13052461. [Online]. Available: <https://www.mdpi.com/2071-1050/13/5/2461>.

- [11] M. Ferriol-Galmés, K. Rusek, J. Suárez-Varela, *et al.*, “Routenet-erlang: A graph neural network for network performance evaluation,” in *IEEE INFOCOM 2022 - IEEE Conference on Computer Communications*, 2022, pp. 2018–2027. DOI: 10.1109/INFOCOM48880.2022.9796944.
- [12] M. Ferriol-Galmés, J. Paillisse, J. Suárez-Varela, *et al.*, “Routenet-fermi: Network modeling with graph neural networks,” *IEEE/ACM Transactions on Networking*, vol. 31, no. 6, pp. 3080–3095, 2023. DOI: 10.1109/TNET.2023.3269983.
- [13] P. Almasan, J. Suárez-Varela, K. Rusek, P. Barlet-Ros, and A. Cabellos-Aparicio, “Deep reinforcement learning meets graph neural networks: Exploring a routing optimization use case,” *Computer Communications*, vol. 196, pp. 184–194, Dec. 2022, ISSN: 0140-3664. DOI: 10.1016/j.comcom.2022.09.029. [Online]. Available: <http://dx.doi.org/10.1016/j.comcom.2022.09.029>.
- [14] M. Ferriol-Galmés, J. Suárez-Varela, J. Paillissé, *et al.*, “Building a digital twin for network optimization using graph neural networks,” *Computer Networks*, vol. 217, p. 109329, 2022, ISSN: 1389-1286. DOI: <https://doi.org/10.1016/j.comnet.2022.109329>. [Online]. Available: <https://www.sciencedirect.com/science/article/pii/S1389128622003681>.
- [15] M. Wang, L. Hui, Y. Cui, R. Liang, and Z. Liu, “Xnet: Improving expressiveness and granularity for network modeling with graph neural networks,” in *IEEE INFOCOM 2022 - IEEE Conference on Computer Communications*, 2022, pp. 2028–2037. DOI: 10.1109/INFOCOM48880.2022.9796726.
- [16] M. Abdel-Basset, H. Hawash, K. M. Sallam, I. Elgendi, and K. Munasinghe, “Digital twin for optimization of slicing-enabled communication networks: A federated graph learning approach,” *IEEE Communications Magazine*, vol. 61, no. 10, pp. 100–106, 2023. DOI: 10.1109/MCOM.003.2200609.
- [17] H. Wang, Y. Wu, G. Min, and W. Miao, “A graph neural network-based digital twin for network slicing management,” *IEEE Transactions on Industrial Informatics*, vol. 18, no. 2, pp. 1367–1376, 2022. DOI: 10.1109/TII.2020.3047843.
- [18] H. Shin, S. Oh, A. Isah, I. Aliyu, J. Park, and J. Kim, “Network traffic prediction model in a data-driven digital twin network architecture,” *Electronics*, vol. 12, no. 18, 2023, ISSN: 2079-9292. DOI: 10.3390/electronics12183957. [Online]. Available: <https://www.mdpi.com/2079-9292/12/18/3957>.
- [19] M. Hata, “Empirical formula for propagation loss in land mobile radio services,” *IEEE Transactions on Vehicular Technology*, vol. 29, no. 3, pp. 317–325, 1980. DOI: 10.1109/T-VT.1980.23859.

Development of a Greedy Auction-Based Distributed Task Allocation Algorithm for UAV Swarms with Long Range Communication

Erdem Can¹ , Mustafa Namdar¹ , and Arif Basgumus² 

¹ Department of Electrical and Electronics Engineering, Kutahya Dumlupinar University, Kutahya, 43100, Turkey

² Department of Electrical and Electronics Engineering, Bursa Uludag University, Bursa, 16059, Turkey

Abstract: This study proposes a greedy auction-based distributed task allocation algorithm (GCAA) for swarm unmanned aerial vehicles (UAVs) with long range (LoRa) communication capabilities. Air-to-air (A2A) communication channels are established using LoRa technology to enable inter-agent communication, while air-to-ground (A2G) communication is facilitated through narrowband Internet of Things (NB-IoT) technology. The negotiation phase is conducted over these communication channels. Using LoRa and NB-IoT parameters, a link budget analysis is performed to determine the A2A reference distance, and a k-means clustering algorithm is developed. The proposed algorithm places base stations at cluster centers and prepares a simulation environment. The decentralized algorithm is compared with a greedy optimization algorithm under uninterrupted and interrupted communication scenarios, and the simulation results are presented in MATLAB. The developed distributed task allocation algorithm demonstrates lower system costs and shorter task completion times compared to the conventional greedy optimization algorithm. Additionally, the performance parameters exhibit more excellent stability in cumulative distribution functions.

Keywords: Greedy auction-based distributed task allocation algorithm, A2A/A2G communication, LoRa, NB-IoT.

Uzak Mesafe Haberleşmesine Sahip İHA Sürüleri için Açgözlü Açık Artırma Temelli Dağıtılmış Görev Tahsis Algoritmasının Geliştirilmesi

Özet: Bu çalışmada uzak mesafe (long range, LoRa) iletişimine sahip sürü insansız hava araçlarında (İHA) açgözlü açık artırma temelli dağıtık görev tahsis algoritması (greedy auction-based distributed task allocation algorithm, GCAA) önerilmiştir. Ajanlar arası haberleşmesinin sağlanabilmesi için LoRa teknolojisi kullanılarak havadan havaya (air-to-air, A2A), dar bant nesnelerin interneti (narrowband Internet of Things, NB-IoT) teknolojisi kullanılarak da havadan yere (air-to-ground, A2G) haberleşme kanalları oluşturulmuş ve müzakere aşaması bu haberleşme kanallarından sağlanmıştır. LoRa ve NB-IoT parametreleri kullanılarak hat bütçe analizi ile A2A referans mesafesi ve k-ortalama kümeleme algoritması geliştirilmiştir. Geliştirilen algoritma ile küme merkezlerine baz istasyonları yerleştirilerek, simülasyon ortamı hazırlanmıştır. Önerilen merkezi olmayan algoritma ile haberleşmenin kesintisiz ve kesintili olduğu ortamda açgözlü optimizasyon algoritması ile karşılaştırılarak, MATLAB ortamında benzetim sonuçları aktarılmıştır. Geliştirilen dağıtık görev tahsis algoritması, geleneksel açgözlü optimizasyon algoritmasına göre sistem maliyetinin ve görev bitirme süresinin daha kısa olduğu gözlenmiştir. Aynı zamanda performans parametrelerinin, birikimsel dağılım fonksiyonlarında daha kararlı olduğu gözlenmiştir.

Anahtar Kelimeler: Açgözlü açık artırma temelli dağıtık görev tahsis algoritması, A2A/A2G haberleşme, LoRa, NB-IoT.

RESEARCH PAPER

Corresponding Author: Mustafa Namdar, mustafa.namdar@dpu.edu.tr

Reference: E. Can, M. Namdar, and A. Basgumus, (2025), "Development of a Greedy Auction-Based Distributed Task Allocation Algorithm for UAV Swarms with Long Range Communication," *ITU-Journ. Wireless Comm. Cyber.*, 2, (1) 37–44.

Submission Date: Mar, 14, 2025

Acceptance Date: Mar, 18, 2025

Online Publishing: Mar, 28, 2025

1 INTRODUCTION

Algorithms used to solve task assignment problems are divided into centralized and distributed decision-making algorithms. In centralized task assignment algorithms, the coordinator manages all task assignments, and thus, conflicts are prevented, and optimum solutions are obtained. In distributed algorithms, there is no coordinator agent, and task sharing is carried out in a distributed manner due to negotiations between agents [1], [2].

Greedy algorithms do not require specific knowledge of the problem they are interested in. They do not require too many control parameters and are suitable for working harmoniously with the operator [3]. In multi-agent systems, the greedy algorithm focuses on the individual benefits of the agents. It aims to maximize the individual return without negotiation between the agents. In [4], the authors have improved the task completion and road coverage in unmanned aerial vehicles (UAVs) using the greedy method. However, since this method is not a negotiation-based algorithm, the UAVs do not share the tasks, and the system performs their optimization. In [5], they developed a distributed task-sharing algorithm by combining the optimization and greedy algorithms. However, the processing load is heavy due to the complex algorithm layout. A decentralized greedy auction-based distributed task allocation algorithm (GCAA) has been proposed in [6]. This study observes an increase in the system cost because more than one agent executes a task. However, communication parameters are not used during task sharing.

In this study, the GCAA algorithm is developed for UAV swarms that communicate long-distance. In order for agents to communicate with each other in the air, air-to-air (A2A) and when A2A communication distance is not sufficient, air-to-ground (A2G) communication channels are established via the base station (BS). The proposed algorithm aims to provide long-distance communication between agents, minimum agent cost, and average signal-to-noise ratio (SNR) values. In the second section of the study, the performance criteria of A2A and A2G communication channels include the maximum communication distances of agents using long range (LoRa) and narrowband Internet of Things (NB-IoT) communication technologies. In the third section of this study, the developed GCAA algorithm is presented. The proposed algorithm consists of four functions. The first function determines the BS locations depending on the tasks using the k-means clustering method. The second function controls the best task selections of the agents. The third function realizes the communication channels for the agents' communication and the primary task sharing. Finally, the last function completes the algorithm by performing the secondary task sharing of the agents. The advantages and disadvantages of the proposed distributed decision-making algorithm and the simulation results with the traditional greedy optimization algo-

gorithm are given in section 4. In the last section, the obtained results are evaluated.

2 DISTANCE ANALYSIS in A2A and A2G for UAVs

This section investigates distance analysis in A2A and A2G communication systems, focusing on signal power calculations, path loss models, and key performance metrics used in UAV networks, including determining the maximum communication range.

2.1 A2A Communication

A2A communication refers to the communication between two or more vehicles in the air. In A2A communication, performance metrics are determined using the two-ray path loss model. In the communication system, the signal power reaching the receiver from the transmitter is shown in (1). Here are wavelength (λ), communication distance (d), transmitter power (P_t), transmitter antenna gain (G_t), receiver antenna gain (G_r), transmitter antenna height (h_t), and receiver antenna height (h_r) [7]–[13],

$$P_r(w) = \frac{\lambda^2}{(4\pi d)^2} 4 \sin^2 \left(\frac{2\pi h_r h_t}{\lambda d} \right) G_r G_t P_t. \quad (1)$$

If the condition of $d\lambda \gg 4h_r h_t$ and $\sin(x) \approx x$ approximation is applied, (1) can be re-written as (2)

$$P_r(w) = P_t G_t G_r \frac{h_r^2 h_t^2}{d^4}. \quad (2)$$

2.2 A2G Communication

A2G communication is used in cases where air vehicles can communicate with targets on the ground or with systems controlled from the ground station [14]–[17]. In A2G communication, performance measurements were determined using the Okumura-Hata model. The Okumura-Hata model is a modified version of the Okumura model that operates in the frequency range of 150 MHz to 1.5 GHz and a distance of 1-100 km. The BS height (h_b) is 30 m to 100 m, while the mobile station height (h_m) is 1 m to 10 m. The path loss for urban areas is given in (3). The operating frequency (f_c) unit is defined in MHz, while (d) is in km, (h_b) and (h_m) are in meters [18]–[20],

$$L_p(\text{urban}) = 69.55 + 26.16 \log(f_c) - 13.82 \log(h_b) - a(h_m) + [44.9 - 6.55 \log(h_b)] \log(d). \quad (3)$$

For smaller cities, $a(h_m)$ can be expressed as in (4)

$$a(h_m) = (1.1 \log(f_c) - 0.7)h_m - (1.56 \log(f_c) - 0.8). \quad (4)$$

In rural or open areas, (3) can be expressed as in (5),

$$L_P(\text{rural}) = L_P(\text{urban}) - 4.78[\log(f_c)]^2 + 18\log(f_c) - 40.94. \quad (5)$$

The received signal power can be concluded as follows

$$P_r(\text{dBm}) = P_t(\text{dBm}) + G_t + G_r - L_P(\text{rural}). \quad (6)$$

SNR is a widely used metric for measuring signal quality in a communication system, as shown by (7). $P_r(w)$ represents the power received by the receiver, and σ^2 represents the thermal noise power,

$$\text{SNR}(w) = \frac{P_r(w)}{\sigma^2(w)}. \quad (7)$$

2.3 Communication Range

Receiver sensitivity is the minimum power level at which the receiver can demodulate and extract the transmitted information from the received weak signal. Due to the innovative modulation scheme, LoRa and NB-IoT systems have low receiver sensitivity. Receiver sensitivity depends on the bandwidth (BW), SNR, and receiver noise factor (NF). At room temperature, it is shown as (8) [17], [19]–[22],

$$R_{\text{sens}}(\text{dBm}) = -174 + 10\log(\text{BW}) + \text{NF} + \text{SNR}. \quad (8)$$

The link margin between the received power and receiver sensitivity is given in (9) to ensure secure communication,

$$\text{LinkMargin}(\text{dB}) = P_r - R_{\text{sens}}. \quad (9)$$

The noise factor as $\text{NF}(\text{dB}) = 10\log(F_{\text{total}})$, is the total amount of power added by the radio frequency (RF) front end at the receiver to the thermal noise power at the input where

$$F_{\text{total}} = F_1 + \frac{F_2 - 1}{G_1} + \frac{F_3 - 1}{G_1 G_2} + \dots + \frac{F_N - 1}{G_1 G_2 \dots G_{N-1}}. \quad (10)$$

Here, $F_{1,\dots,N}$ represents the linear noise factor of the RF stages, and $G_{1,\dots,N-1}$ represents the linear gain of these stages.

Table 1 LoRa and NB-IoT parameters

Parameters	LoRa	NB-IoT
Frequency (MHz)	868	800
Bandwidth (kHz)	125	180
Rx sensitivity (dBm)	-139.5	-129
Transmitted power, P_t (dBm)	14	23
Thermal noise power, σ^2	5.01×10^{-23}	3.98×10^{-21}
Receiver antenna gain, G_r	1	1
Transmitter antenna gain, G_t	1	1
Link margin (dB)	10	10
Agent speed (m/s)	1	1
Agent height (h_t, h_m, h_r) (m)	10	10
Base station height, h_b (m)	30	30

In this study, LoRa is used by UAVs, and BSs use NB-IoT. SX1301 parameters are taken as LoRa gateway, and Quectel BC95-G parameters are taken as NB-IoT references. The spreading factor (SF) is assumed to be 12 for long-distance communication. LoRa, NB-IoT, and UAV parameters are presented in Table 1 [22], [23].

3 GREEDY AUCTION-BASED DISTRIBUTED TASK ALLOCATION ALGORITHM

The k-means algorithm is centralized. This method starts with random ‘k’ cluster centers. Starting points affect the clustering process and results. Euclidean and similar distance functions measure object similarity [24], [25].

The clusters and centers of the tasks are determined with the proposed k-means algorithm (Algorithm 1). The d_{\min} and d_{\max} explained in Algorithm 1 represent the minimum and maximum communication distance. The minimum reference distance is the maximum communication range between agents, as shown in (11). The maximum reference distance is the maximum range agents communicate with the BS and is given in (12).

$$\log(d_{\min}) = \frac{L_P + 10\log(G_t G_r) + 20\log(h_t h_r)}{40}, \quad (11)$$

$$\log(d_{\max}) = \frac{A + B}{44.9 - 6.55\log(h_b)} \quad (12)$$

where $A = L_P(\text{rural}) - 27.81 - 46.05\log(f_c) + 13.82\log(h_b)$ and $B = (1.1\log(f_c) - 0.7)h_m + 4.78(\log(f_c))^2$.

Algorithm 1 k-means Clustering Algorithm

```

1 function CLUSTERING( $T, k = 10, d_{\min}, d_{\max}$ )
2    $T = \{t_1, t_2, \dots, t_n\}$ ,  $t_i = (x_i, y_i)$   $\triangleright$  Randomly initialize task points
3    $C = \{c_1, c_2, \dots, c_k\}$ ,  $c_i = (x_i, y_i)$   $\triangleright$  Randomly initialize cluster centers
4    $\text{id}_x(i) \leftarrow \arg \min d(t_i, c_j)$ ,  $\forall t_i \in T$   $\triangleright$  Find the nearest cluster center for each task
5   while true do
6     for  $i \in [1, k]$  do
7       if cluster_element is not empty then
8          $C_j = \frac{1}{|S_j|} \sum_{t_i \in S_j} t_i$ ,  $S_j = \{t_i \mid \text{id}_x(i) = j\}$   $\triangleright$  Update cluster centers
9       else
10        Select a random cluster center
11      end if
12    end for
13    for  $i \in [1, T]$  do  $\triangleright$  Check the distance between tasks and cluster centers
14      if  $d(t_i, c_{\text{id}_x(i)}) < d_{\min}$  then
15        Search for another cluster center
16      else if  $d_{\min} \leq d(t_i, c_j) \leq d_{\max}$  then
17        Assign the task to this cluster
18      else
19         $k = k + 1$ ,  $C = C \cup \{c_{\text{new}}\}$   $\triangleright$  Add a new cluster
20      end if
21    end for
22    if  $d_{\min} \leq d(c_i, c_j) \leq d_{\max}$  then  $\triangleright$  Check the distance between cluster centers
23      break
24    else
25       $k = k - 1$   $\triangleright$  Remove unnecessary clusters
26    end if
27  end while
28 end function
    
```

Algorithm 2 Greedy Auction-Based Task Allocation Algorithm

```

1 function TASKALLOCATION(Clustering(), BestTask(), CommunicationChannel(),
  SecondaryTask())
2    $\tau = 1$  ▷ Iteration counter
3   Clustering( $T = 30, 50$ )
4   BestTask(0) = 0
5   CommunicationChannel(0) = 0
6   SecondaryTask(0) = 0
7   while not empty( $T$ ) or not empty( $u_{xy}$ ) do
8     BestTask( $\tau$ )
9     CommunicationChannel( $\tau$ )
10    SecondaryTask( $\tau$ )
11     $\tau \leftarrow \tau + 1$ 
12  end while
13 end function
    
```

Algorithm 3 Selecting the Best Task

```

1 function BESTTASK( $T$ )
2   for  $i \in [1, u_n]$  do
3      $t = \frac{dt}{v}$  ▷ Drag energy
4      $dt = \sqrt{(u_x(t) - T_x(t))^2 + (u_y(t) - T_y(t))^2}$ 
5      $E_i = \frac{1}{2} C_D \rho v^3 S_i$ 
6      $H_i = (P_{D0} - E_i)$ 
7      $b_i(t) \leftarrow \max(H_i)$ 
8      $idx_A(t) \leftarrow \arg \max(H_i)$ 
9   end for
10 end function
    
```

The greedy auction-based distributed task allocation algorithm (Algorithm 2) is a negotiation algorithm that tries to make the best short-term decision that maximizes the individual benefits of the agents. The auction process is the first stage of the algorithm. Each agent calculates its costs for all tasks with the published task coordinates. The calculated cost values are subtracted from the agent's utility value P_{D0} to determine individual benefits (remaining energy). The b_i set of the relevant agent is updated by taking the maximum value of the determined benefits. This set also represents the agent's utility for the task it requests. The idx_A value defines the task number the agent requests. The auction stage of the agents and the best task selection are presented in Algorithm 3.

Agents calculate the distance between the starting point and the desired task and create a return E_b cost matrix. If the remaining energy value of the agents is less than the return energy, the agent is disabled and returns to the starting position. If the remaining energy value of the agents is more than the return energy, the agent broadcasts a Y_A message. When the agents broadcast the same task and, therefore, the same Y_A value, the negotiation process begins. During the negotiation process, agents first broadcast their locations. Agents calculate the distance between them according to the broadcasted location values. Agents within the d_{min} reference distance perform A2A communication among themselves and share tasks due to the negotiation process. The negotiation process with A2G communication through the defined BS to prevent interruption of communication and increase in system cost is presented in Algorithm 4.

Algorithm 4 Communication Channels and Primary Task Sharing

```

1 function COMMUNICATIONCHANNEL( $idx_A(\tau), b_i(\tau)$ )
2    $d_B = \sqrt{(x_{B_i} - idx_{A_{x_i}})^2 + (y_{B_j} - idx_{A_{y_j}})^2}$ 
3    $t_b = R_B / v$ 
4    $E_b = \frac{1}{2} C_D \rho v^3 S_b$ 
5   if  $b_i > E_b$  then
6      $Y_A(t) = idx_{A_i}$ 
7   else
8     Broadcast the number of the disabled agent
9   end if
10  if  $Y_{A_i}(t) == Y_{A_j}(t)$  then
11     $d_k = \sqrt{(u_{x_i}(t) - u_{x_j}(t))^2 + (u_{y_i}(t) - u_{y_j}(t))^2}$ 
12    if  $d_k < d_{min}$  then
13      comA2A( $\tau$ ) =  $[u_i, u_j]$ 
14      Broadcast numbers of agents communicating via A2A
15    else
16      comA2G( $\tau$ ) =  $[u_i, u_j]$ 
17      Broadcast numbers of agents communicating via A2G
18    end if
19    if agents communicate only via A2A then
20      for  $i \in [1, \text{comA2A}_n]$  do
21        if  $d_k \lambda \geq 4h_i h_r$  then
22          Equation (1), Equation (7)
23        else
24          Equation (2), Equation (7)
25        end if
26        Broadcast  $b_i$  values of agents participating in bilateral negotiations
27        Broadcast the numbers of winning and losing agents
28        if  $\text{comA2A}_W \cup \text{comA2A}_L$  then
29          The agent cannot receive a task
30        else
31          The agent whose task assignment is finalized in bilateral negotiations broadcasts its number
32           $P_{D0i} = b_i(\text{comA2A}_W, u_{xy}(t) = T(idx_A))$ 
33          Broadcast the number of the agent who lost the bilateral negotiation ( $P_{D0i} = 0$ )
34        end if
35      end for
36    else if agents communicate via both A2A and A2G then
37      for  $i \in [1, \text{comA2A}_n$  and  $\text{comA2G}_n]$  do
38        if  $\text{comA2A}_n$  then
39          if  $d_k \lambda \geq 4h_i h_r$  then
40            Equation (1), Equation (7)
41          else
42            Equation (1), Equation (7)
43          end if
44        else
45          if  $\text{comA2G}_n$  then
46             $P_r(w) = 10^{(P_r(\text{dBm})/10) - 3}$ 
47            Equation (7)
48          end if
49        end if
50      end for
51      Broadcast the number of the agent who won the task in A2A comm.
52      Broadcast the number of the agent who won the task in A2G comm.
53      The common winner in A2A and A2G communication wins the task and broadcasts its number
54       $P_{D0i} = b_i(\text{comA2A}_W \cap \text{comA2G}_W, u_{xy}(t) = T(idx_A))$ 
55       $P_{D0i} = 0$ 
56    else if agents communicate only via A2G then
57      for  $i \in [1, \text{comA2G}_n]$  do
58        if  $\text{comA2G}_n$  then
59           $P_r(w) = 10^{(P_r(\text{dBm})/10) - 3}$ 
60          Equation (7)
61        end if
62        Broadcast  $b_i$  values of agents participating in bilateral negotiations
63        Broadcast the numbers of winning and losing agents
64        if  $\text{comA2G}_W \cup \text{comA2G}_L$  then
65          The agent cannot receive a task
66        else
67          The agent whose task assignment is finalized in bilateral negotiations broadcasts its number
68           $P_{D0i} = b_i(\text{comA2G}_W, u_{xy}(t) = T(idx_A))$ 
69          Broadcast the number of the agent who lost the bilateral negotiation ( $P_{D0i} = 0$ )
70        end if
71      end for
72    end if
73  end if
74 end function
    
```

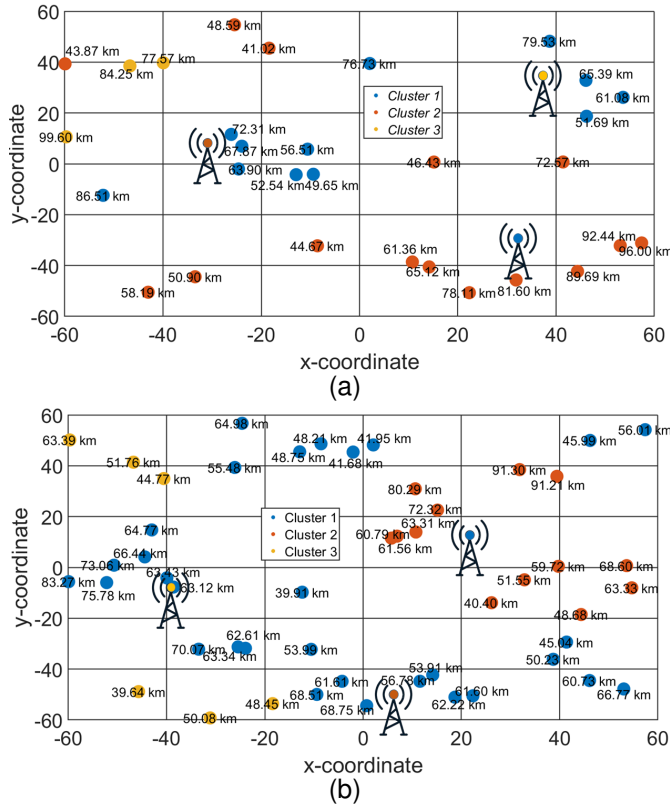



Fig. 1 BS and task positions a) 30 tasks, b) 50 tasks.

In the first stage of task sharing, the agents that lost due to the negotiation publish their numbers. In the first negotiation stage, the losing agents are subjected to the second negotiation process to not fall behind the other agents in the swarm and maximize individual benefit. In this stage, only the losing agents share the remaining tasks while the others wait to execute the tasks they won. The second stage of negotiation is presented in Algorithm 5. The BS and task sets determined in Algorithm 1 are presented in Fig. 1.

4 NUMERICAL RESULTS

The simulation results of the designed algorithm in MATLAB environment are presented on a Windows 11 operating system computer with an Intel Core i7-12700H processor, NVIDIA GeForce RTX 3050 graphics card, and 16 GB RAM hardware. The system cost, SNR values of communication channels, and agent task completion times are taken as reference for the developed algorithm. The performance metrics taken as reference for the developed algorithm are compared with the greedy optimization algorithm in the uninterrupted communication environment and the environment without A2G communication.

For agents to be able to communicate A2A and A2G, the maximum reference distances were calculated as $d_{min} = 38.681$ km and $d_{max} = 145.02$ km using (11) and (12). However, since the Okumura-Hata model works 0-100 km, the simulation was run at a reference distance of d_{max} 100 km.

Algorithm 5 Secondary Task Assignment

```

1 function SECONDARYTASK( $P_{D0i} = 0$ , CommunicationChannel())
2    $P_{D0i} = []$ ,  $u_{xy} = []$ ,  $T = []$ 
3   while any( $P_{D0i} == 0$ ) do
4     BestTask( $P_{D0i} = 0$ )
5     CommunicationChannel( $P_{D0i} = 0$ )
6   end while
7 end function
    
```

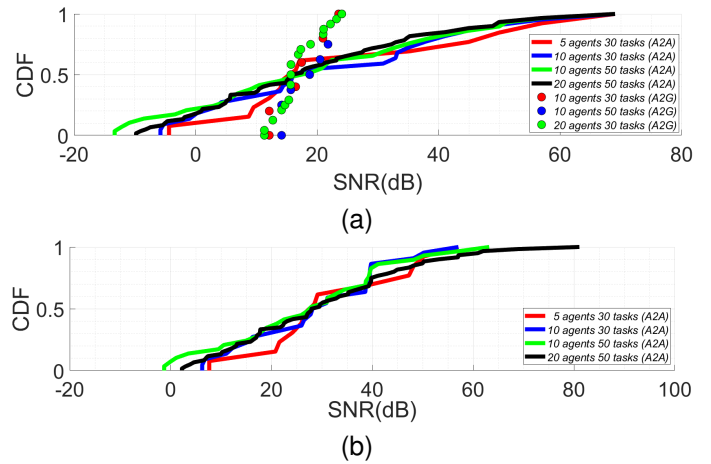


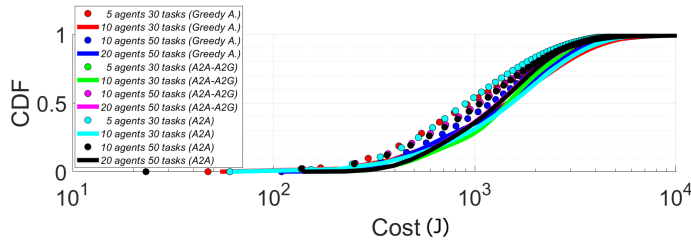
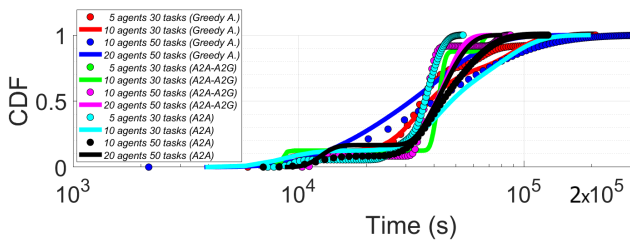
Fig. 2 Cumulative distribution function (CDF) of the communication channel during bilateral negotiation a) A2A-A2G environment b) Only A2A environment.

The cumulative distribution function of the communication channel during bilateral negotiation is shown in Fig. 2. In all simulation environments, the distributed decision-making algorithm, including A2G and A2A communication, observed an average SNR value of 22.427 dB in A2A communication and an average SNR value of 18.083 dB in A2G communication. The distributed decision-making algorithm, including only A2A communication, observed an average SNR value of 28.481 dB.

The number of bilateral negotiations varies according to the communication environments where the agents are located. In the 5-agent 30-task system, it was observed that the number of bilateral negotiations was equal in the environment containing A2A and A2G communication and in the environment containing only A2A communication, and the negotiations contained only A2A communication. It was observed that the algorithm containing only an A2A communication medium showed lower density at lower costs compared to the greedy optimization algorithm. It was observed that the algorithm containing an A2A-A2G communication medium could reach the same density level at a lower cost than the greedy optimization algorithm. When we look at the general cost, the distributed task allocation algorithm containing the uninterrupted communication medium reached the saturation level with a lower cost than the other two algorithms, as presented in Fig. 3.

Table 2 Algorithms' performances for different scenarios

	5 Agents 30 Tasks			10 Agents 30 Tasks			10 Agents 50 Tasks			20 Agents 50 Tasks		
	Greedy Algorithm	GCAA (A2A-A2G)	GCAA (A2A)	Greedy Algorithm	GCAA (A2A-A2G)	GCAA (A2A)	Greedy Algorithm	GCAA (A2A-A2G)	GCAA (A2A)	Greedy Algorithm	GCAA (A2A-A2G)	GCAA (A2A)
Iterations	8	9	9	4	3	4	6	6	6	3	3	3
Tasks	28	30	30	30	30	30	50	50	50	50	50	50
Messages	78	151	151	146	428	425	201	486	470	320	1989	1918
Cost (J)	4.535×10^4	3.878×10^4	3.878×10^4	6.232×10^4	5.898×10^4	6.628×10^4	8.175×10^4	7.105×10^4	7.223×10^4	8.175×10^4	7.105×10^4	7.223×10^4
Time (s)	7.242×10^5	6.26×10^5	6.26×10^5	3.712×10^5	3.238×10^5	4.184×10^5	5.483×10^5	4.548×10^5	5.389×10^5	2.019×10^5	2.283×10^5	2.34×10^5
Active Agents	0	1	1	4	3	4	5	5	5	20	20	20
Same Task Preference	0	13	13	0	0	3	0	0	3	0	0	6
Pairwise Negotiations	-	-	-	-	27	22	-	37	29	-	84	60
A2A Average SNR (dB)	-	26.481	26.481	-	23.456	29.568	-	20.104	27.652	-	19.667	30.224
A2G Average SNR (dB)	-	-	-	-	18.116	-	-	19.154	-	-	16.980	-


Fig. 3 Cumulative distribution function for task cost.

Fig. 4 Cumulative distribution function for task completion time.

It is observed that the greedy optimization algorithm shows changes in time performance with the increase in the number of tasks. The algorithm that only includes A2A communication is observed to have the longest completion time in the 50-task system. It is observed that the A2G-A2A algorithm offers a more stable completion time compared to the other two algorithms. The curves show a more controlled and steep increase, and the task completion speed increases after a certain period, whereas the curve shifts to the right more as the number of tasks increases (50 tasks), as observed in Fig. 4. The performance values of the greedy optimization and auction-based distributed task allocation algorithms are presented in Table 2.

5 CONCLUSION

This study proposes a distributed task allocation algorithm solution for swarm UAVs with long-distance communication. Simulation results for the proposed algorithm are evaluated through the parameters of the number of agents, number of tasks, task location, BS locations, A2A reference distance, and initial energy of the agents. When the distributed decision-making algorithm tested in MATLAB environment is compared with the optimization algorithm, it is seen that the system cost, the number of disabled agents, and the

task duration are less depending on the system parameters. At the same time, while the greedy optimization algorithm is a faster and more effective method for small and medium-sized tasks, it is observed that the developed distributed decision-making algorithm provides more balanced performance in variable task sets. It is observed that the optimization algorithm performs better in the number of messages broadcasted. In the distributed decision-making algorithm where communication is limited, it is concluded that some agents choose the same task, and the performance values are lower than the A2G-A2A distributed algorithm. It is observed from the simulation results that the active agents complete the tasks that the disabled agents cannot complete.

AUTHOR CONTRIBUTIONS

The authors Erdem Can contributed to the writing, investigation, and software; Mustafa Namdar and Arif Basgumus contributed to the methodology, validation, and editing.

REFERENCES

- [1] E. Can, B. I. Kirklar, M. Namdar, and A. Basgumus, "Deep learning based target tracking and diving algorithm in kamikaze UAVs," in *Innovations in Intelligent Systems and App. Conf. (ASYU)*, 2024, pp. 1–6. DOI: 10.1109/ASYU62119.2024.10757004.
- [2] E. Can, Z. Yildirim, Y. Kaya, M. Eser, M. Namdar, and A. Basgumus, "Development of greedy auction-based distributed decision-making algorithm and agent communication language in swarm unmanned aerial vehicles," in *IEEE National Conf. on Electrical and Electronics Eng. (ELECO)*, 2024, pp. 1–5. DOI: 10.1109/ELECO64362.2024.10847247.
- [3] Y. Demir, "Tekrarli acgozlu algoritma uzerine kapsamli bir analiz," *Journal of the Institute of Science and Technology*, vol. 11, no. 4, pp. 2716–2728, 2021. DOI: 10.21597/jist.935652.
- [4] Y. Jia, S. Zhou, Q. Zeng, *et al.*, "The UAV path coverage algorithm based on the greedy strategy and ant colony optimization," *Electronics*, vol. 11, no. 17, p. 2667, 2022. DOI: 10.3390/electronics11172667.

- [5] J. Zhou, X. Zhao, X. Zhang, D. Zhao, and H. Li, "Task allocation for multi-agent systems based on distributed many-objective evolutionary algorithm and greedy algorithm," *IEEE Access*, vol. 8, pp. 19306–19318, 2020. DOI: 10.1109/ACCESS.2020.2967061.
- [6] M. Braquet and E. Bakolas, "Greedy decentralized auction-based task allocation for multi-agent systems," *IFAC-PapersOnLine*, vol. 54, no. 20, pp. 675–680, 2021. DOI: 10.1016/j.ifacol.2021.11.249.
- [7] C. Sommer, S. Joerer, and F. Dressler, "On the applicability of two-ray path loss models for vehicular network simulation," in *IEEE Vehicular Netw. Conf.*, 2012, pp. 64–69. DOI: 10.1109/VNC.2012.6407446.
- [8] E. Zöchmann, K. Guan, and M. Rupp, "Two-ray models in mmWave communications," in *IEEE Int. Workshop on Signal Proc. Adv. in Wireless Comm.*, 2017, pp. 1–5. DOI: 10.1109/SPAWC.2017.8227681.
- [9] K. Uchida, J. Honda, T. Tamaki, and M. Takematsu, "Handover simulation based on a two-rays ground reflection model," in *IEEE Int. Conf. on Complex, Intelligent, and Software Intensive Systems*, 2011, pp. 414–419. DOI: 10.1109/CISIS.2011.119.
- [10] R. He, Z. Zhong, B. Ai, J. Ding, and K. Guan, "Analysis of the relation between fresnel zone and path loss exponent based on two-ray model," *IEEE Antennas and Wireless Propagation Letters*, vol. 11, pp. 208–211, 2012. DOI: 10.1109/LAWP.2012.2187270.
- [11] S. Kurt and B. Tavli, "Path-loss modeling for wireless sensor networks: A review of models and comparative evaluations," *IEEE Antennas Propag. Mag.*, vol. 59, no. 1, pp. 18–37, 2017. DOI: 10.1109/MAP.2016.2630035.
- [12] J. Walfisch and H. L. Bertoni, "A theoretical model of uhf propagation in urban environments," *IEEE Trans. Antennas Propag.*, vol. 36, no. 12, pp. 1788–1796, 1988. DOI: 10.1109/8.14401.
- [13] S. Duangsuwan and P. Jamjareegulgarn, "Exploring ground reflection effects on received signal strength indicator and path loss in far-field air-to-air for unmanned aerial vehicle-enabled wireless communication," *Drones*, vol. 8, no. 11, p. 677, 2024. DOI: 10.3390/drones8110677.
- [14] J. Lee, S. Lee, S. H. Chae, and H. Lee, "Performance analysis of cooperative dynamic framed slotted-ALOHA with random transmit power control in A2G communication networks," *IEEE Access*, vol. 10, pp. 106699–106707, 2022. DOI: 10.1109/ACCESS.2022.3211943.
- [15] S. Lee, H. Yu, and H. Lee, "Multiagent Q-learning-based multi-UAV wireless networks for maximizing energy efficiency: Deployment and power control strategy design," *IEEE Internet of Things Journal*, vol. 9, no. 9, pp. 6434–6442, 2021. DOI: 10.1109/JIOT.2021.3113128.
- [16] S. Lee, S. Lim, S. H. Chae, B. C. Jung, C. Y. Park, and H. Lee, "Optimal frequency reuse and power control in multi-UAV wireless networks: Hierarchical multi-agent reinforcement learning perspective," *IEEE Access*, vol. 10, pp. 39555–39565, 2022. DOI: 10.1109/ACCESS.2022.3166179.
- [17] A. Almarhabi, A. J. Aljohani, and M. Moinuddin, "Lora and high-altitude platforms: Path loss, link budget and optimum altitude," in *IEEE Int. Conf. Intell. Adv. Syst.*, 2021, pp. 1–6. DOI: 10.1109/ICIAS49414.2021.9642705.
- [18] A. Goldsmith, *Wireless communications*. Cambridge university press, 2005, ISBN: 978-0-521-83716-3.
- [19] K. Akpado, O. Oguejiofor, A. Adewale, and A. Ejiofor, "Pathloss prediction for a typical mobile communication system in nigeria using empirical models," *IRACST-Int. J. Comput. Netw. Wirel. Commun.*, vol. 3, no. 2, pp. 207–211, 2013, ISSN: 2250-3501.
- [20] M. Al Rashdi, Z. Nadir, and H. Al-Lawati, "Applicability of okumura-hata model for wireless communication systems in Oman," in *IEEE Int. IOT, Electronics and Mechatronics Conf. (IEMTRONICS)*, 2020, pp. 1–6. DOI: 10.1109/IEMTRONICS51293.2020.9216441.
- [21] Z. K. Adeyemo, O. K. Ogunremi, and I. A. Ojedokun, "Optimization of okumura-hata model for long term evolution network deployment in Lagos, Nigeria," *terrain*, vol. 4, no. 7, p. 14, 2016. DOI: 10.15866/irecap.v6i3.9012.
- [22] K. L. B. Ponce, S. Inca, D. Díaz, and M. Núñez, "Towards adaptive lora wireless sensor networks: Link budget and energy consumption analysis," in *IEEE Int. Conf. Electron. Electr. Eng. Comput.*, 2021, pp. 1–4. DOI: 10.1109/INTERCON52678.2021.9532685.
- [23] H. Soy, "Coverage analysis of LoRa and NB-IoT technologies on LPWAN-based agricultural vehicle tracking application," *Sensors*, vol. 23, no. 21, p. 8859, 2023. DOI: 10.3390/s23218859.
- [24] M. Mardi and M. R. Keyvanpour, "GBKM: A new genetic based k-means clustering algorithm," in *IEEE Int. Conf. on Web Research (ICWR)*, 2021, pp. 222–226. DOI: 10.1109/ICWR51868.2021.9443113.
- [25] S. Kapil, M. Chawla, and M. D. Ansari, "On K-means data clustering algorithm with genetic algorithm," in *IEEE Int. Conf. Parallel Distrib. Grid Comput.*, 2016, pp. 202–206. DOI: 10.1109/PDGC.2016.7913145.

Prediction of Power Amplifier Performance via Fine and Coarse Modeling Along with Deep Neural Network

Lida Kouhalvandi¹ , Mohammad Alibakhshikenari² , and Serdar Ozoguz³ 

¹ Department of Electrical and Electronics Engineering, Dogus University, Istanbul, 34775, Turkey

² Department of Electronics Engineering, University of Rome Tor Vergata, Rome, 00133, Italy

³ Department of Electronics and Communication Engineering, Istanbul Technical University, Istanbul, 34469, Turkey

Abstract: The power amplifier (PA) is a nonlinear design for which an accurate characterization is required for modeling and optimizing effectively. To tackle this difficulty, we present a method based on the fine and coarse modeling approach along with the implementation of deep neural networks (DNNs). For this case, firstly the executed transistor is modeled with the X-parameters and the DNN, as the 'fine modeling'. Then, the S-parameters are modeled with the help of configured hidden-layer structure at the previous step as the 'coarse modeling' leads to facilitate the overall PA sizing. Finally, the PA is modeled through the optimized DNN, which leads to estimating the performances of PA at the extended frequency in terms of S-parameters, output power, power gain, and efficiency. The presented fine and coarse modeling is powerful enough to configure the hidden-layer configuration of DNNs without any need for other optimization methods for determining the number of hidden layers with neurons in each one. The presented methodology is validated by designing and optimizing a PA with a power gain of more than 11 dB and a power-added efficiency of around 60% operating with 600 MHz band frequency.

Keywords: Fine and coarse modeling, deep neural network, optimization, power amplifier.

Derin Sinir Ağı Tabanlı İnce ve Kaba Modelleme Yoluyla Güç Kuvvetlendirici Performansının Tahmini

Özet: Güç kuvvetlendiricileri (GK), tasarımında yüksek doğruluklu bir karakterizasyonun kritik öneme sahip olduğu lineer olmayan bir devre bloğudur ve zorlayıcı isterlere göre tasarlanması için etkin bir şekilde modellenip optimize edilmesi gerekmektedir. Bu amaçla, öncelikle yapıda kullanılan transistörün X parametreleri ve DNN kullanılarak "ince modeli" elde edilir. Ardından, önceki adımda yapılandırılmış gizli katman yapısıyla transistörün bu sefer S parametreleri elde edilir, çünkü bu "kaba model" genel PA boyutlandırmasını kolaylaştırmaktadır. Son olarak, GK, optimize edilmiş DNN aracılığıyla modellenir ve bu da GK'nın genişletilmiş frekanstaki performanslarının S parametreleri, çıkış gücü, güç kazancı ve verimlilik açısından tahmin edilmesine olanak tanır. Önerilen ince ve kaba modelleme yöntemi, DNN'lerin gizli katman yapılandırmasını belirlemek için yeterli olup, gizli katman sayısı veya her katmandaki nöron sayısı gibi hiperparametreleri belirlemek için ek bir optimizasyon yöntemine ihtiyaç duymamaktadır. Sunulan yöntem, 600 MHz bant frekansında çalışan, 11 dB'den fazla güç kazancı ve yaklaşık %60'lık güç eklenen verimliliğe sahip bir GK'nin tasarlanması ile doğrulanmıştır.

Anahtar Kelimeler: İnce ve kaba modelleme, derin sinir ağı, optimizasyon, güç kuvvetlendirici.

THEORETICAL PAPER

Corresponding Author: Serdar Ozoguz, ozoguz@itu.edu.tr

Reference: L. Kouhalvandi, M. Alibakhshikenari, and S. Ozoguz, (2025), "Prediction of Power Amplifier Performance via Fine and Coarse Modeling Along with Deep Neural Network," *ITU-Journ. Wireless Comm. Cyber.*, 2, (1) 45–50.

Submission Date: Mar, 14, 2025

Acceptance Date: Mar, 18, 2025

Online Publishing: Mar, 28, 2025

1 INTRODUCTION

With the exponential advances in wireless communication systems, high-performance power amplifiers (PAs) for transmitting signals are becoming necessary [1] and the bandwidth of these systems is increasing day-by-day [2]. Hence, designing and modeling PAs require diverse techniques and topologies to meet the targeted specifications [3]. Recently, various optimization methods have been introduced for the accurate modeling of PAs including active and passive components. Among the diversely presented methods, the neural networks (NNs) are used for modeling the PAs which are able to approximate the nonlinear functions accurately [4].

In [5], a signal reconstruction deep residual neural network is introduced for digital pre-distortion (DPD) linearization which results in generating the out-of-band spectrum. The mixed-precision neural network is employed in [6] for energy-efficient DPD which reduces the computational complexity to the greatest degree. The convolutional neural network is introduced in [7] for modeling the PA with low computational complexity. In another study, [8], the deep neural network (DNN) is used for reducing the training time with the help of transfer learning. The recurrent neural network as another type of NN is used in [9] for behavioral modeling of PA. In [10], the DNN is executed for modeling and sizing the PA through the long short-term memory (LSTM)-based technique.

The NN can also be used for modeling the active device that in [11], it is employed for generating an automated optimization process. In summary, various methods are also introduced for modeling the transistors through NNs [12]. As it is obvious, starting the optimization process of PA from the transistor level is significant enough [13]–[15]. For this case, we propose an intelligence-based optimization method based on firstly modeling the high-electron-mobility transistor (HEMT) through the X-parameters with DNN as the 'fine modeling'. Afterward with the trained network, focus on the structure of hidden layers, a new DNN is constructed with the S-parameters of PA in which the constructed DNN is as the 'coarse modeling'. Finally, with the configured DNN in which the number of hidden layers with the number of neurons are known from the previously constructed DNNs, a new DNN is trained for optimizing the PA in terms of the S-parameters (i.e., S_{11} , S_{22} , S_{21}), power gain (G_p), output power (P_{out}), and power added efficiency (PAE). The proposed methodology is executed in a fully automated way leads to optimize design parameters of any PA that result in high-performance outcomes. In this study, we design and optimize a PA operating from 1.7 GHz to 2.3 GHz in which Gallium nitride (GaN) HEMT is used as an active device.

This work is organized as follows: Section 2 is devoted to presenting the methodology that is based on the fine and coarse modeling in which the DNNs are constructed. The

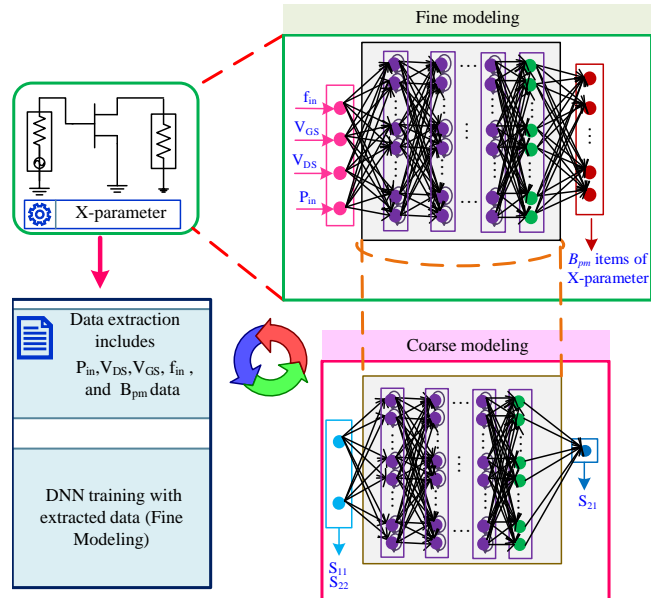


Fig. 1 A flowchart of presented fine and coarse modeling approach in this study.

effectiveness of the proposed approach is validated by designing and optimizing a PA with 600 MHz bandwidth and the related simulation results are presented in Sec. 3. Finally, Sec. 4 concludes this study.

2 PROPOSED METHODOLOGY BASED ON FINE AND COARSE MODELING ALONG WITH TRAINING DNNs

As previously presented, the DNN method is strong enough for learning nonlinear behavior between input and output corresponding data. For this case, we propose an automated methodology that is based on i) modeling HEMT device through X-parameters (fine modeling), ii) modeling PA with S-parameters with the help of constructed DNN at the previous step (coarse modeling), and iii) optimizing the PA in terms of one-tone continuous wave (CW) performances. For all the trained DNNs, the normalized root mean square error (RMSE) is a factor for calculating the convergence of NN and also the rectified linear unit (ReLU) function is executed as the activation function. This section is devoted to presenting the proposed methodology in which the flowchart of 'fine and coarse modeling' through DNNs is depicted in Figure 1.

2.1 Fine Modeling

X-parameters are frequency-dependent parameters, highly accurate, and widely used modeling tools for nonlinear high-frequency structures. It consists of three additional terms as X^F , X^S , and X^T in the output spectrum. X^F captures a large signal harmonic response and X^S with X^T captures the small signal sensitivity by representing the inci-

dent and scattered waves. Functions for B_{pm} are reflected waves (labeled with port p and harmonic m), and are given small extraction tones as A_{qn} (labeled with port q and harmonic n). The detailed definitions are presented in (1) and (2).

$$B_{pm} = X_{pm}^{(F)}(|A_{11}|)P^m + X_{pm,qn}^{(S)}(|A_{11}|)P^{m-n}A_{qn} + X_{pm,qn}^{(T)}(|A_{11}|)P^{m+n}A_{qn}^* \quad (1)$$

where,

$$P = \frac{A_{11}}{|A_{11}|} \quad (2)$$

As the first step of optimization, the GaN HEMT transistor is modeled through the LSTM-based DNN in which the X-parameters are used as a dataset for training. As Figure 1 shows in the fine modeling step, the input layer of LSTM-based DNN includes specification as the input frequency (f_{in}), input power (P_{in}), gate-source (V_{gs}) and drain-source (V_{ds}) and the output layer is the B_{pm} . Here, the LSTM-based DNN is constructed and the RMSE specification is considered. If this specification is suitable enough, then the constructed hidden layers (including the number of LSTM layers with neurons in each one) are fixed for modeling the next DNNs.

2.2 Coarse Modeling

After modeling the HEMT device through the X-parameters and achieving the hidden-layer structure, this configuration of hidden layers is employed for modeling the PA through S-parameters. The general structure of LSTM-based DNN used for coarse modeling is depicted in Figure 1. For this kind of network, the input layer includes S_{11} and S_{22} specifications and the output layer represents S_{21} result. This step of modeling will lead to improving the optimization process in which the overall performance of PA will be enhanced based on S-parameters and one-tone continuous wave (CW) performances in the next step.

2.3 Overall PA Optimization

After completing the fine and coarse modeling, the PA must be optimized in terms of existing parameters (here, capacitor (C) and inductor (L)) to achieve high-performance outcomes in terms of S_{11} , S_{22} , S_{21} , G_p , P_{out} , and PAE specifications. Figure 2 shows the DNN structure leading to i) optimizing the PA in terms of inserted design parameters, and ii) estimating the output specifications at the determined frequencies. For this kind of DNN, the hidden-layer structure is the one achieved from fine modeling.

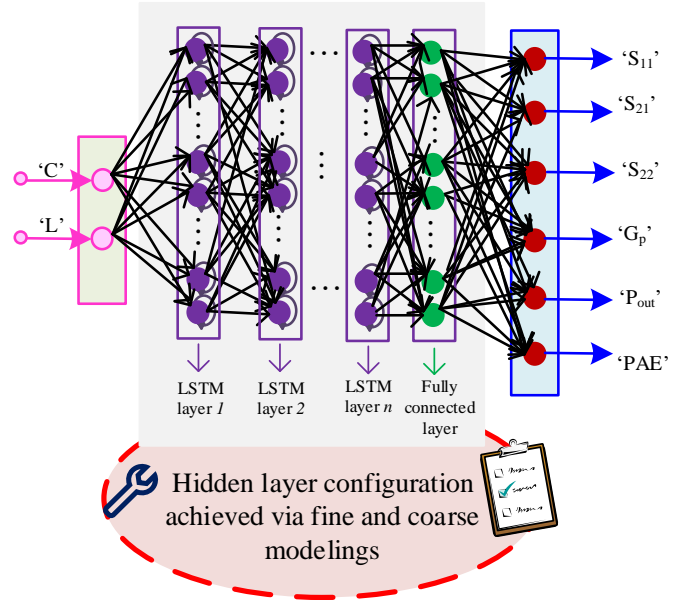


Fig. 2 Structure of LSTM-based DNN for optimizing the PA and achieving the optimal design parameters along with predicting the extended frequencies.

3 SIMULATION RESULTS

For executing the proposed methodology, a CPU environment with an Intel Core i7-4790 CPU @ 3.60 GHz and 32.0 GB RAM is prepared first. Then, a GaN HEMT transistor as an active device namely 'Ampleon CLF1G0060-10' is selected. For the presented procedure, the automated environment is generated by the combination of 'Keysight ADS' and 'MATLAB' as the electronic design automation tool and numerical analyzer, respectively. For all the trained DNNs, the solver is set to 'adam' and 'gradient threshold' is set to 1. This section describes the practical implementation of the proposed method for the PA operating with 600 MHz band frequency.

As the first step, the fine modeling is executed based on the X-parameters generated by the f_{in} , P_{in} , V_{gs} , V_{ds} [16], and B_{pm} specifications as presented in Eq. (1). Here, the modeling is executed for $p=2$ and $m=5$. With the help of 500 data (achieved from random iteration), the LSTM-based DNN is trained results in the normalized RMSE value presented in Figure 3. As it is obvious, the trained DNN achieved 0.087 RMSE value when the number of hidden layers is 4 with 200 neurons in each one.

Afterward, the coarse modeling is executed with the help of configured PA through the simplified real frequency technique [17] and also by the generated gate and drain impedances through the load-pull simulation. Figure 4 presents the configured PA that input and output matching networks include 4-LC with 2-LC ladders, respectively. For the presented PA, Rogers RO4350B with $\epsilon_r=3.66$ and

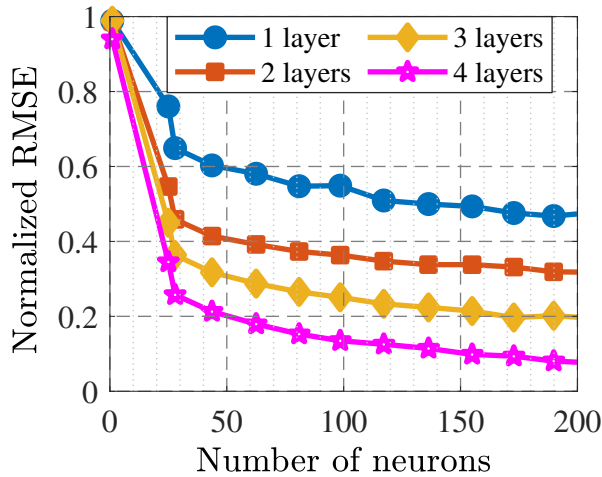


Fig. 3 Accuracy of the trained DNN at the fine modeling step.

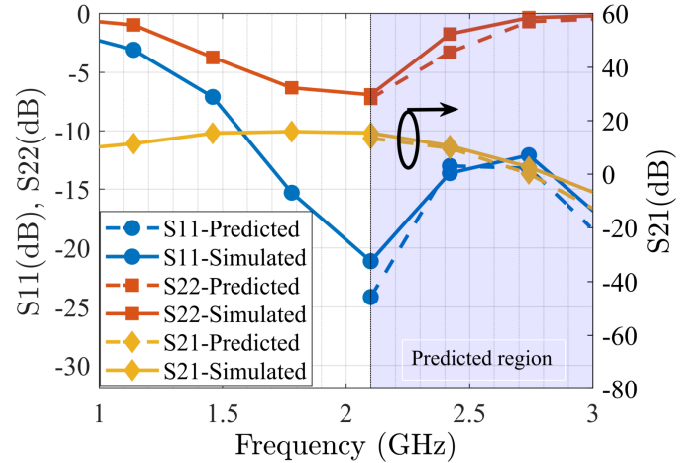


Fig. 5 S-parameter performances of the optimized PA.

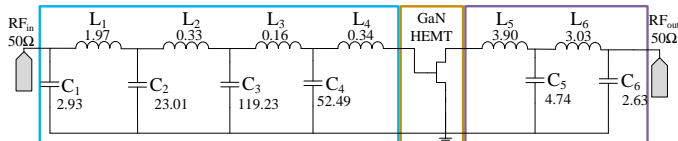


Fig. 4 Optimized PA with the executed GaN HEMT device; Unit of each capacitor and inductor are (pF) and (nH), respectively.

a thickness of 0.508 mm is used as a substrate and it is biased with a drain-source voltage of 50 V and quiescent drain-source current of 40 mA. With this constructed PA, 800 sequences include multi-segment S_{11} , S_{12} , and S_{22} specifications are generated for training the LSTM-based DNN as the coarse modeling step. In this stage, the hidden-layer configuration constructed from the fine modeling step is exactly substituted. This step leads to facilitating the sizing optimization of configured PA.

For the optimized PA operating from 1.7 GHz to 2.3 GHz, various results in terms of S-parameters and one-tone CW performances (i.e., P_{out} , G_p , and PAE at 3-dB gain compression) are performed. Figure 5 shows the detailed results for S_{11} , S_{22} , and S_{21} specifications. Here, the simulated S-parameters are compared with the estimated results with the help of trained DNN from 2.1 to 3 GHz. Additionally, one-tone CW performances are also presented in terms of simulated and predicted results in Figure 6. For the used HEMT device and the configured PA, a maximum PAE value of 60.2% with a linear G_p value larger than 11 dB at 40 dBm output power is achieved. It is observed that the predicted regions in both Figure 5 and Figure 6 are tracking the results achieved from simulations in an acceptable manner. The stability factor is well-enough in the whole bandwidth, which shows that the input and output matching networks are optimized in an improved way.

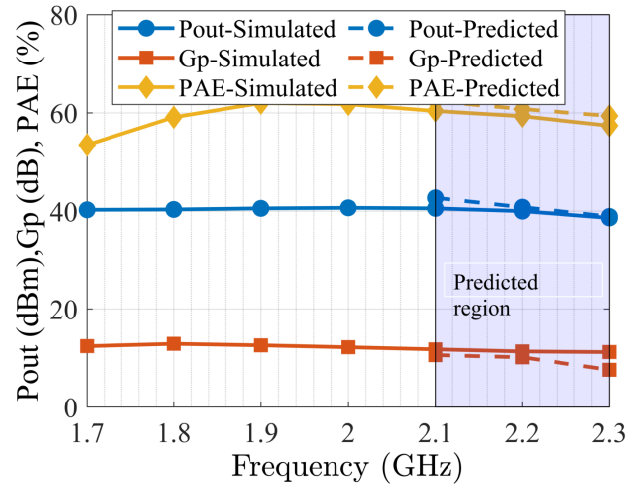


Fig. 6 P_{out} , G_p , and PAE results at 3-dB gain compression.

4 CONCLUSIONS

In this work, a DNN-based optimization method based on fine and coarse modeling is proposed. Firstly, the executed HEMT device is modeled through X-parameters, and then the S-parameters of PA are modeled through the configured DNN at the fine modeling stage. The presented procedure is effective enough since the hidden-layer configuration generated from fine modeling is employed for the DNNs at the coarse modeling stage and an NN is trained for sizing the PA. The fine and coarse modeling helps designers to configure the hidden layers of DNNs in a fast way without any need for optimization methods. The whole procedure is automated way, and a 10 W PA is designed and optimized to prove the effectiveness of the methodology operating from 1.7 GHz to 2.3 GHz.

AUTHOR CONTRIBUTIONS

Conceptualization, L.K. and M.A.; methodology, L.K, M.A., and S.O.; software, L.K.; validation, M.A., and S.O.; formal analysis, L.K.; investigation, M.A.; resources, S.O.; data curation, L.K.; writing—original draft preparation, L.K.; writing—review and editing, M.A., S.O; visualization, S.O.; supervision, S.O.; project administration, M.A. and S.O.; funding acquisition, S.O. All authors have read and agreed to the published version of the manuscript.

REFERENCES

- [1] W. Li, H. Zeng, L. Huang, *et al.*, “A review of terahertz solid-state electronic/optoelectronic devices and communication systems,” *Chinese Journal of Electronics*, vol. 34, no. 1, pp. 26–48, 2025. DOI: 10.23919/cje.2023.00.282.
- [2] U. Ghafoor, “Strengthening data confidentiality in 6g cognitive networks through secrecy rate optimization,” *IEEE Communications Letters*, pp. 1–1, 2025. DOI: 10.1109/LCOMM.2025.3537285.
- [3] D. Zeng, H. Zhu, G. Shen, *et al.*, “A compact 24–30-ghz gan front-end module with coupled-resonator-based transmit/receive switch for 5g millimeter-wave applications,” *IEEE Transactions on Microwave Theory and Techniques*, pp. 1–13, 2025. DOI: 10.1109/TMTT.2025.3530435.
- [4] D. Wang, M. Aziz, M. Helaoui, and F. M. Ghannouchi, “Augmented real-valued time-delay neural network for compensation of distortions and impairments in wireless transmitters,” *IEEE Transactions on Neural Networks and Learning Systems*, vol. 30, no. 1, pp. 242–254, 2019. DOI: 10.1109/TNNLS.2018.2838039.
- [5] J. Wang, R. Su, J. Lv, G. Xu, and T. Liu, “Signal reconstruction deep residual neural network-based bandwidth augmented methods for dpd linearization,” *IEEE Microwave and Wireless Technology Letters*, vol. 33, no. 3, pp. 243–246, 2023. DOI: 10.1109/LMWC.2022.3217691.
- [6] Y. Wu, A. Li, M. Beikmirza, *et al.*, “Mp-dpd: Low-complexity mixed-precision neural networks for energy-efficient digital predistortion of wideband power amplifiers,” *IEEE Microwave and Wireless Technology Letters*, vol. 34, no. 6, pp. 817–820, 2024. DOI: 10.1109/LMWT.2024.3386330.
- [7] Z. Liu, X. Hu, L. Xu, W. Wang, and F. M. Ghannouchi, “Low computational complexity digital predistortion based on convolutional neural network for wideband power amplifiers,” *IEEE Transactions on Circuits and Systems II: Express Briefs*, vol. 69, no. 3, pp. 1702–1706, 2022. DOI: 10.1109/TCSII.2021.3109973.
- [8] S. Zhang, X. Hu, Z. Liu, *et al.*, “Deep neural network behavioral modeling based on transfer learning for broadband wireless power amplifier,” *IEEE Microwave and Wireless Components Letters*, vol. 31, no. 7, pp. 917–920, 2021. DOI: 10.1109/LMWC.2021.3078459.
- [9] A. Fischer-Bühner, L. Anttila, M. Turunen, M. Dev Gomony, and M. Valkama, “Augmented phase-normalized recurrent neural network for rf power amplifier linearization,” *IEEE Transactions on Microwave Theory and Techniques*, vol. 73, no. 1, pp. 412–422, 2025. DOI: 10.1109/TMTT.2024.3484581.
- [10] L. Kouhalvandi, O. Ceylan, and S. Ozoguz, “Automated deep neural learning-based optimization for high performance high power amplifier designs,” *IEEE Transactions on Circuits and Systems I: Regular Papers*, vol. 67, no. 12, pp. 4420–4433, 2020. DOI: 10.1109/TCSI.2020.3008947.
- [11] C. Belchior, L. C. Nunes, P. M. Cabral, and J. C. Pedro, “Towards the automated rf power amplifier design,” in *2023 19th International Conference on Synthesis, Modeling, Analysis and Simulation Methods and Applications to Circuit Design (SMACD)*, 2023, pp. 1–4. DOI: 10.1109/SMACD58065.2023.10192148.
- [12] L. Kouhalvandi and S. D. Guerrieri, “Modeling of hemt devices through neural networks: Headway for future remedies,” in *2023 10th International Conference on Electrical and Electronics Engineering (ICEEE)*, 2023, pp. 261–267. DOI: 10.1109/ICEEE59925.2023.00054.
- [13] L. Kouhalvandi and S. D. Guerrieri, “Nonlinear behavioral modeling of fets: Toward the implementation of deep neural networks through large signal data and eda tools,” in *2024 19th European Microwave Integrated Circuits Conference (EuMIC)*, 2024, pp. 307–310. DOI: 10.23919/EuMIC61603.2024.10732844.
- [14] P. Chen, J. Xia, B. M. Merrick, and T. J. Brazil, “Multi-objective bayesian optimization for active load modulation in a broadband 20-w gan doherty power amplifier design,” *IEEE Transactions on Microwave Theory and Techniques*, vol. 65, no. 3, pp. 860–871, 2017. DOI: 10.1109/TMTT.2016.2636146.
- [15] P. Chen, B. M. Merrick, and T. J. Brazil, “Bayesian optimization for broadband high-efficiency power amplifier designs,” *IEEE Transactions on Microwave Theory and Techniques*, vol. 63, no. 12, pp. 4263–4272, 2015. DOI: 10.1109/TMTT.2015.2495360.
- [16] *Ampleon*, <https://www.ampleon.com/>, Accessed: 2025-02-23.
- [17] S. Yarman, “Design of ultra wideband power transfer networks,” *New York, NY, USA: Wiley*, 2010. DOI: 10.1002/9780470688922.

